OAK RIDGE NATIONAL LABORATORY
operated by
UNION CARBIDE CORPORATION
for the
U. S. ATOMIC ENERGY COMMISSION

ORNL - TM - 2647

AN EVALUATION OF THE MOLTEN-SALT REACTOR EXPERIMENT HASTELLOY N SURVEILLANCE SPECIMENS - THIRD GROUP

H. E. McCoy, Jr.

ORNL-TM-2647

Contract No. W-7405-eng-26

METALS AND CERAMICS DIVISION

AN EVALUATION OF THE MOLTEN-SALT REACTOR EXPERIMENT HASTELLOY N SURVEILLANCE SPECIMENS — THIRD GROUP

H. E. McCoy, Jr.

JANUARY 1970

OAK RIDGE NATIONAL LABORATORY
Oak Ridge, Tennessee
operated by
UNION CARBIDE CORPORATION
for the
U.S. ATOMIC ENERGY COMMISSION

CONTENTS

AN EVALUATION OF THE MOLTEN-SALT REACTOR EXPERIMENT HASTELLOY N SURVEILLANCE SPECIMENS – THIRD GROUP

H. E. McCoy, Jr.

ABSTRACT

We have examined the third group of Hastelloy N surveillance samples removed from the Molten-Salt Reactor Experiment. Standard Hastelloy N was removed from the core after exposure to a thermal fluence of 9.4×10^{20} neutrons/cm^2 over a time period of 15,289 hr at 650°C and from outside the reactor vessel after exposure to a thermal fluence of 2.6×10^{19} neutrons/cm^2 over a time period of 20,789 hr at 650°C. The former samples were exposed to the fuel salt and the later samples were exposed to nitrogen plus 2 to 5% O_2. The material seemed quite compatible with both environments. Postirradiation tests showed that the fracture strain was reduced at 25°C and above 500°C. The reduction in ductility at 25°C is likely due to carbide precipitation and the reduction above 500°C is due to the presence of helium from the $^{10}B(N,\alpha)^7Li$ transmutation. The accumulated results in this series of experiments allow us to follow the changes in fracture strain over the thermal fluence range 1.3×10^{19} to 9.4×10^{20} neutrons/cm^2.

Two heats of modified Hastelloy N were removed from the core after irradiation to a thermal fluence of 5.3×10^{20} neutrons/cm^2 over a time period of 9789 hr at 650°C. The postirradiation properties of these alloys were better than those of standard Hastelloy N.

INTRODUCTION

The Molten-Salt Reactor Experiment (MSRE) is a single region reactor that is fueled by a molten fluoride salt (65 LiF–29.1 BeF_2–5 ZrF_4–0.9 UF_4, mole %), moderated by unclad graphite, and contained by Hastelloy N (Ni–16 Mo–7 Cr–4 Fe–0.05 C, wt %). The details of the reactor design and construction can be found elsewhere.[1] We knew that the neutron

[1] R. C. Robinson, MSRE Design and Operations Report, Pt. 1, Description of Reactor Design, ORNL-TM-728 (January 1965).

environment would produce some changes in the two structural materials – graphite and Hastelloy N. Although we were very confident of the compatibility of these materials with the fluoride salt, we needed to keep abreast of the possible development of corrosion problems within the reactor itself. For these reasons, we developed a surveillance program that would allow us to follow the property changes of graphite and Hastelloy N specimens as the reactor operated.

The reactor went critical on June 1, 1965, and after numerous small problems were solved, assumed normal operation in May 1966. We have removed three groups of surveillance samples and the results of tests on the Hastelloy N specimens from the first and second groups[2,3] were reported previously. This report will deal primarily with the results of tests on the Hastelloy N samples removed with the third group of surveillance samples. The third group included two heats of standard Hastelloy N that had been used in fabricating the MSRE and two heats with modified chemistry that had better mechanical properties after irradiation and appear attractive for use in future molten-salt reactors. The respective history of each lot was (1) standard Hastelloy N, exposed in the MSRE cell to an environment of N_2 + 2 to 5% O_2 for 20,789 hr at 650°C to a thermal fluence of 2.6×10^{19} neutrons/cm^2, (2) standard Hastelloy N, exposed in the MSRE core to fluoride salt for 15,289 hr at 650°C to a thermal fluence of 9.4×10^{20} neutrons/cm^2, and (3) modified Hastelloy N, exposed in the MSRE core to fluoride salt for 9789 hr at 650°C to a thermal fluence of 5.3×10^{20} neutrons/cm^2. The results of tests on these materials will be presented in detail and some comparisons will be made with the data from the groups removed previously.

---

[2]H. E. McCoy, An Evaluation of the Molten-Salt Reactor Experiment Hastelloy N Surveillance Specimen – First Group, ORNL-TM-1997 (November 1967).

[3]H. E. McCoy, An Evaluation of the Molten-Salt Reactor Experiment Hastelloy N Surveillance Specimen – Second Group, ORNL-TM-2359 (February 1969).

EXPERIMENTAL DETAILS

Surveillance Assemblies

The core surveillance assembly was designed by W. H. Cook and others, and the details have been reported previously.[4] The specimens are arranged in three stringers. Each stringer is about 62 in. long and consists of two Hastelloy N rods and a graphite section made up of various pieces that are joined by pinning and tongue-and-groove joints. The Hastelloy N rod has periodic-reduced sections 1 1/8 in. long by 1/8 in. in diameter and can be cut into small tensile specimens after it is removed from the reactor. Three stringers are joined together so that they can be separated in a hot cell and reassembled with one or more new stringers for reinsertion into the reactor. The assembled stringers fit into a perforated Hastelloy N basket that is inserted into an axial position about 3.6 in. from the core center line.

A control facility is associated with the surveillance program. It utilizes a "fuel salt" containing depleted uranium in a static pot that is heated electrically. The temperature is controlled by the MSRE computer so that the temperature matches that of the reactor. Thus, these specimens are exposed to conditions similar to those in the reactor except for the static salt and the absence of a neutron flux.

There is another surveillance facility for Hastelloy N located outside the core in a vertical position about 4.5 in. from the vessel. These specimens are exposed to the cell environment of N_2 + 2 to 5% O_2.

Materials

The compositions of the two heats of standard Hastelloy N are given in Table 1. These heats were air melted by Stellite Division of Union Carbide Corporation. Heat 5085 was used for making the cylindrical portion of the reactor vessel and heat 5065 was used for forming the top

---

[4]W. H. Cook, MSR Program Semiann. Progr. Rept. Aug. 31, 1965, ORNL-3872, p. 87.

Table 1. Chemical Analysis of Surveillance Heats

Element	Content, wt %			
	Heat 5065	Heat 5085	Heat 67-502	Heat 67-504
Cr	7.2	7.3	7.18	6.94
Fe	3.9	3.5	0.034	0.05
Mo	16.5	16.7	12.0	12.4
C	0.065	0.052	0.05	0.07
Si	0.60	0.58	0.015	0.010
Co	0.08	0.15	0.02	0.02
W	0.04	0.07	2.15	0.03
Mn	0.55	0.67	0.14	0.12
V	0.22	0.20	0.06	0.01
P	0.004	0.0043	0.001	0.002
S	0.007	0.004	< 0.002	0.003
Al	0.01	0.02	0.02	0.03
Ti	0.01	< 0.01	0.49	< 0.02
Cu	0.01	0.01	0.04	0.03
O	0.0016	0.0093	0.0002	< 0.0001
N	0.011	0.013	< 0.0001	0.0003
Zr		< 0.002	< 0.01	0.01
Hf			< 0.01	0.50
	Analysis, ppm			
B	24,37, 20,10	38	1	0.3

and bottom heads. These materials were given a mill anneal of 1 hr at 1177°C and a final anneal of 2 hr at 900°C at ORNL after fabrication.

The chemical compositions of the two modified alloys are given in Table 1. The modifications in composition were made principally to improve the alloy's resistance to radiation damage and to bring about general improvements in the fabricability, weldability, and ductility.[5] These alloys were small 100-lb heats made by Stellite Division of Union Carbide Corporation by vacuum melting. They were finished to 1/2 in. plate by working at 870°C. We cut strips 1/2 in. by 1/2 in. from the plates and swaged them to 1/4-in. diam. rod. Two sections of rod were

[5]H. E. McCoy and J. R. Weir, Materials Development for Molten-Salt Breeder Reactors, ORNL-TM-1854 (June 1967).

welded together to make 62-in.-long rods for fabricating the samples. The rods were annealed for 1 hr at 1177°C in argon and then the reduced sections were machined.

Test Specimens

The surveillance rods inside the core are 62 in. long and those outside the vessel are 84 in. long. They both are 1/4 in. in diameter with reduced sections 1/8 in. in diameter by 1 1/8 in. long. After removal from the reactor, the rods are sawed into small mechanical property specimens having a gage section 1/8 in. in diameter by 1 1/8 in. long.

The first rods were machined as segments and then welded together, but we described previously an improved technique in which we use a milling cutter to machine the reduced sections in the rod.[3] This technique is quicker, cheaper, and requires less handling of the relatively fragile rods than the previous method of making the rods into segments.

IRRADIATION CONDITIONS

The irradiation conditions for the three groups of surveillance specimens that have been removed are summarized in Table 2. The environment in the core facility is the molten-fluoride fuel salt. The specimens outside the core (designated "vessel" specimens) are exposed to the cell environment of N_2 + 2 to 5% O_2.

Testing Techniques

The laboratory creep-rupture tests of unirradiated control specimens were run in conventional creep machines of the dead-load and lever-arm types. The strain was measured by a dial indicator that showed the total movement of the specimen and part of the load train. The zero strain measurement was taken immediately after the load was applied. The temperature accuracy was ±0.75%, the guaranteed accuracy of the Chromel-P–Alumel thermocouples used.

Table 2. Summary of Exposure Conditions of Surveillance Samples[a]

	Group 1	Group 2		Group 3		
	Core Standard Hastelloy N	Core Modified Hastelloy N	Vessel Standard Hastelloy N	Core Standard Hastelloy N	Core Modified Hastelloy N	Vessel Standard Hastelloy N
Date inserted	9/8/65	9/13/66	8/24/65	9/13/66	6/5/67	8/24/65
Date removed	7/28/66	5/9/67	6/5/67	4/3/68	4/3/68	5/7/68
Mwhr on MSRE at time of insertion	0.0066	8682	0	8682	36,247	0
Mwhr on MSRE at time of removal	8682	36,247	36,247	72,441	72,441	72,441
Temperature, °C	650 ± 10	650 ± 10	650 ± 10	650 ± 10	650 ± 10	650 ± 10
Time at temperature, hr	4800	5500	11,000	15,289	9789	20,789
Peak fluence, neutrons/cm^2						
Thermal (< 0.876 ev)	1.3×10^{20}	4.1×10^{20}	1.3×10^{19}	9.4×10^{20}	5.3×10^{20}	2.6×10^{19}
Epithermal (> 0.876 ev)	3.8×10^{20}	1.2×10^{21}	2.5×10^{19}	2.8×10^{21}	1.6×10^{21}	5.0×10^{19}
(> 50 kev)	1.2×10^{20}	3.7×10^{20}	2.1×10^{19}	8.5×10^{20}	4.8×10^{20}	4.2×10^{19}
(> 1.22 Mev)	3.1×10^{19}	1.0×10^{20}	5.5×10^{18}	2.3×10^{20}	1.3×10^{20}	1.1×10^{19}
(> 2.02 Mev)	1.6×10^{19}	0.5×10^{20}	3.0×10^{18}	1.1×10^{20}	0.7×10^{20}	6.0×10^{18}
Peak flux, neutrons cm^{-2} sec^{-1} Mw^{-1}						
Thermal (< 0.876 ev)	4.1×10^{12} (b,c)	4.1×10^{12} (b,c)	1.0×10^{11} (b)	4.1×10^{12} (b,c)	4.1×10^{12} (b,c)	1.0×10^{11} (b)
Epithermal (> 0.876 ev)	1.2×10^{13} (c)	1.2×10^{13} (c)	1.9×10^{11} (b,c)	1.2×10^{13} (c)	1.2×10^{13} (c)	1.9×10^{11} (b,c)
(> 50 kev)	3.7×10^{12} (c)	3.7×10^{12} (c)	1.6×10^{11} (c)	3.7×10^{12} (c)	3.7×10^{12} (c)	1.6×10^{11} (c)
(> 1.22 Mev)	1.0×10^{12} (b,c)	1.0×10^{12} (b,c)	4.2×10^{10} (b)	1.0×10^{12} (b,c)	1.0×10^{12} (b,c)	4.2×10^{10} (b)
(> 2.02 Mev)	0.5×10^{12} (b,c)	0.5×10^{12} (b,c)	2.3×10^{10} (b)	0.5×10^{12} (b,c)	0.5×10^{12} (b,c)	2.3×10^{10} (b)

[a] Information compiled by R. C. Steffy. Revised for full-power operation at 8 Mw.

[b] Experimentally determined.

[c] Calculated.

The postirradiation creep-rupture tests were run in lever-arm machines that were located in hot cells. The strain was measured by an extensometer with rods attached to the upper and lower specimen grips. The relative movement of these two rods was measured by a linear differential transformer, and the transformer signal was recorded. The accuracy of the strain measurement is difficult to determine. The extensometer (mechanical and electrical portions) produced measurements that could be read to about ±0.02% strain; however, other factors (temperature changes in the cell, mechanical vibrations, etc.) probably combined to give an overall accuracy of ±0.1% strain. This is considerably better than the specimen-to-specimen reproducibility that one would expect for relatively brittle materials. The temperature measuring and control system was the same as that used in the laboratory with only one exception. In the laboratory, the control system was stabilized at the desired temperature by use of a recorder with an expanded scale. In the tests in the hot cells, the control point was established by setting the controller without the aid of the expanded-scale recorder. This error and the thermocouple accuracy combine to give a temperature uncertainty of about ±1%.

The tensile tests were run on Instron Universal Testing Machines. The strain measurements were taken from the crosshead travel and generally are accurate to ±2% strain.

The test environment was air in all cases. Metallographic examination showed that the depth of oxidation was small and we feel that the environment did not appreciably influence the test results.

EXPERIMENTAL RESULTS

Visual and Metallographic Examination

W. H. Cook was in charge of the disassembly of the core surveillance fixture. As shown in Fig. 1 the assembly was in excellent mechanical condition when removed. The graphite and Hastelloy N surfaces were very clean with markings such as numbers and tool marks clearly visible. The

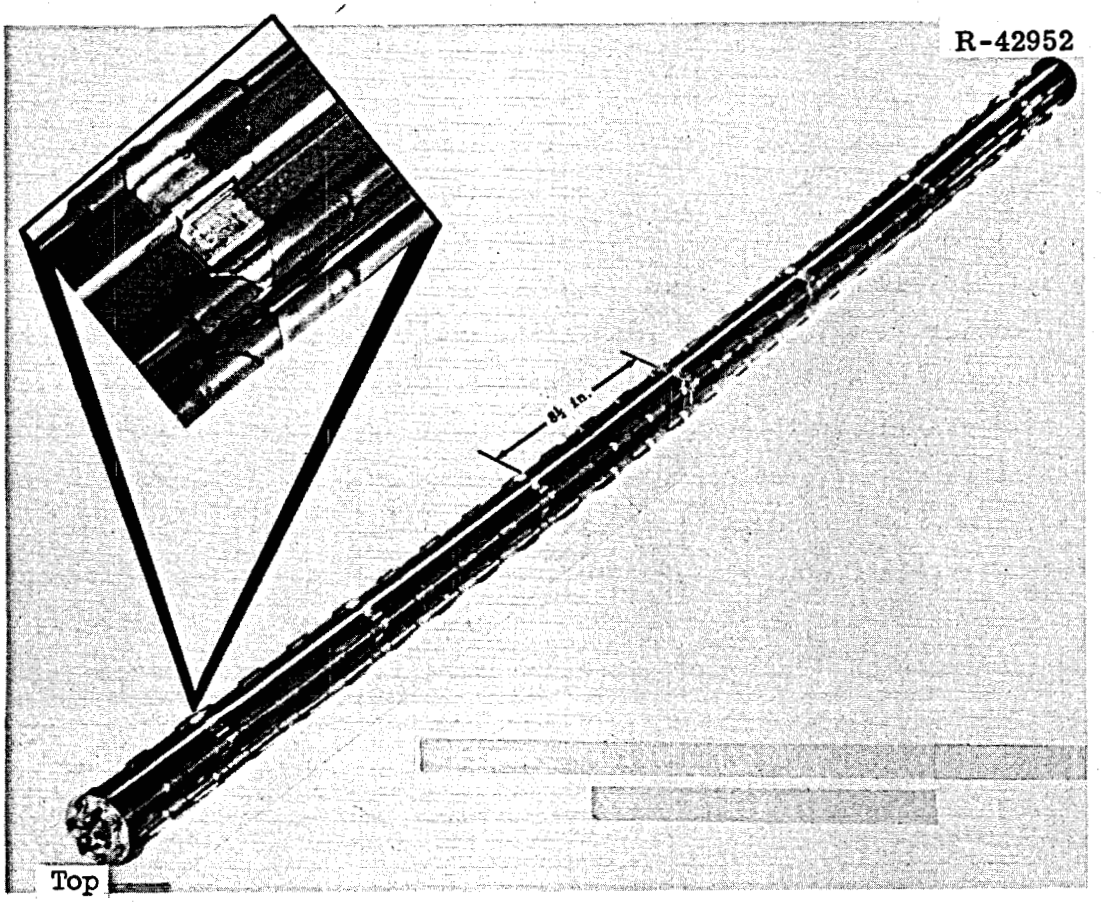

Fig. 1. Molten-Salt Reactor Experiment Surveillance Specimens from Run 14 (Stringers RS3, RL2, and RR2).

Hastelloy N was discolored slightly. The Hastelloy N surveillance rods outside the reactor vessel were oxidized, but the oxide was tenacious.

We examined polished cross sections of segments from each of the surveillance rods. Typical micrographs of the rods of standard Hastelloy N that were located outside the reactor vessel are shown in Figs. 2 and 3. The cell environment of N_2 + 2 to 5% O_2 is oxidizing to the alloy, but there is no evidence of nitriding. There is some internal oxidation to a depth of 1 to 2 mils and a very thin uniform surface oxide. The general microstructure is characterized by large M_6C-type carbides that are distributed during the primary working and by finer M_6C-type carbides that formed during the long thermal anneal of 20,789 hr at 650°C.

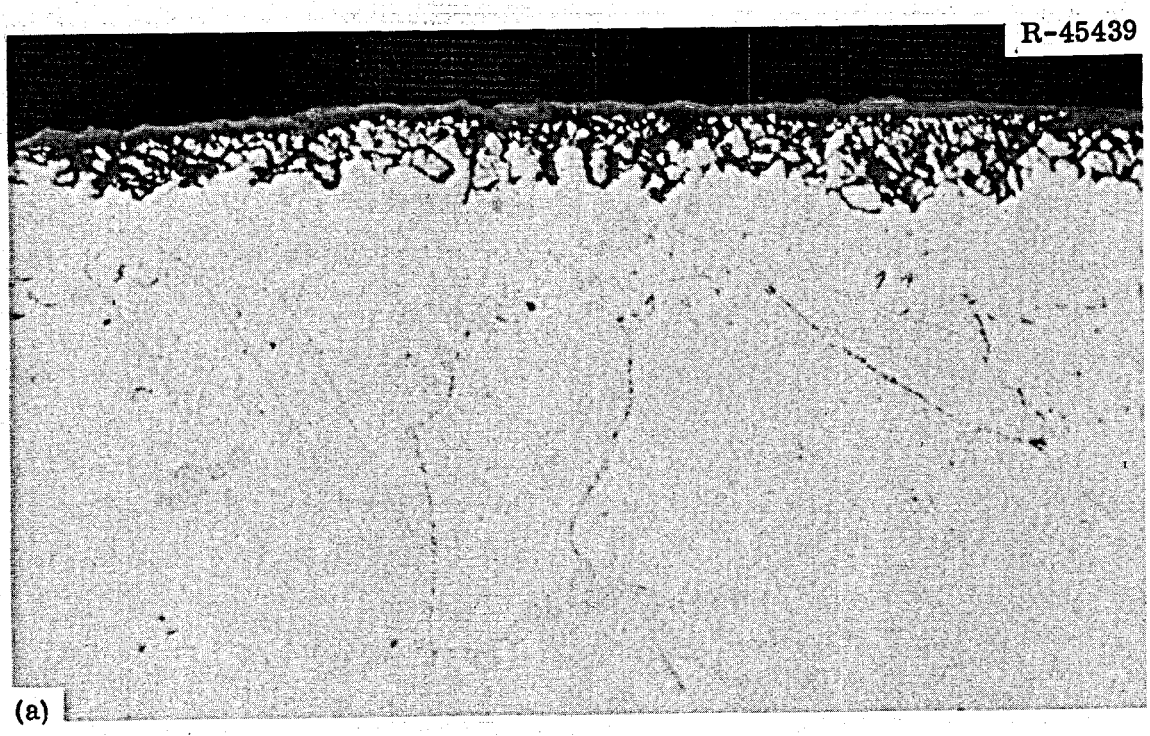

(a)

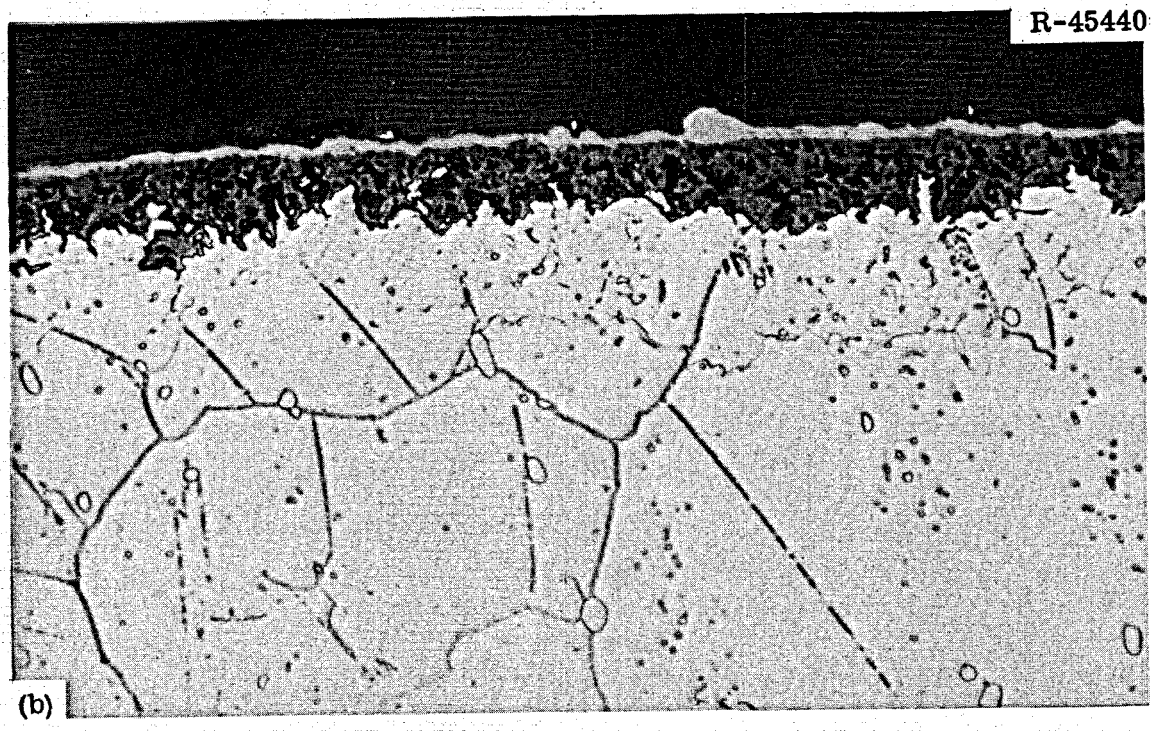

(b)

Fig. 2. Photomicropgraphs of Hastelloy N (Heat 5085) Surveillance Specimens Exposed to the Cell Environment of N_2 + 2 to 5% O_2 for 20,789 hr at 650°C. 500×. (a) Unetched showing surface oxidation. (b) Etched (glyceria regia) showing shallow modification of microstructure due to reaction with cell environment.

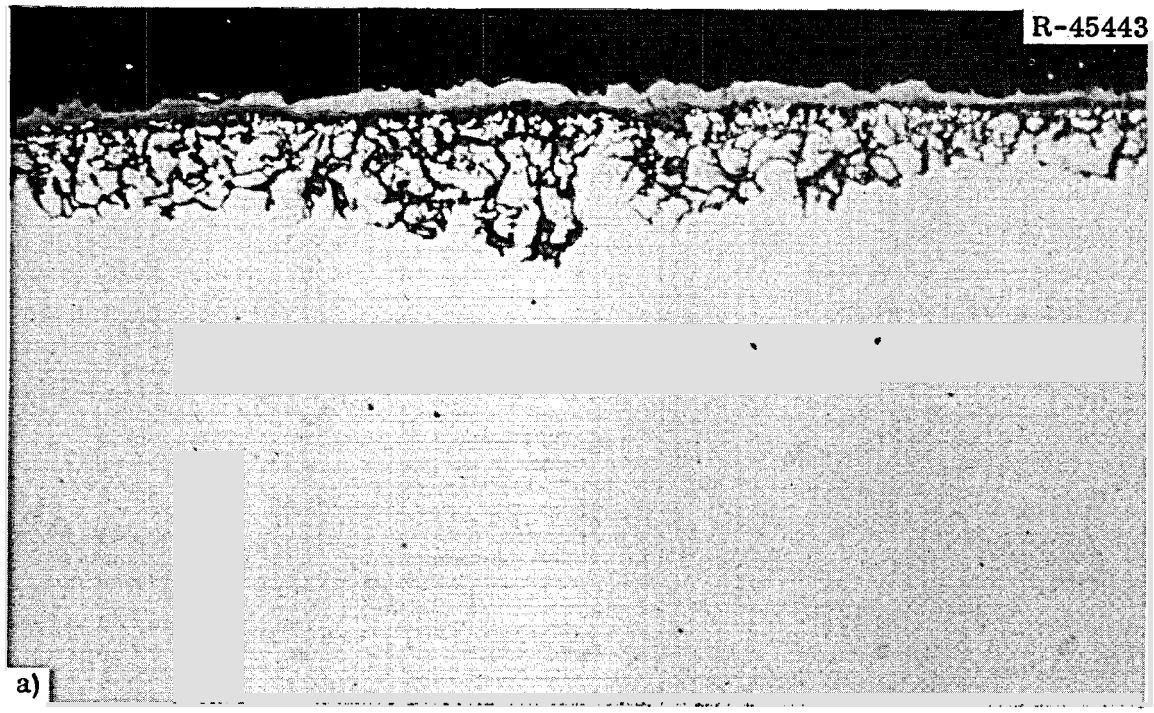

Fig. 3. Photomicrographs of Hastelloy N (Heat 5065) Surveillance Specimens Exposed to the Cell Environment of N_2 + 2 to 5% O_2 for 20,789 hr at 650°C. 500×. (a) Unetched showing surface oxidation. (b) Etched (glyceria regia) showing shallow modification of microstructure due to reaction with cell environment.

Typical photomicrographs of the standard Hastelloy N samples exposed to the MSRE fuel salt for 15,289 hr at 650°C are shown in Figs. 4 and 5. There is a thin layer of modified structure less than 0.5 mil thick at the surface. This modified structure was noted previously.[6] As shown in Figs. 6 and 7, a similar product is formed on the surfaces of the control specimens. We originally suspected that this product formed only where the Hastelloy N was in intimate contact with graphite, but a closer examination shows that the modified structure exists around the complete circumference of the rod and not just where it makes tangential contact with graphite. From the practical standpoint, the modified layer has not changed detectably since we first observed the samples removed after 4800 hr of exposure and we feel that it will not influence the mechanical properties of the material.

The amount of fine M_6C-type precipitates is not detectably different for the material aged while being irradiated (Figs. 4 and 5) and that aged in the absence of irradiation (Figs. 6 and 7). There does seem to be more precipitate present in heat 5065 than in heat 5085, an observation in keeping with the higher carbon content of heat 5065 (Table 1, p. 4). Extracted precipitates were found to be of the M_6C type with a lattice parameter of 11.02 A. Some of the material exposed to the highest thermal fluence of 9.4×10^{20} neutrons/cm^2 was examined in transmission. A typical electron photomicrograph is shown in Fig. 8 where helium bubbles are clearly visible along several of the grain boundaries. This sample had not been stressed and the rather large sizes of these bubbles attests to the initial inhomogeneous distribution of the boron. However, the observation of bubbles of this size only serves to support the formation of gas bubbles in metals during irradiation and really is not informative from a mechanistic standpoint. Deformation takes place on an atomistic scale (few angstroms) and our ability to see details in the grain boundaries of such specimens is limited to about 50 A, so we are not yet able to see details of the size involved in deformation.

---

[6]H. E. McCoy, An Evaluation of the Molten-Salt Reactor Experiment Hastelloy N Surveillance Specimen - First Group, ORNL-TM-1997 (November 1967).

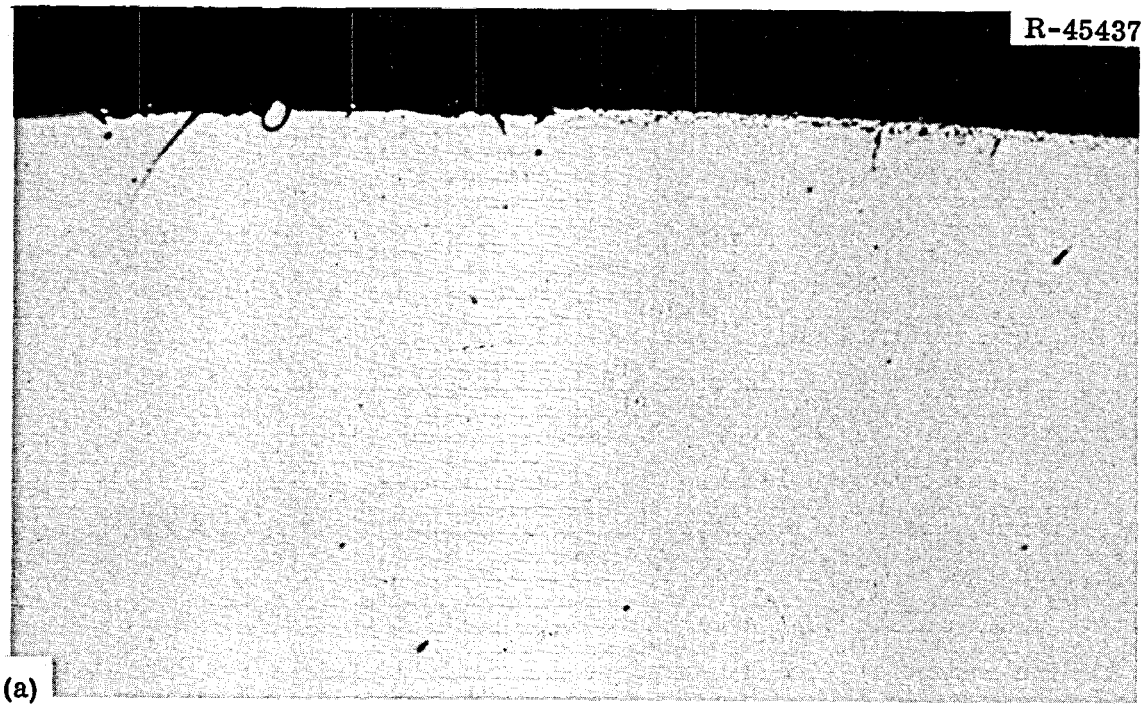

Fig. 4. Photomicrographs of Hastelloy N (Heat 5085) Surveillance Specimens Exposed to Fuel Salt for 15,289 hr at 650°C. 500×. (a) Unetched. (b) Etched (glyceria regia) photomicrographs showing shallow reaction layer near surface.

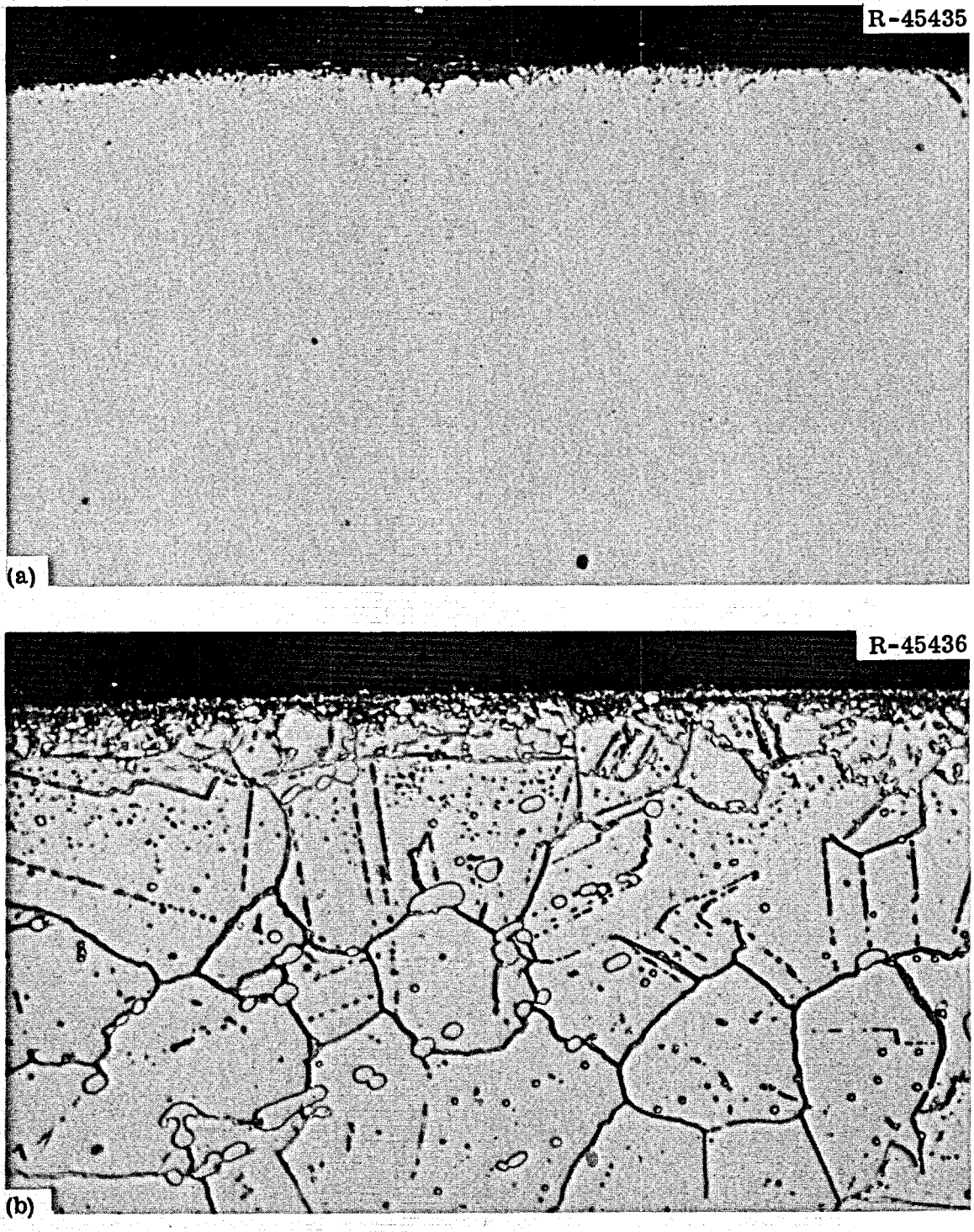

Fig. 5. Photomicrographs of Hastelloy N (Heat 5065) Surveillance Specimens Exposed to Fuel Salt for 15,289 hr at 650°C. 500X. (a) Unetched. (b) Etched (glyceria regia) photomicrographs showing shallow reaction layer near surface.

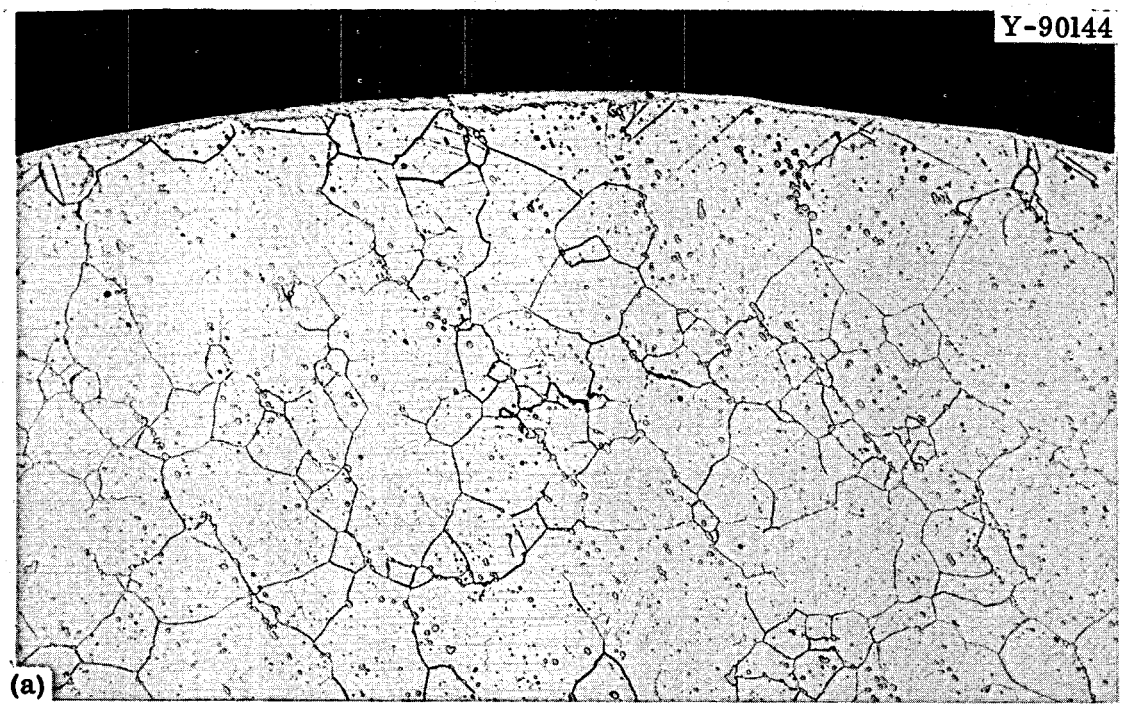

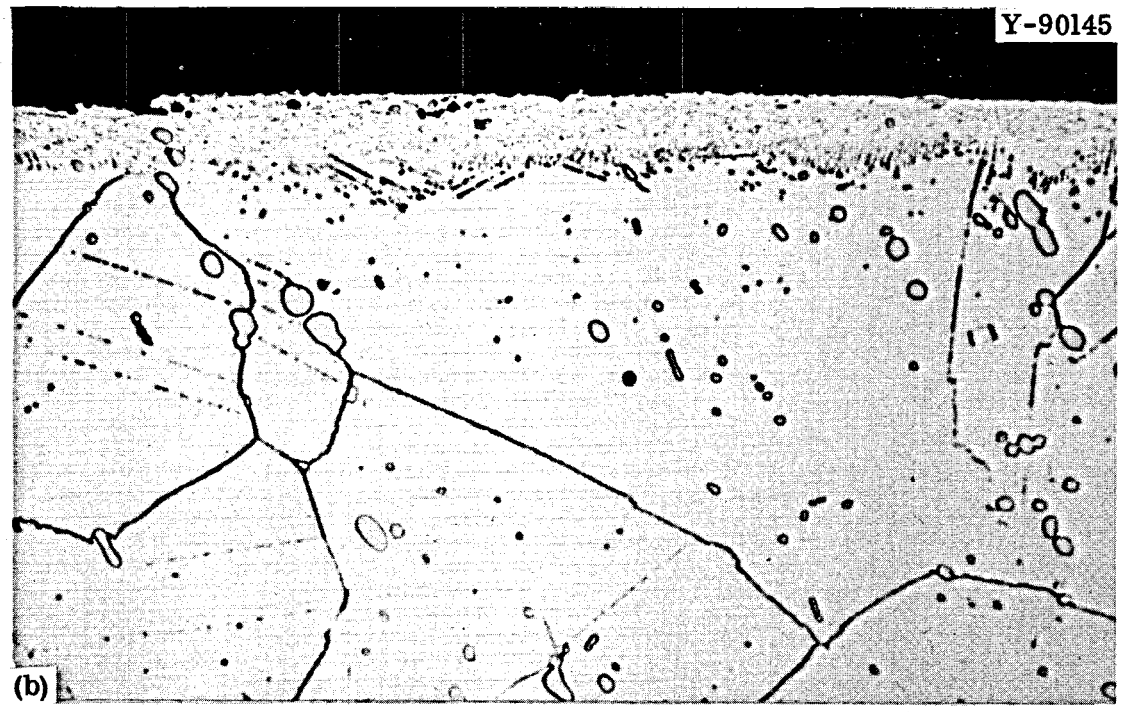

Fig. 6. Photomicrographs of Hastelloy N (Heat 5085) Surveillance Control Specimens Exposed to Static Barren Fuel Salt for 15,289 hr at 650°C. Note the shallow reaction layer near the surface. (a) Etched, 100×. (b) Etched, 500×. Etchant: glyceria regia.

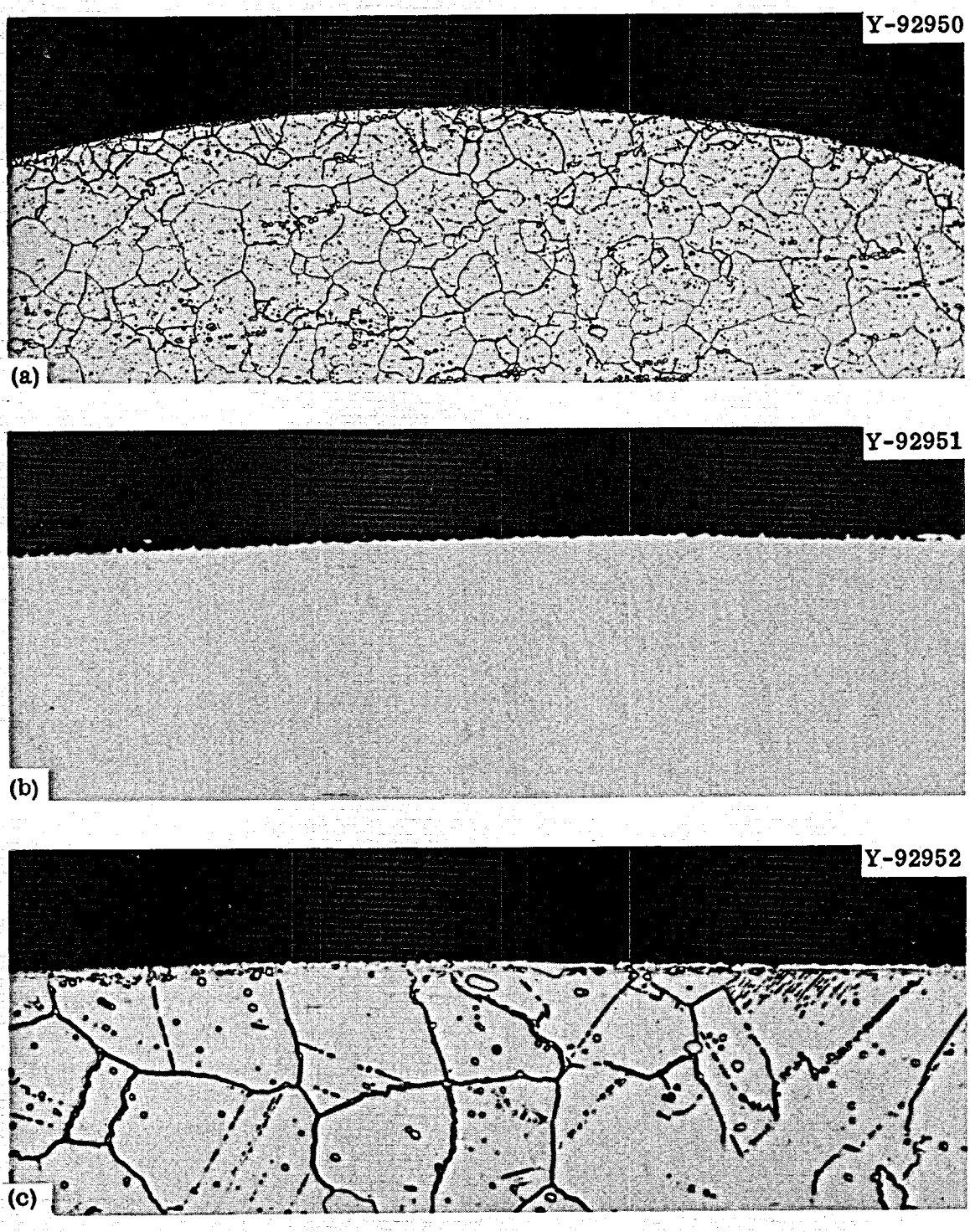

Fig. 7. Photomicrographs of Hastelloy N (Heat 5065) Surveillance Control Specimens Exposed to Static Barren Fuel Salt for 15,289 hr at 650°C. Note the shallow reaction layer near the surface. (a) Etched. 100X. (b) As polished. 500X. (c) Etched. 500X. Etchant: glyceria regia.

Fig. 8. Transmission Electron Photomicrograph of Hastelloy N (Heat 5085) Exposed to the MSRE Core for 15,289 hr at 650°C. The thermal fluence was 9.4×10^{20} neutrons/cm^2, enough to transmute most of the ^{10}B in this material to helium.

Typical photomicrographs of the modified Hastelloy N are shown in Figs. 9 and 10. The grain size in this material is rather large due to the high preirradiation anneal of 1 hr at 1177°C and the absence of the carbide stringers. There is a thin layer on the surface, which has the appearance of being a deposit rather than where material has been removed by corrosion. X-ray studies indicate the presence of iron. Since these alloys contain only trace quantities of iron compared with 4 to 5% for the rest of the material in the MSRE and in the control facility, it is quite reasonable that iron should be deposited on the surfaces of the modified alloys. The general microstructure contains a finely dispersed precipitate with larger amounts along the grain boundaries.

Mechanical Property Data – Standard Hastelloy N

Tensile Properties

The postirradiation tensile properties of heat 5085 after exposure to the cell environment of N_2 + 2 to 5% O_2 for 20,789 hr are given in Table A-1 (Appendix) and the fracture strain is plotted as a function of test temperature in Fig. 11. There are significant reductions in the fracture strain at 25°C and above 500°C. The fracture strain decreased with decreasing strain rate at the elevated temperatures. One particularly interesting observation was that the fracture strain at room temperature could be improved by a postirradiation anneal of 8 hr at 870°C. This anneal is quite often used as a postweld anneal and is sufficient to precipitate (or redissolve) carbides and to relieve residual stresses, but does not cause grain-boundary motion. Thus, the recovery of the room-temperature ductility by this anneal supports the supposition that the reduction in ductility at 25°C is due to carbide precipitation.

The results of tensile tests on heat 5065 after exposure to the MSRE cell environment for 20,789 hr at 650°C are given in Table A-2 (Appendix) and the fracture strain is shown as a function of test temperature in Fig. 12. This heat does not exhibit the reduction in ductility at 25°C, but does show a substantial loss in ductility above 500°C due to irradiation. The effect of strain rate is qualitatively the same as that shown in Fig. 11 for heat 5085, but the scatter in experimental results does not allow a quantitative comparison.

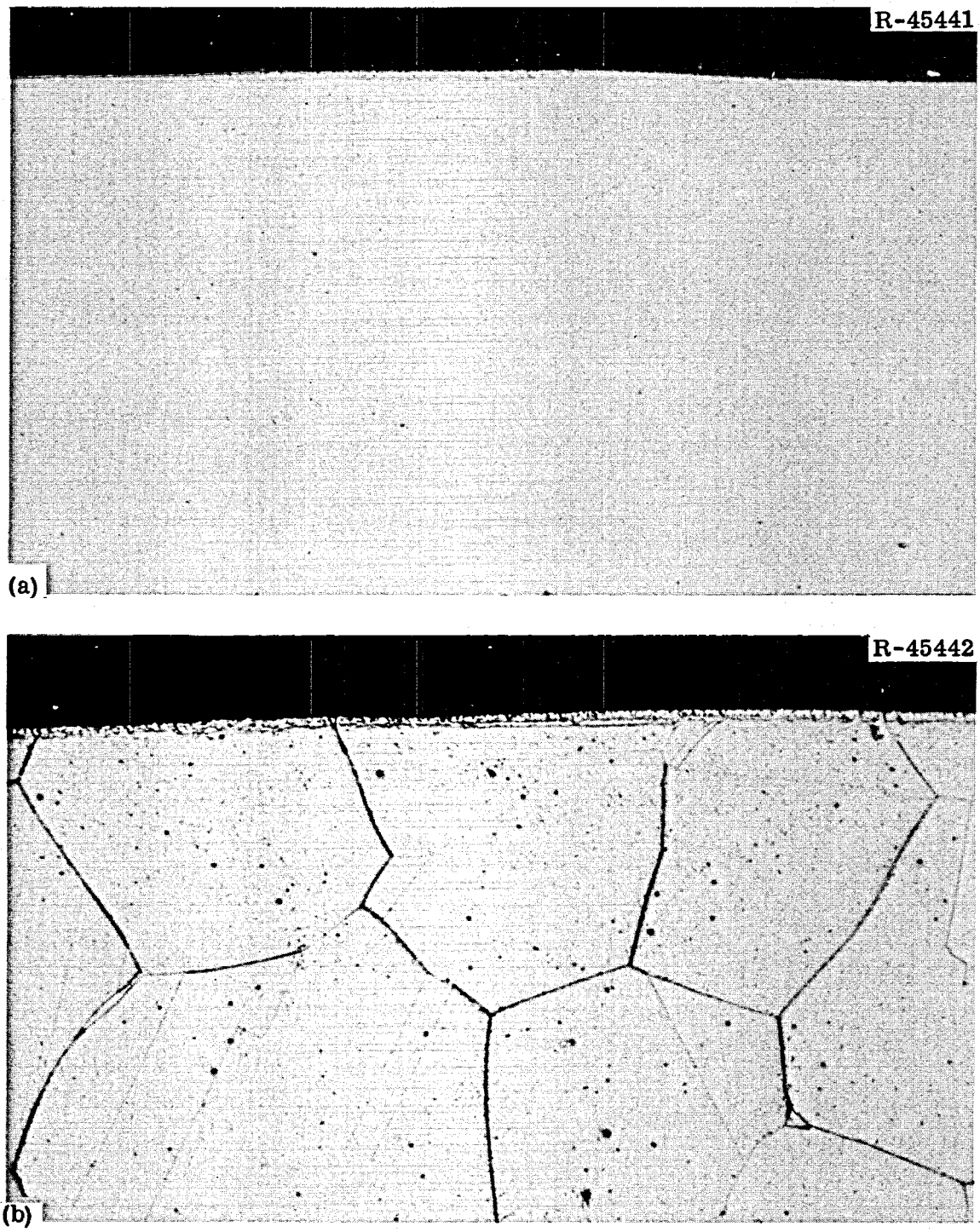

Fig. 9. Photomicrographs of Modified Hastelloy N Containing 2% W and 0.5% Ti (Heat 67-502) After Exposure to the MSRE Core for 9789 hr at 650°C and a Thermal Fluence of 5.3×10^{20} neutrons/cm^2. 500X.
(a) As polished. (b) Etchant: glyceria regia. This structure is also representative of that of a heat of material containing 0.5% Hf (Heat 67-504) that had a similar exposure.

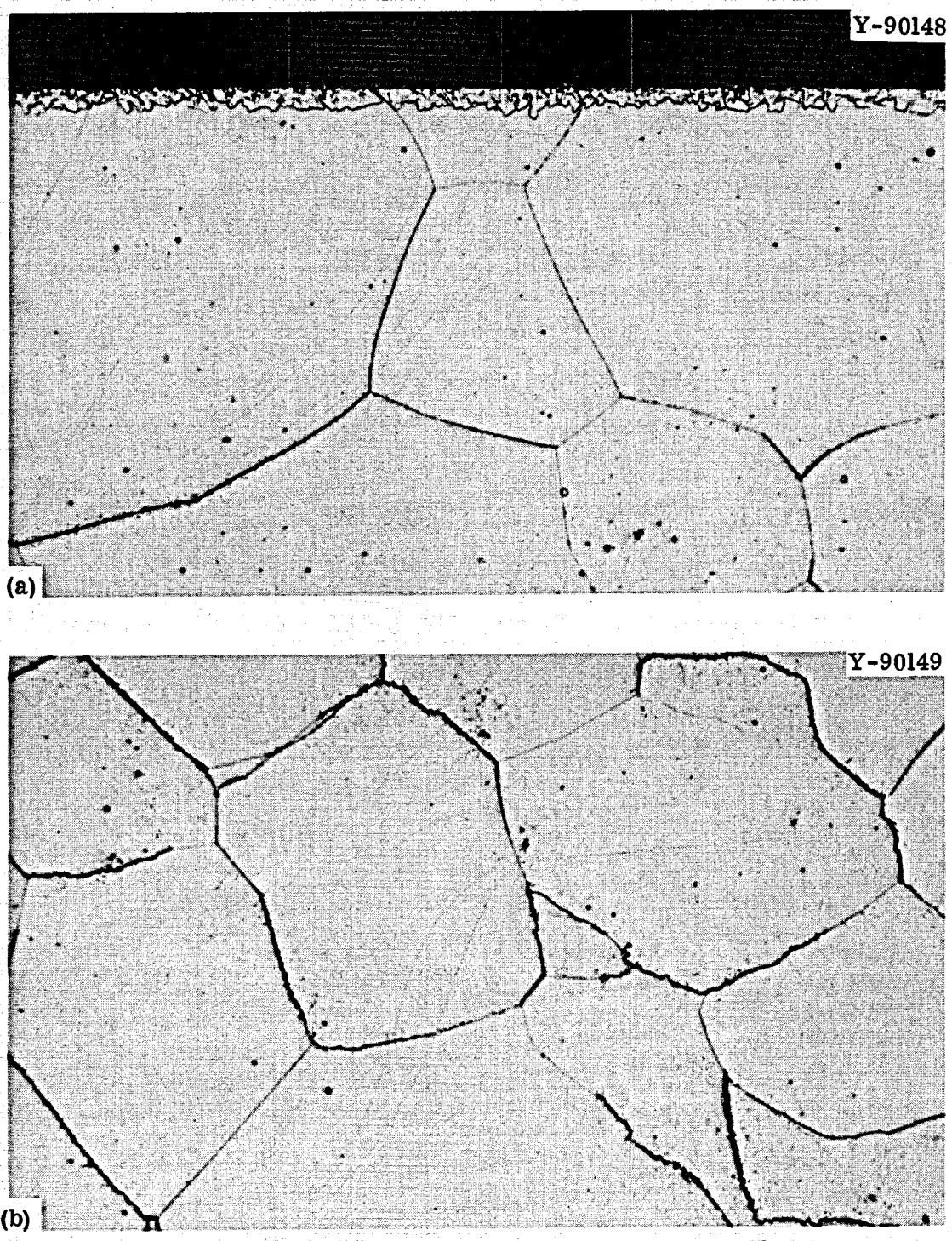

Fig. 10. Photomicrographs of Modified Hastelloy N Containing 2% W and 0.5% Ti (Heat 67-502) After Exposure to Static Barren Fuel Salt for 9789 hr at 650°C. 500×. (a) Edge and (b) typical matrix. Etchant: glyceria regia. This structure is also representative of that of a heat of material containing 0.5% Hf (heat 67-504) that had a similar exposure.

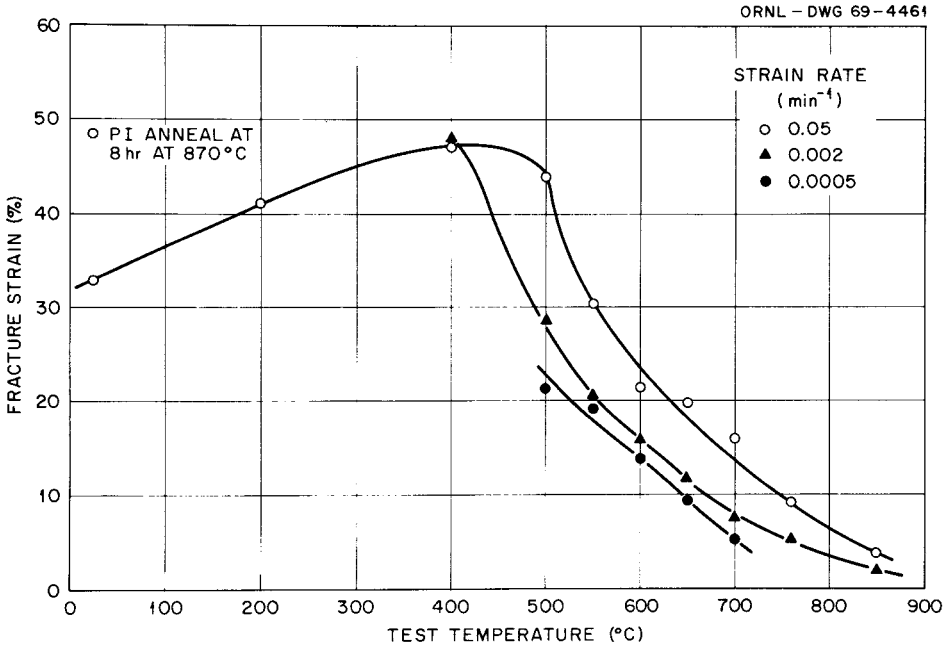

Fig. 11. Postirradiation Tensile Properties of Hastelloy N (Heat 5085) After Irradiation to a Thermal Fluence of 2.6×10^{19} neutrons/cm^2 Over 20,789 hr at 650°C.

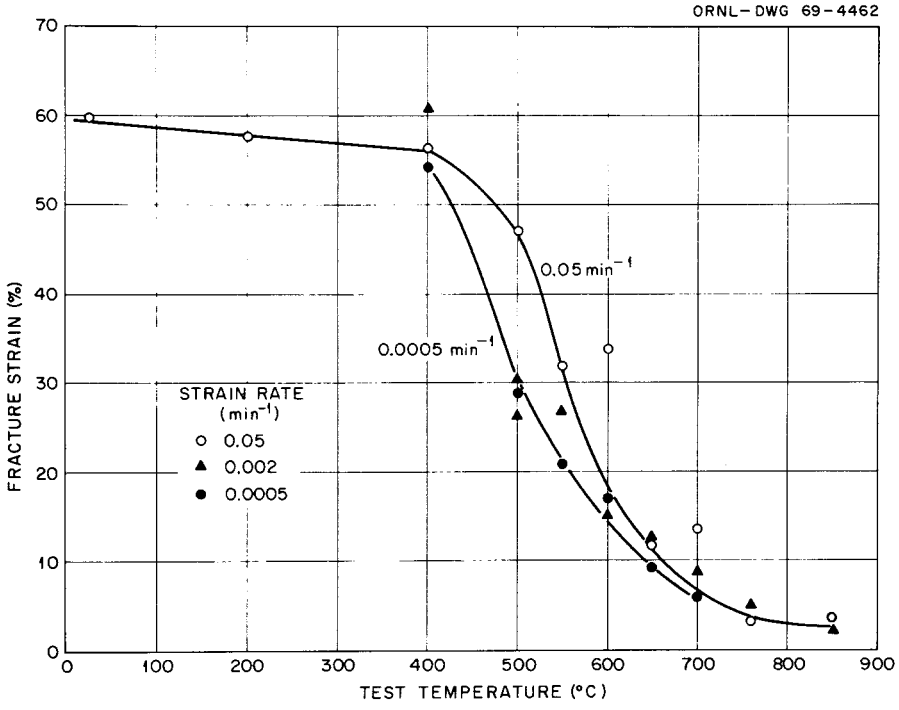

Fig. 12. Postirradiation Tensile Properties of Hastelloy N (Heat 5065) After Irradiation to a Thermal Fluence of 2.6×10^{19} neutrons/cm^2 Over 20,789 hr at 650°C.

Heats 5085 and 5065 were also removed from the core surveillance and control facilities after 15,289 hr of exposure. The detailed tensile data on these specimens are given in Tables A-3 through A-6 (Appendix). The variation of the fracture strain with test temperature is shown in Fig. 13 for heat 5085 after exposure in the core surveillance facility to a thermal fluence of 9.4×10^{20} neutrons/cm^2 and in Fig. 14 for heat 5085 after exposure in the control facility. The irradiated samples (Fig. 13) showed reduced fracture strains compared with the control samples (Fig. 14) over the entire test temperature range studied. Similar plots of the variation of fracture strain with test temperature are shown for heat 5065 after removal from the core surveillance facility (Fig. 15) and the control facility (Fig. 16). There is a slight reduction in the fracture strain at 25°C due to irradiation, but the reduction is not nearly as great as noted for heat 5085 (Fig. 13). The fracture strain of heat 5065 is reduced above 500°C by irradiation, and the resulting strains are lower than those for heat 5085 (Fig. 13). For example, at a test temperature of 650°C and a strain rate of 0.002 min^{-1} heat 5085 (Fig. 13) fractures at a strain of 5% and heat 5065 (Fig. 15) fractures at 3.5%. The unirradiated samples from the control facility show a greater reduction in fracture strain for heat 5085 (Fig. 14) than for heat 5065 (Fig. 16) at 25°C, but the fracture strains at 650°C are not appreciably different for the two heats.

Heat 5085 has been carried throughout our surveillance program, so we now have accumulated enough data to see how the fracture strain is varying with neutron fluence. The fracture strain is shown as a function of test temperature in Fig. 17 for heat 5085. Generally, the fracture strain is decreased with increasing fluence. At low fluence the ductility reduction at low test temperatures is restricted to 25°C and recovers at higher test temperatures, but at higher fluences the fracture strain is reduced over a wider temperature range. We attribute this embrittlement to carbide precipitation and, as shown in Fig. 11, the ductility can be recovered by postirradiation annealing. The ductility reduction above 500°C is associated with the presence of helium and the increased tendency for intergranular fracture. The fracture strain at a given temperature above 500°C generally decreases with increasing thermal fluence.

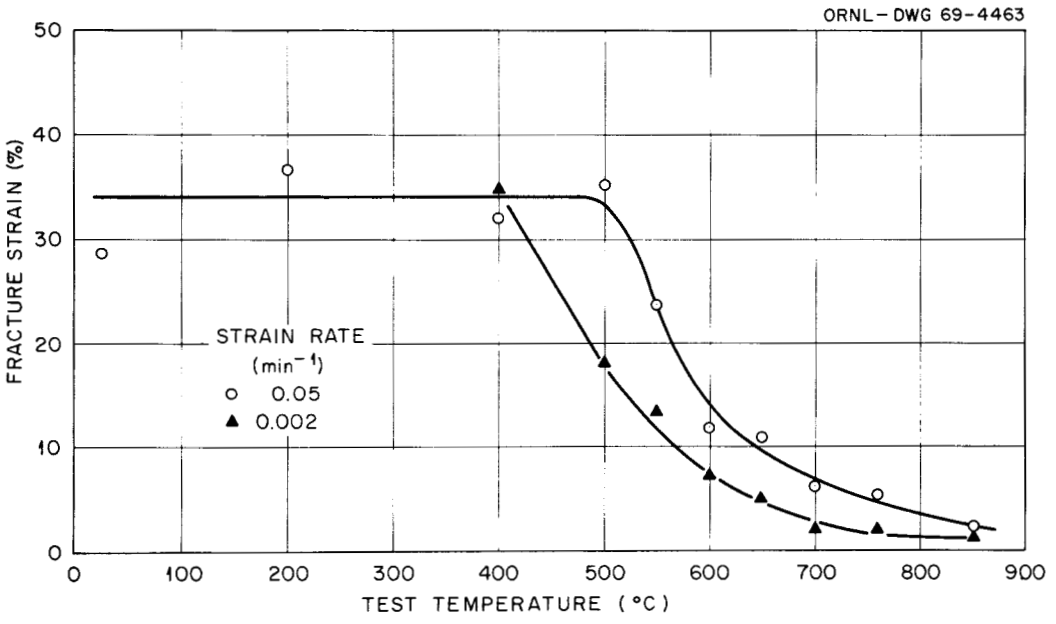

Fig. 13. Postirradiation Tensile Properties of Hastelloy N (Heat 5085) After Irradiation to a Thermal Fluence of 9.4×10^{20} neutrons/cm^2 Over 15,289 hr at 650°C.

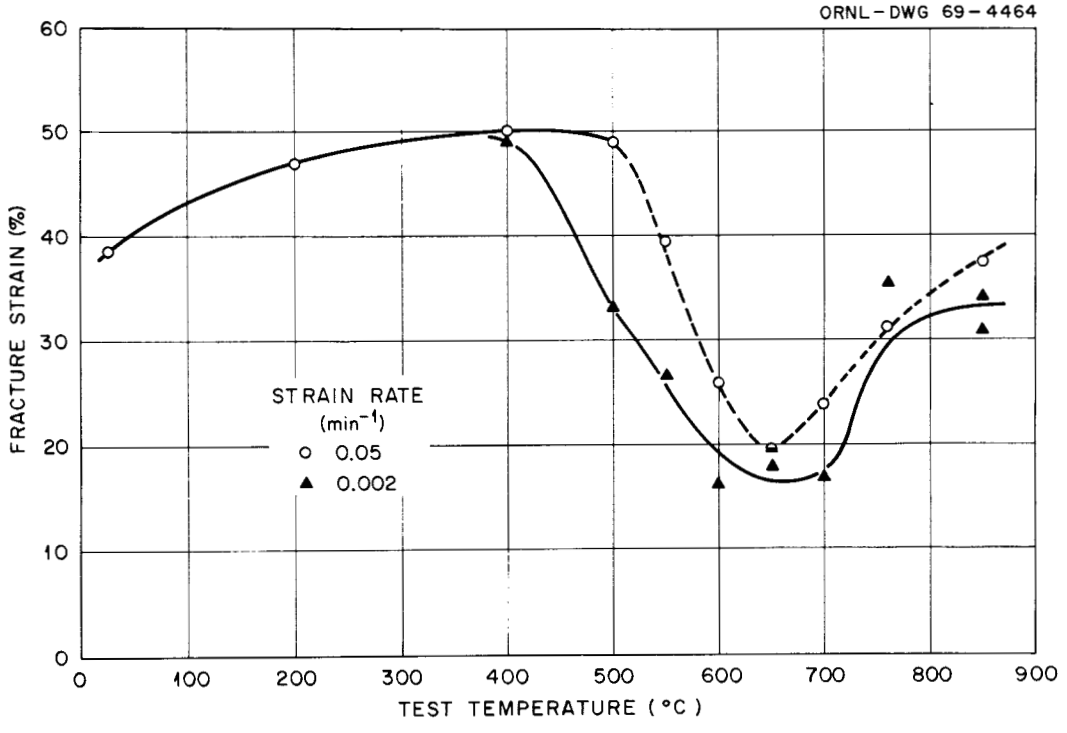

Fig. 14. Tensile Properties of Hastelloy N (Heat 5085) After Aging for 15,289 hr at 650°C in Static Barren Fuel Salt.

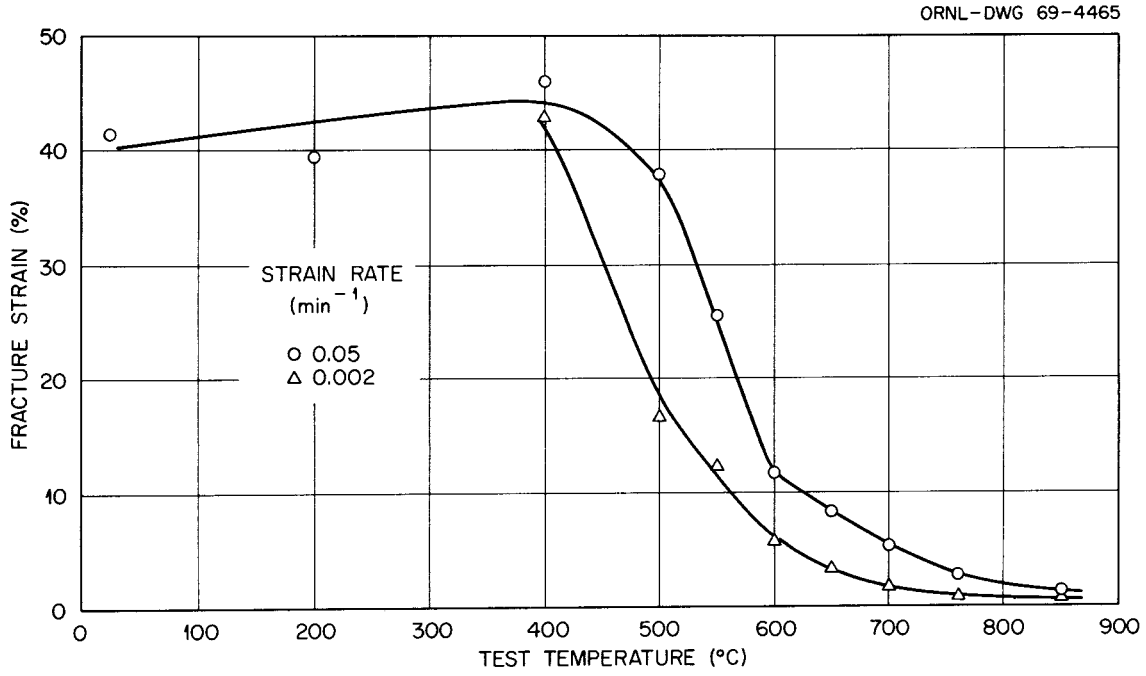

Fig. 15. Postirradiation Tensile Properties of Hastelloy N (Heat 5065) After Irradiation to a Thermal Fluence of 9.4×10^{20} neutrons/cm^2 Over 15,289 hr at 650°C.

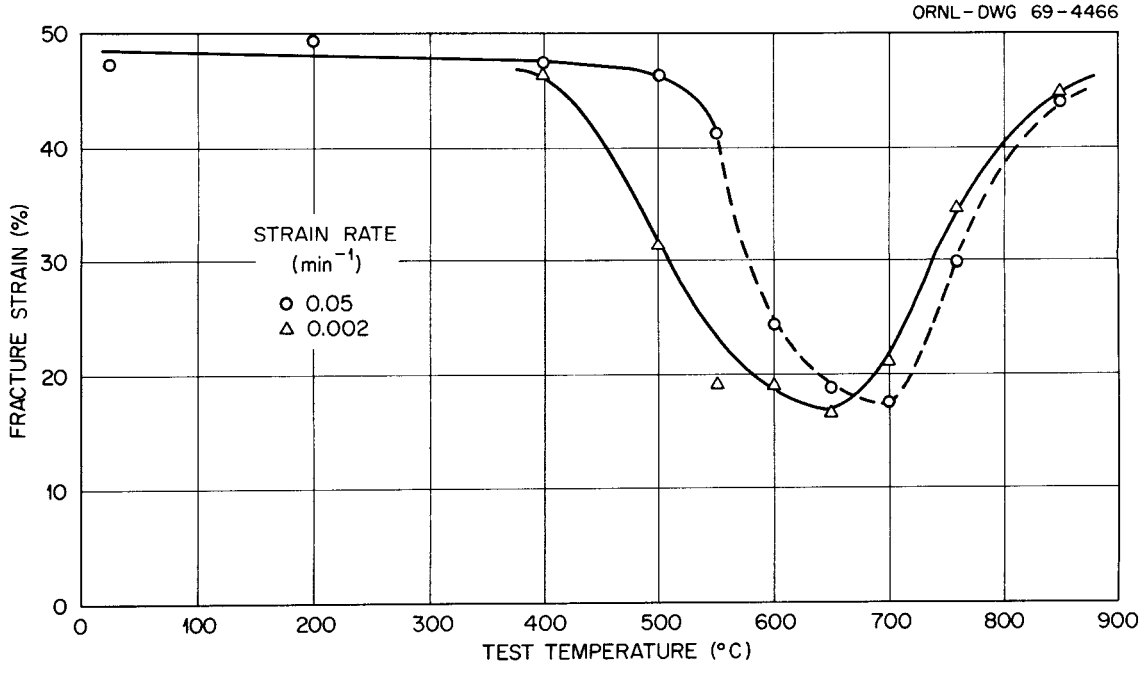

Fig. 16. Tensile Properties of Hastelloy N (Heat 5065) After Aging for 15,289 hr at 650°C in Static Barren Fuel Salt.

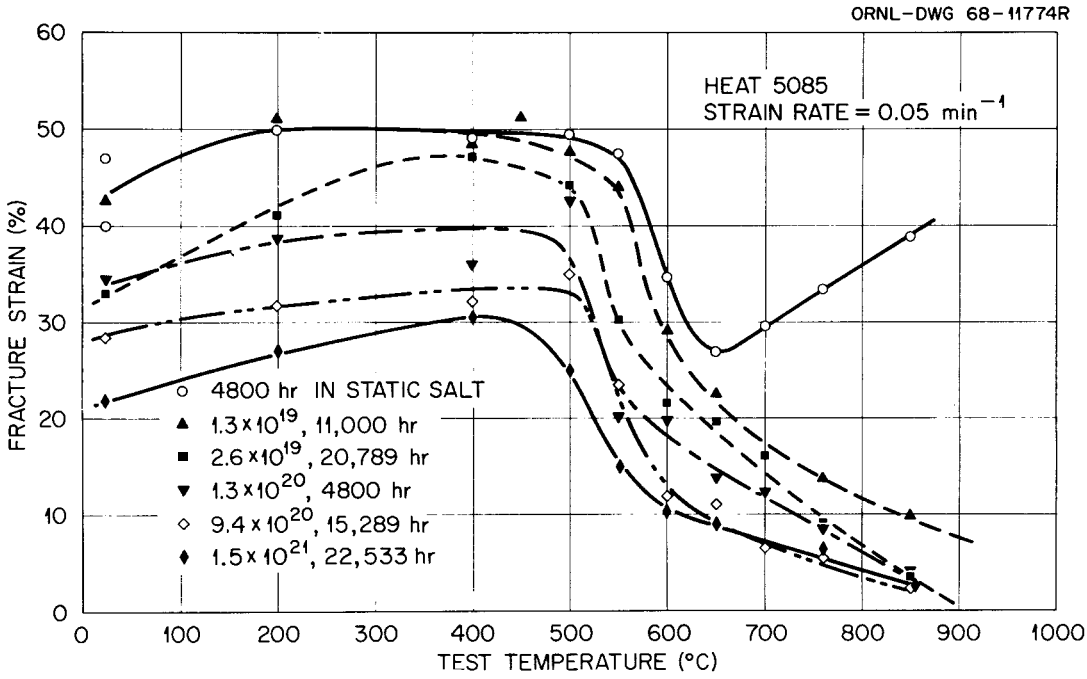

Fig. 17. Postirradiation Tensile Properties of MSRE Surveillance Samples.

The fracture strains for heat 5085 at a slower strain rate, 0.002 min^{-1}, are shown in Fig. 18. The behavior as a function of fluence is similar to that shown in Fig. 17 at a higher strain rate. An important exception is the observation that as the test temperature is increased, the fracture strain depends on fluence to a lesser extent.

One very important question that arises is "How much of the reduction in fracture strain in Fig. 17 can be attributed to thermal aging?" Several of the tensile results obtained on samples from the control facility are shown in Fig. 19. The results show generally that the fracture strain is reduced at all test temperatures by aging at 650°C. However, the reductions in fracture strain due to aging do not account for nearly all the reduction noted for irradiated samples. For example, the fracture strains at test temperatures of 25 and 650°C are 53.0 and 33.6% for as-annealed samples, 38.6 and 19.6% after aging for 15,289 hr at 650°C (Fig. 19), and 28.5 and 11.0% after irradiation to a fluence of 9.4×10^{20} neutrons/cm^2 over a period of 15,289 hr at 650°C. We do not have as much data on the response of heat 5065 to aging, but a

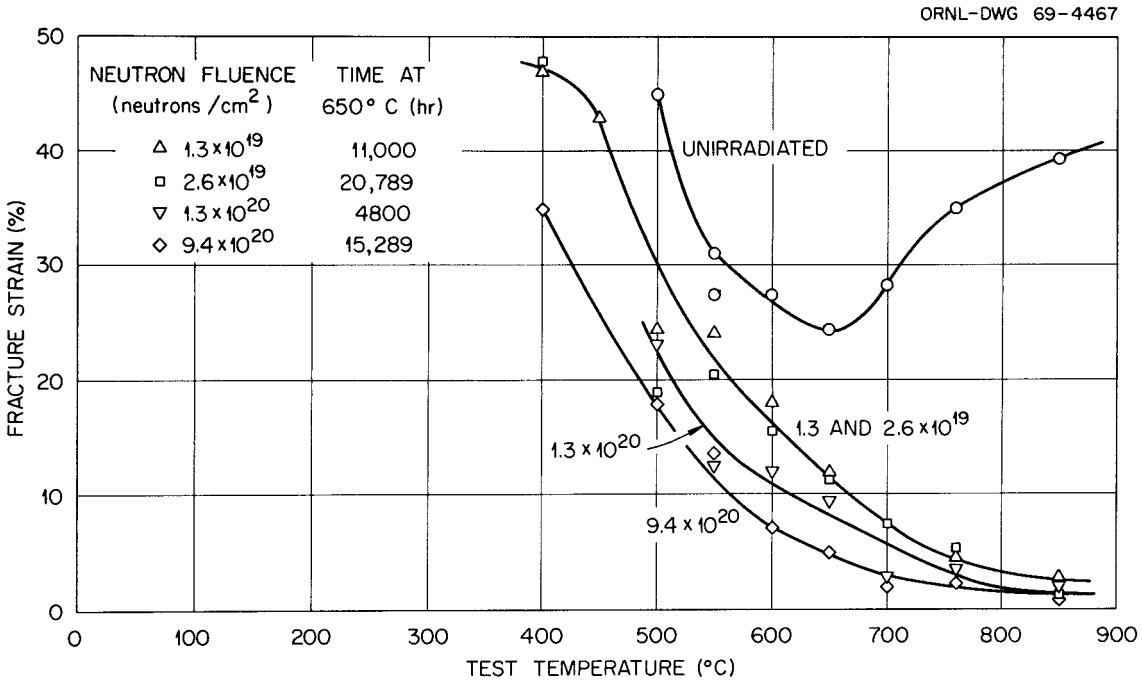

Fig. 18. Postirradiation Tensile Properties (Strain Rate of 0.002 min^{-1}) of Hastelloy N (Heat 5085) After Exposure to Various Neutron Fluences.

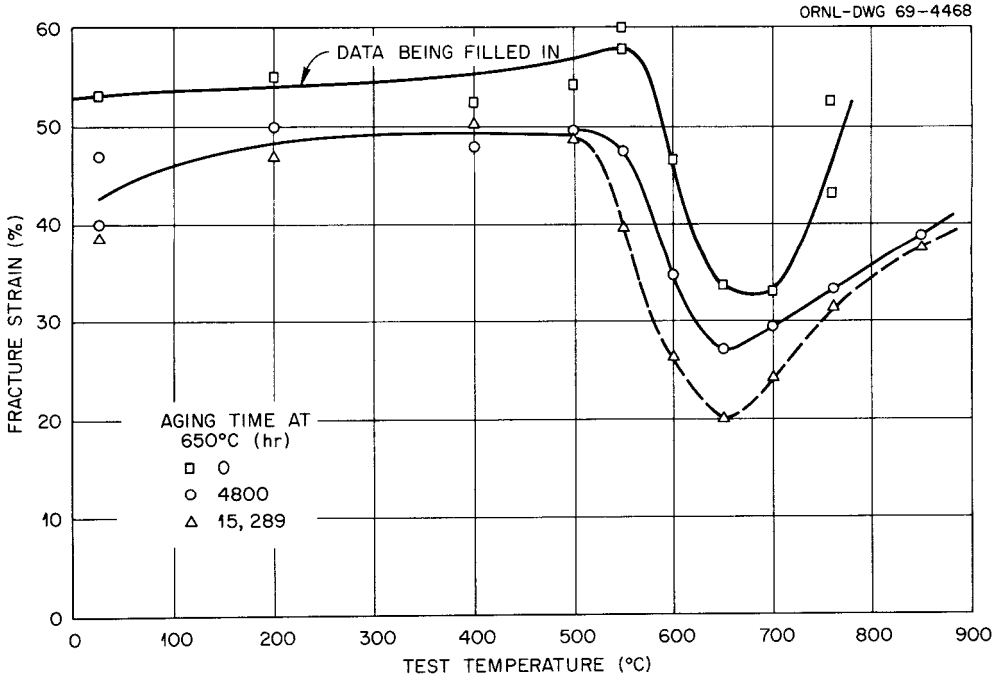

Fig. 19. Variation of the Tensile Properties (Strain Rate of 0.5 min^{-1}) of Hastelloy N (Heat 5085) with Aging Time in Barren Fuel Salt at 650°C.

comparison of Figs. 14 and 16, pp. 22 and 23, of the fracture strain for heats 5065 and 5085 after aging for 15,289 hr at 650°C indicates very similar properties of the two heats at 650°C and higher fracture strain for heat 5065 at 25°C.

The combined observations on the change in the fracture strain at a test temperature of 25°C are shown in Fig. 20. The results are plotted as if aging time were the controlling variable, and the results on the unirradiated samples (open symbols) indicate that aging time is an important factor. However, for the cases where irradiated and unirradiated samples were tested after similar thermal histories, the irradiated samples showed the larger reduction in fracture strain. Thus, neutron fluence as well as time at temperature are important factors in the reduction of the fracture strain at low temperatures. The question of whether the role of irradiation is to produce defects that enhance the growth rates of precipitates or to produce transmutation products that aid in stabilizing a precipitate nucleus yet remains unanswered. The data shown for heat 5065 in Fig. 20 indicate that this material is less susceptible to this type of embrittlement than heat 5085.

Creep-Rupture Properties

Some of the samples were tested under creep conditions at 650°C. The detailed results of these experiments are presented in Tables A-7 through A-9 (Appendix) and some correlations of these results with those obtained from previous surveillance samples[7,8] will be presented.

A stress-rupture plot for heat 5085 is shown in Fig. 21. The results obtained on the unirradiated samples show that the rupture life is reduced slightly by prolonged aging at 650°C, the magnitude of the effect decreasing with decreasing stress level. The rupture life is decreased markedly by irradiation even at thermal fluences as low as

---

[7]H. E. McCoy, An Evaluation of the Molten-Salt Reactor Experiment Hastelloy N Surveillance Specimen – First Group, ORNL-TM-1997 (November 1967).

[8]H. E. McCoy, An Evaluation of the Molten-Salt Reactor Experiment Hastelloy N Surveillance Specimen – Second Group, ORNL-TM-2359 (February 1969).

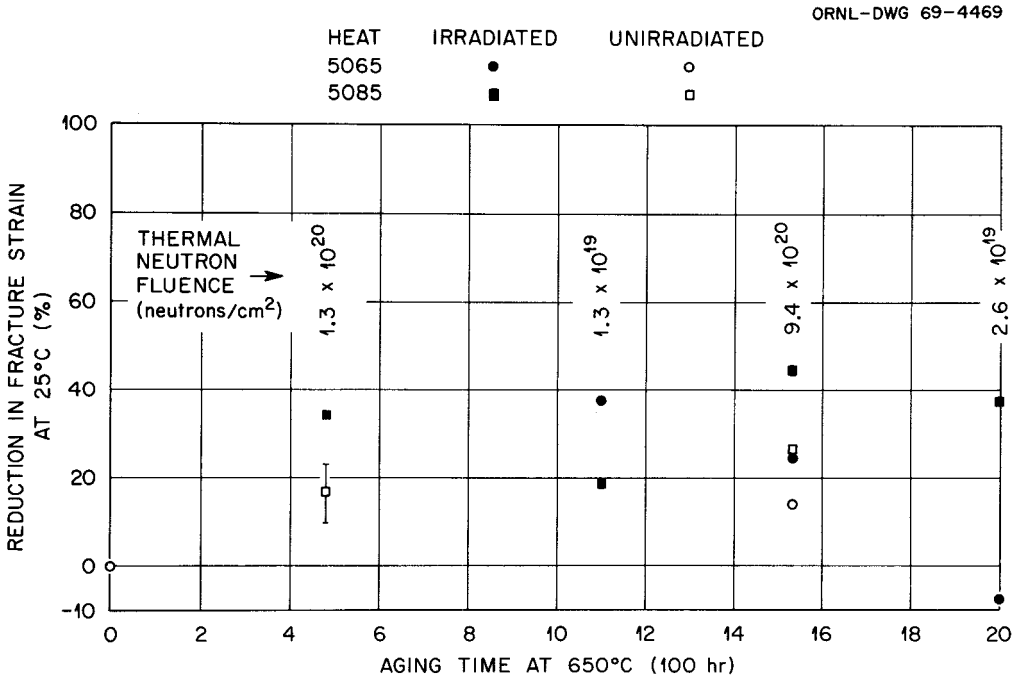

Fig. 20. Variation of the Fracture Strain at 25°C with Aging and Irradiation.

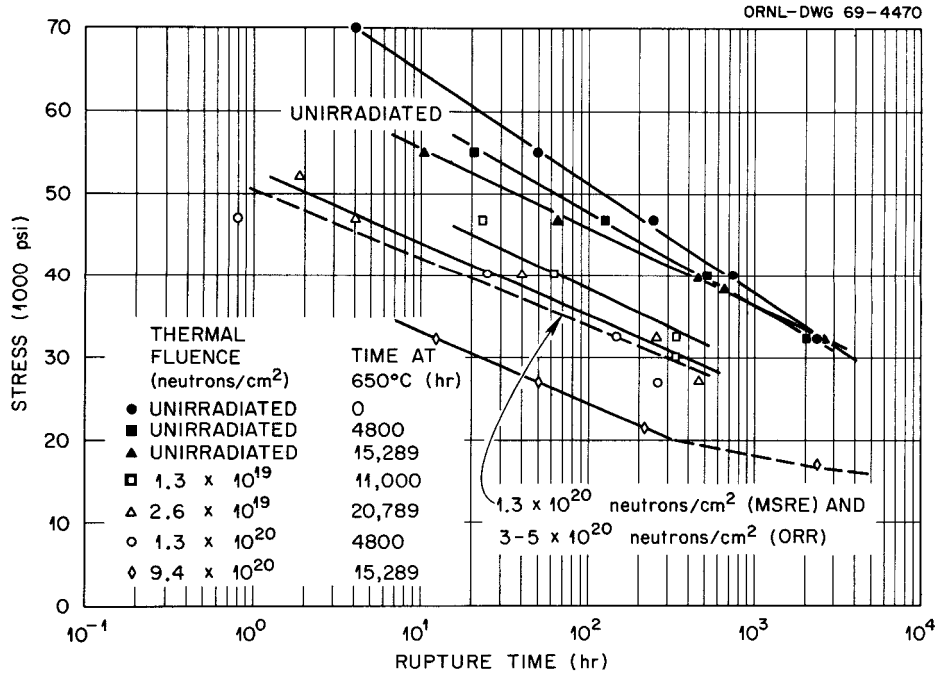

Fig. 21. Postirradiation Stress Rupture Properties of MSRE Surveillance Specimens (Heat 5085) at 650°C.

1.3×10^{19} neutrons/cm^2. The rupture life is reduced progressively by increasing fluence with a large step occurring between fluences of 1.3 and 9.4×10^{20} neutrons/cm^2.

The minimum creep rate is shown as a function of stress level in Fig. 22 for these same samples from heat 5085. The results on unirradiated samples show that the creep rate is increased slightly at high stress levels by prolonged aging at 650°C. A few irradiated samples tested at high stress levels and the samples irradiated to 9.4×10^{20} neutrons/cm^2 have a higher minimum creep rate. This is likely due to the tests being so short and the fracture strains so low that the steady-state creep period (the period in which the minimum creep rate usually occurs) was not reached and the rate that we measured was too high. However, generally at lower stress levels irradiation and aging seem to have little effect on the minimum creep rate.

The fracture strains are shown as a function of minimum creep rate in Fig. 23 for the irradiated samples of heat 5085. The scatterband shown in this figure was determined from numerous tests on samples of these same heats of standard Hastelloy N that had been irradiated in the Oak Ridge Research Reactor (ORR) to thermal fluences of 2 to 5×10^{20} neutrons/cm^2. In samples removed from the MSRE the fracture strain was decreased from about 20% for unirradiated material to about 2.3% by a thermal fluence of 1.3×10^{19} neutrons/cm^2. Progressively higher fluences reduced the fracture strain even further. The limited number of data points for each lot of material do not give a very strong indication of the very distinct ductility minimum noted in our ORR irradiations. This may be associated with the much larger times involved in the MSRE irradiations (5000 to 20,000 hr) compared with those in the ORR (1000 hr).

The effects of aging in the absence of irradiation on the fracture strain of heat 5085 at 650°C are shown in Fig. 24. After annealing for 2 hr at 900°C the fracture strain is 30 to 40%, almost independent of strain rate. After aging for 4800 hr at 650°C the fracture strains are now in the range of 20 to 30%. Aging for 15,289 hr causes a small further reduction in the fracture strain at high strain rates, but no significant change in the fracture strain at low strain rates. Thus, the

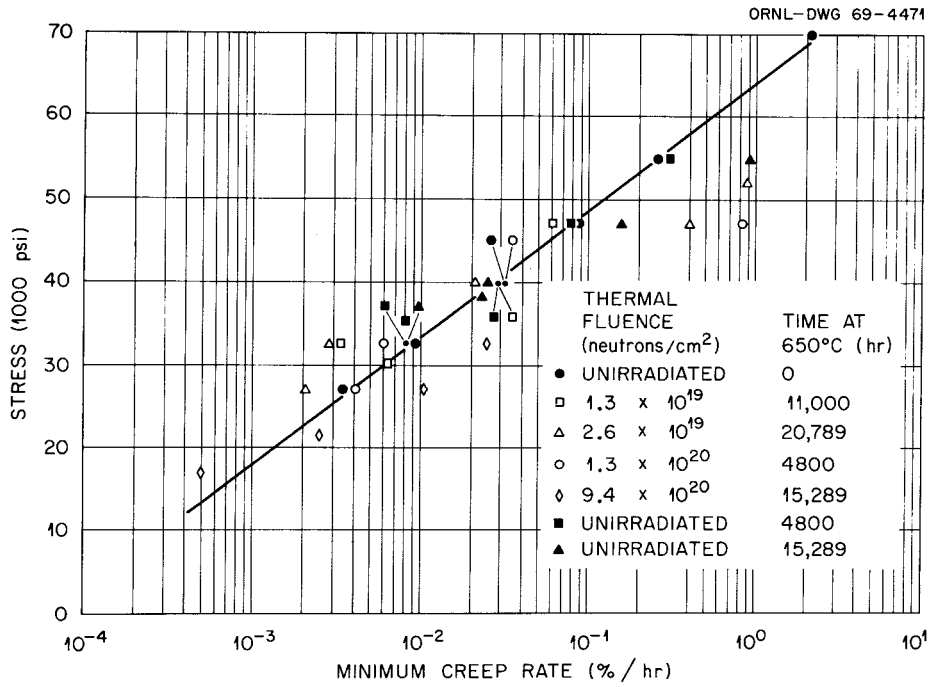

Fig. 22. Minimum Creep Rate of Hastelloy N (Heat 5085) Surveillance Specimens from MSRE at 650°C.

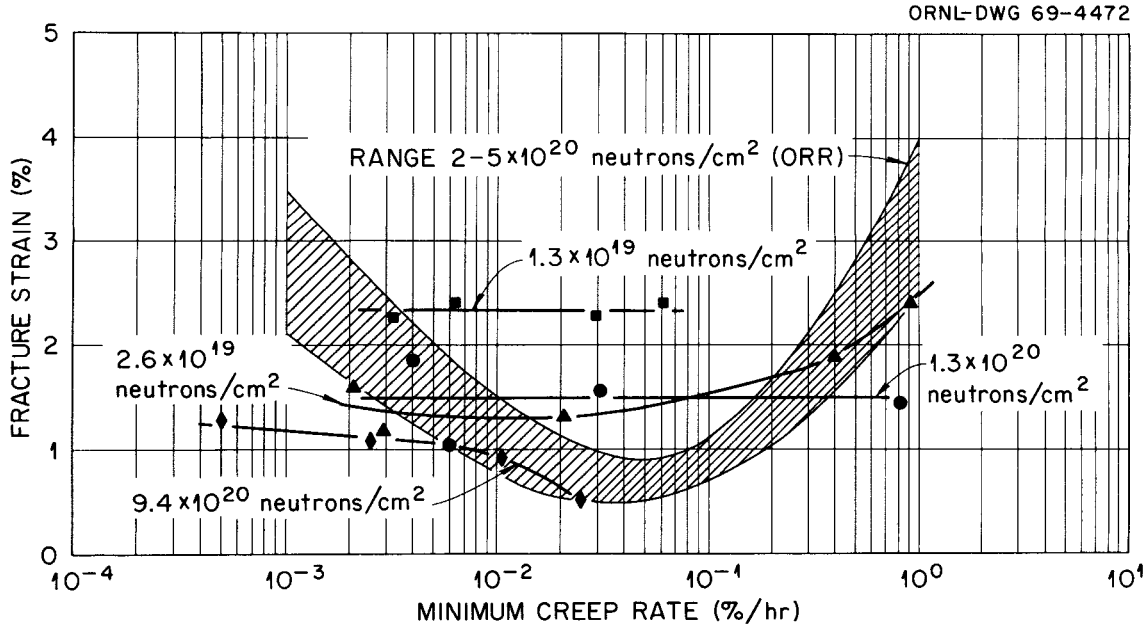

Fig. 23. Variation of Fracture Strain with Strain Rate for Hastelloy N (Heat 5085) Surveillance Specimens at 650°C.

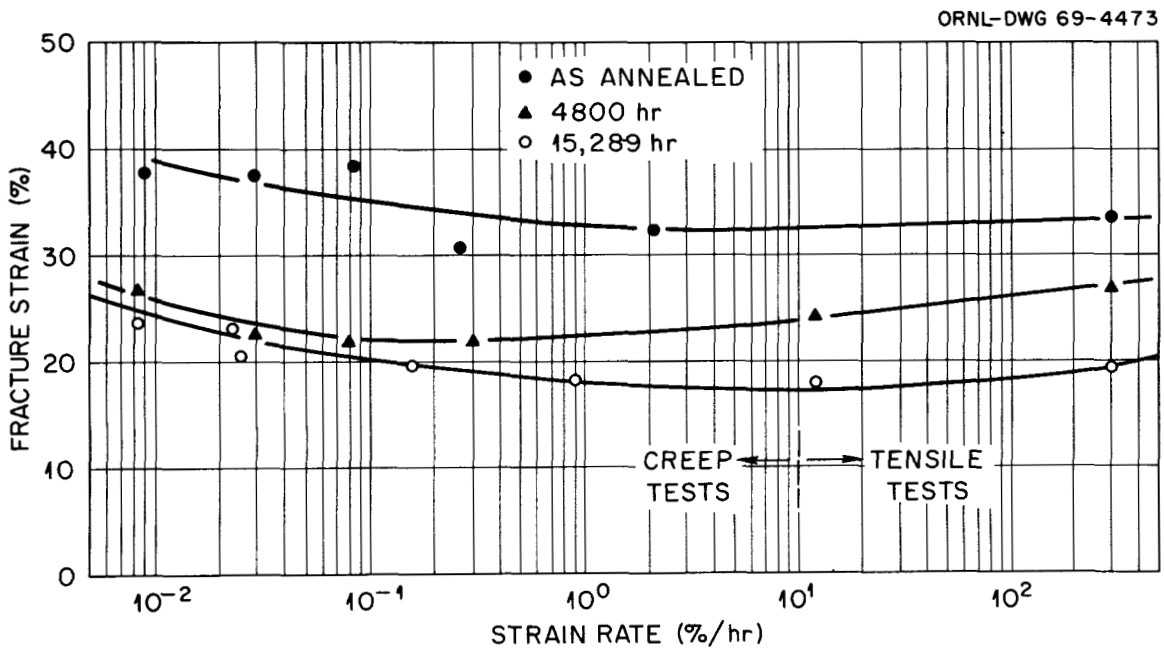

Fig. 24. Influence of Aging at 650°C on the Fracture Strain of Hastelloy N (Heat 5085) When Tested at 650°C.

fracture strain in a sample strained at a rate of 0.1%/hr at 650°C is about 20% for heat 5085 after aging 15,289 hr at 650°C (Fig. 24) and only 0.5% (Fig. 23) after a thermal fluence of 9.4×10^{20} neutrons/cm^2.

The results of our stress-rupture tests on heat 5065 are summarized in Fig. 25. Contrary to the behavior of heat 5085 (Fig. 21), thermal aging seems to have no effect on the creep-rupture properties of heat 5065. However, the rupture life is reduced appreciably by irradiation and the resulting lifetimes at a given stress are quite comparable for heats 5065 and 5085.

The minimum creep rate is shown as a function of stress level for heat 5065 in Fig. 26. The minimum creep rate is increased slightly by thermal aging at 650°C. The creep rates seem to be high for some of the irradiated samples, but this is likely associated with the fracture strain being so low that the minimum creep rate was not established.

The variation of fracture strain with minimum creep rate for the irradiated samples of heat 5065 is shown in Fig. 27. The ductility of this heat is about the same as that shown in Fig. 23 for heat 5085, except for the material irradiated to a thermal fluence of

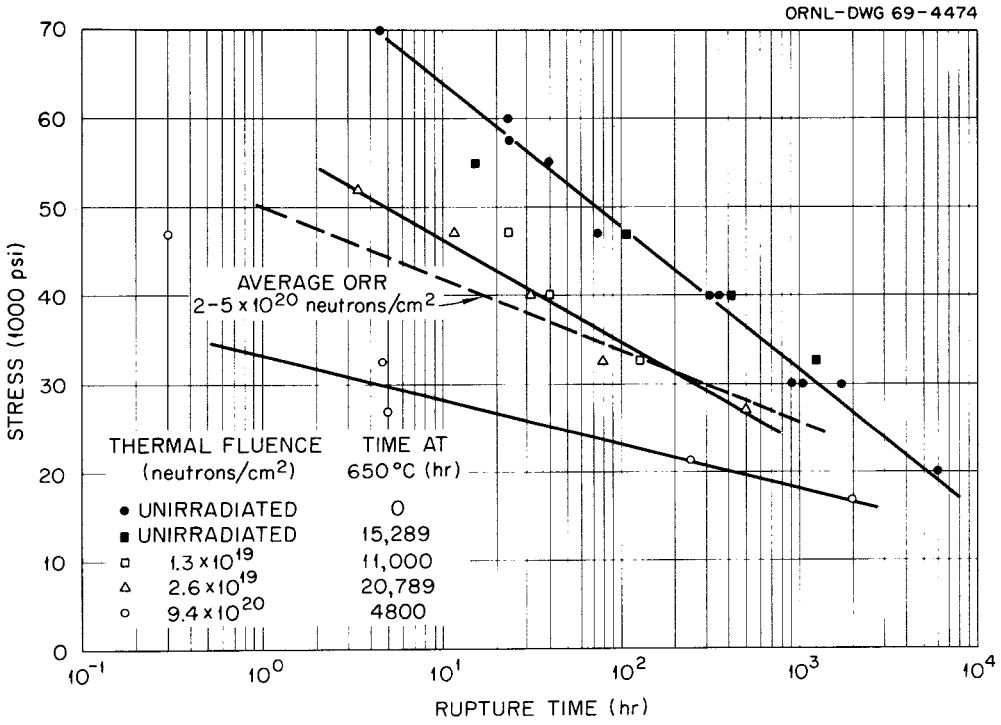

Fig. 25. Stress Rupture Properties of MSRE Surveillance Specimens (Heat 5065) at 650°C.

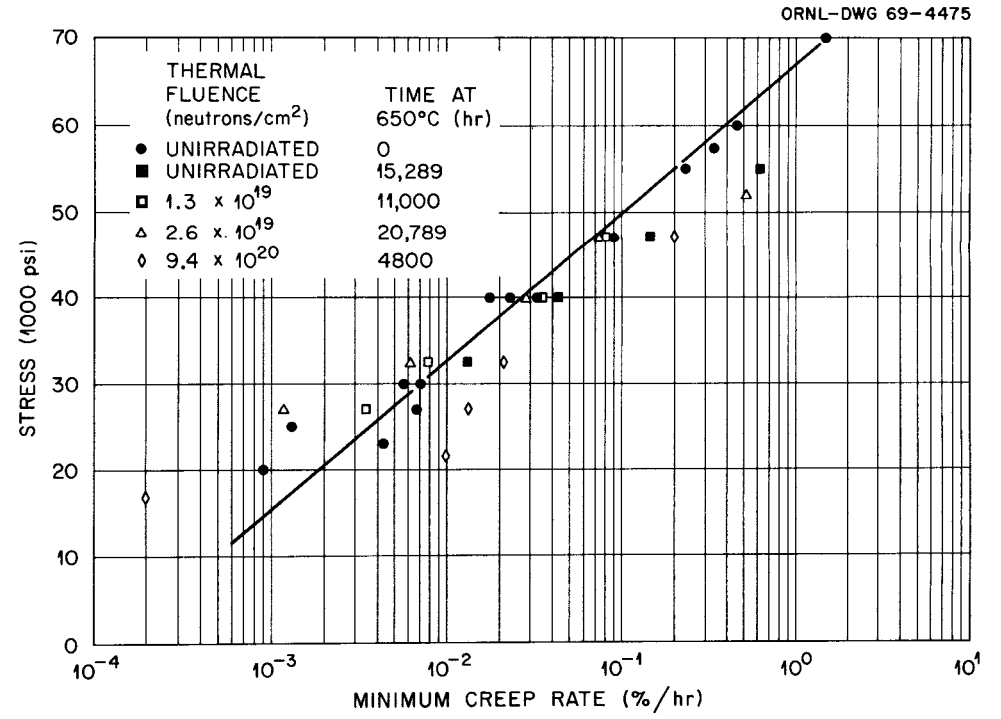

Fig. 26. Minimum Creep Rate of Hastelloy N (Heat 5065) Surveillance Samples from MSRE at 650°C.

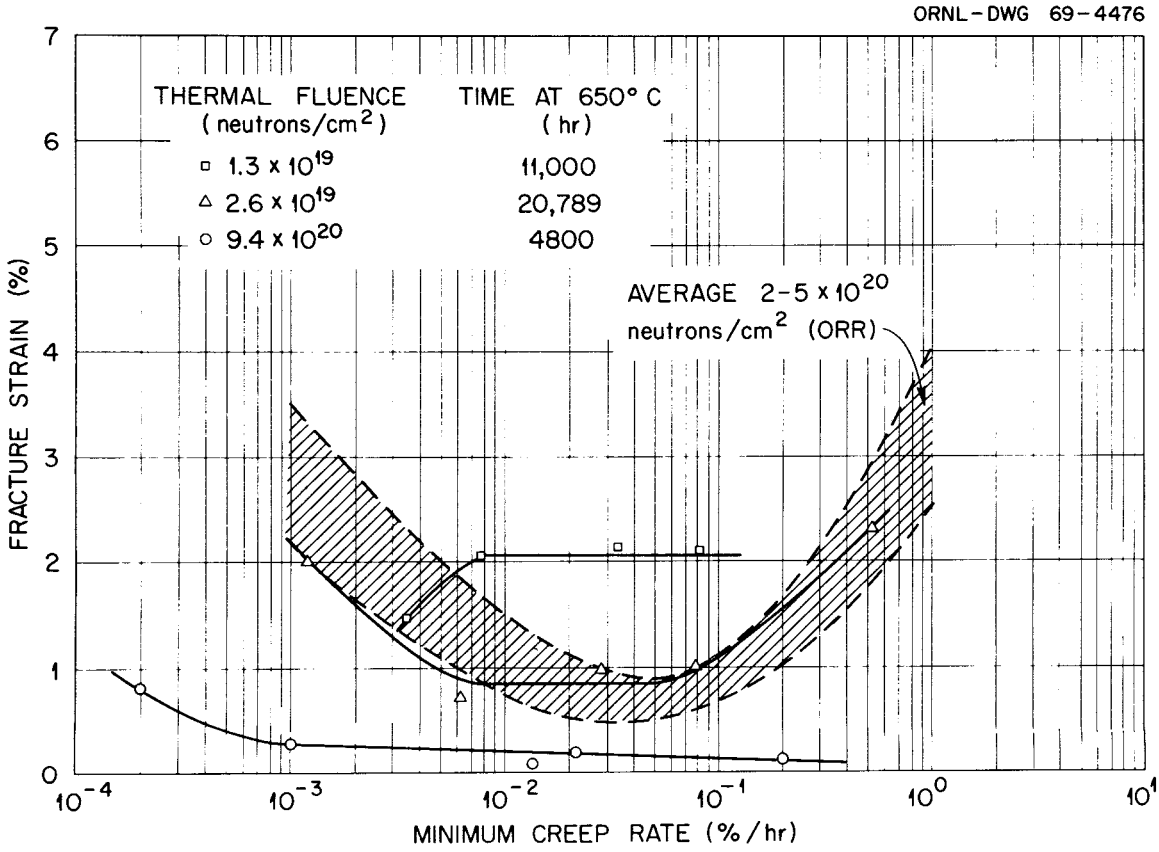

Fig. 27. Variation of Fracture Strain with Strain Rate for Hastelloy N (Heat 5065) Surveillance Specimens at 650°C.

9.4×10^{20} neutrons/cm^2 for which heat 5065 has much lower fracture strains.

Our observations on the variation of fracture strain of surveillance specimens with strain rate are summarized in Fig. 28. Data are included in this figure for both tensile and creep tests. The scatterband based on our observations on samples irradiated in the ORR is also shown in Fig. 28 (ref. 9). The fracture strain varies widely with fluence at high strain rates and varies much less at low strain rates. At low strain rates, the fracture strains for the samples irradiated to 1.3×10^{19} neutrons/cm^2 fall above the scatterband and those for samples irradiated to 9.4×10^{20} neutrons/cm^2 fall below the scatterband.

---

[9]H. E. McCoy, "Variation of the Mechanical Properties of Irradiated Hastelloy N with Strain Rate," J. Nucl. Mater. 31(1), 67–85 (May 1969).

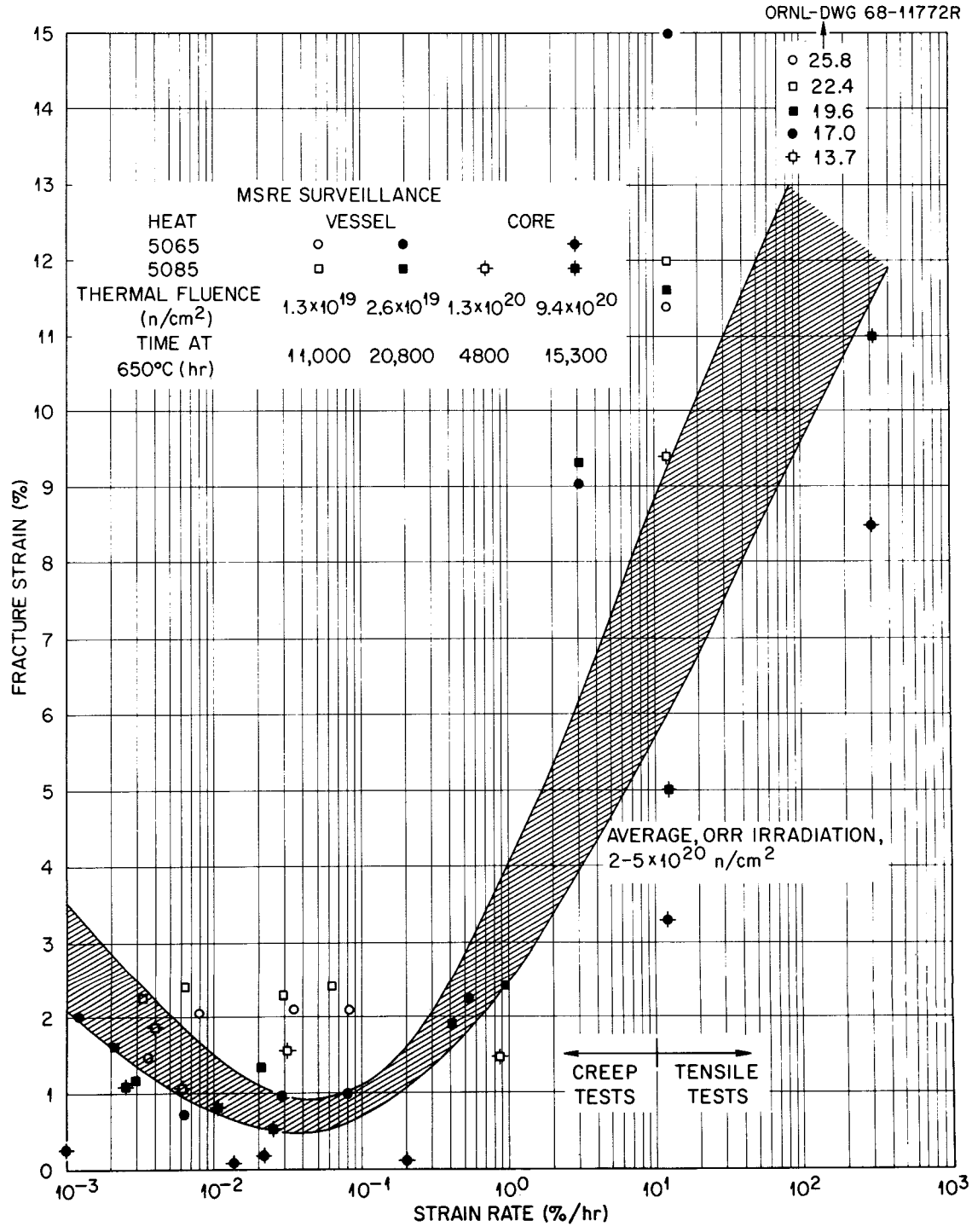

Fig. 28. Variation of Fracture Strain with Strain Rate for Hastelloy N Surveillance Specimens at 650°C.

Mechanical Property Data — Modified Hastelloy N

Tensile Properties

Two heats of modified Hastelloy N (Table 1, p. 4) were included in both the core surveillance facility and the control facility. Heat 67-502 contained a nominal 0.5% Ti and 2% W and heat 67-504 contained a nominal addition of 0.5% Hf. These samples were exposed to salt 9789 hr at 650°C and those in the MSRE received a thermal neutron fluence of 5.3×10^{20} neutrons/cm^2. The detailed results of tensile tests on these materials are given in Tables A-10 through A-13 (Appendix).

The fracture strains at a strain rate of 0.05 min^{-1} are compared in Fig. 29 for the modified alloys. In the unirradiated condition, heat 67-502 had higher fracture strains than heat 67-504 up to about 600°C where the opposite trend was noted. The shapes of these curves are different from those shown in Figs. 14 and 16, pp. 22 and 23, for the standard alloy. The fracture strain of the standard alloy decreases rapidly with increasing temperature above about 500°C and a ductility minimum occurs at about 650°C. For the modified alloys, the fracture strain does not begin to decrease with temperature until about 600°C and the strain continues to decrease up to 850°C, the highest temperature investigated. The fracture strains of the modified alloys after irradiation, also shown in Fig. 29, are reduced at temperatures above about 500°C. Both alloys have about the same fracture strains, and a comparison with Fig. 17, p. 24, shows that the modified alloys irradiated to 5.3×10^{20} neutrons/cm^2 have better fracture strains than those of the standard alloy irradiated to 1.3×10^{19} neutrons/cm^2. One test indicates that the fracture strain of heat 67-504 at 25°C may be reduced by irradiation. This will have to be checked further.

The fracture strains observed in tensile tests at a strain rate of 0.002 min^{-1} for heat 67-502 and -504 are shown in Fig. 30. The postirradiation properties of the two heats are about the same and, although reduced considerably by irradiation, they are much better than those shown in Fig. 18, p. 25, for standard Hastelloy N.

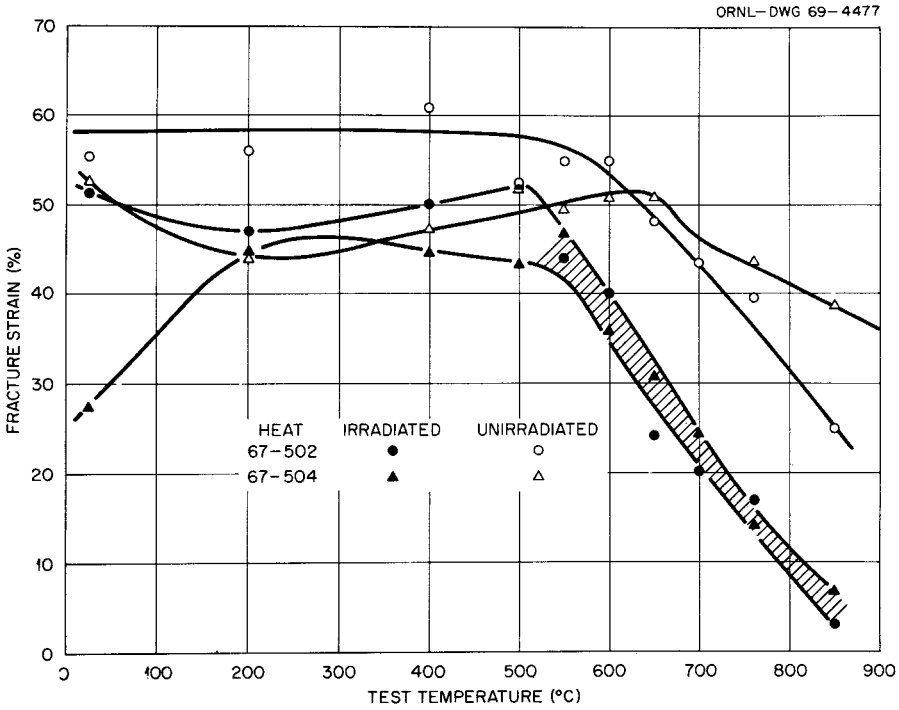

Fig. 29. Tensile Properties (Strain Rate of 0.05 min^{-1}) of Two Compositions of Modified Hastelloy N Following Irradiation (Thermal Fluence of 5.3×10^{20} neutrons/cm^2) or Annealing (Control Samples) for 9789 hr at 650°C.

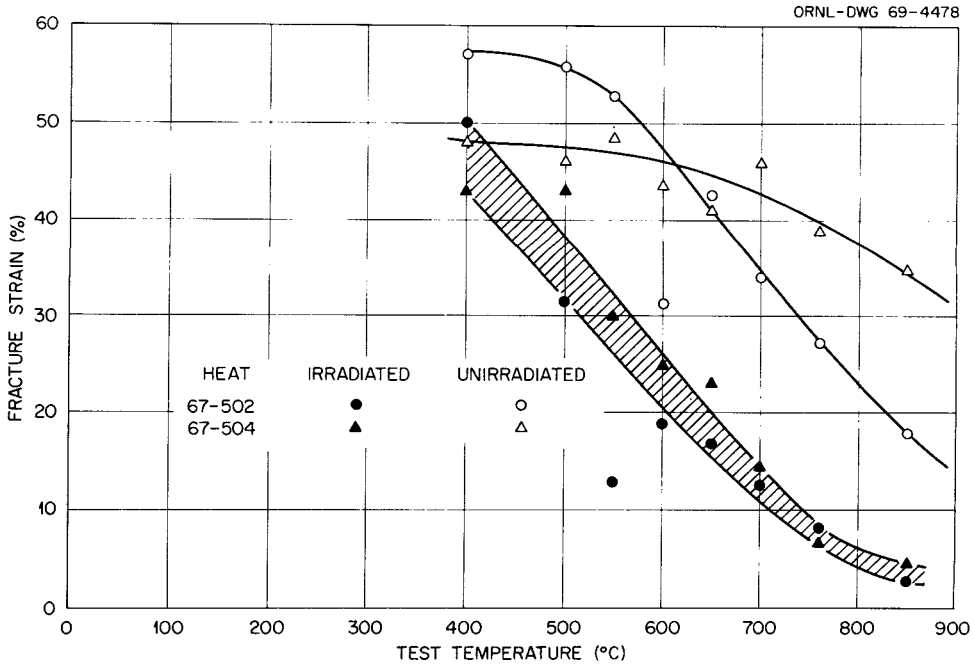

Fig. 30. Tensile Properties (Strain Rate of 0.002 min^{-1}) of Two Compositions of Modified Hastelloy N Following Irradiation (Thermal Fluence of 5.3×10^{20} neutrons/cm^2) or Annealing (Control Samples) for 9789 hr at 650°C.

Creep-Rupture Properties

The results of creep-rupture tests on heats 67-502 and -504 are given in Tables A-14 and A-15 (Appendix). The stress-rupture properties of heat 67-502 are shown in Fig. 31. Aging for 9789 hr at 650°C increased the rupture life by about 30% and neutron irradiation to a fluence of 5.3×10^{20} neutrons/cm^2 decreased the rupture life by about 30% compared with the as-annealed material. The minimum creep rate, shown in Fig. 32, was increased by the aging treatment and the samples that were aged and irradiated simultaneously had the same minimum creep rates as the as-annealed material.

The creep-rupture strength of heat 67-504 (Fig. 33) was not altered appreciably by aging at 650°C. However, irradiation decreased the rupture life of the material by about 50%. The minimum creep rate (Fig. 34) was increased by the combined irradiation and aging treatment, but was increased even more by just the aging treatment.

The fracture strains of heats 67-502 and -504 at 650°C are shown in Fig. 35 as a function of strain rate. In the unirradiated condition, both heats show a trend of decreasing fracture strain with decreasing strain rate. Aging improves the fracture strain of both heats and irradiation decreases the fracture strain. The irradiated material has a fracture strain of about 6% under creep conditions.

Metallographic Examination of Mechanical Property Specimens

Several of the tested samples were examined metallographically. Photomicrographs are shown in Fig. 36 for a sample of heat 5085 that was tensile tested at 25°C after being exposed to the cell environment for 20,789 hr at 650°C. The fracture under these test conditions would normally be transgranular, but the fracture shown in Fig. 36 is primarily intergranular. This change in fracture mode probably accounts for the fracture strain of this sample being only 33% (Fig. 11, p. 20) compared with about 55% for unirradiated, unaged material. The photomicrographs shown in Fig. 37 were made on another sample of heat 5085 from outside the vessel that was tested at 650°C. The fracture is largely intergranular and there are very few cracks near the fracture.

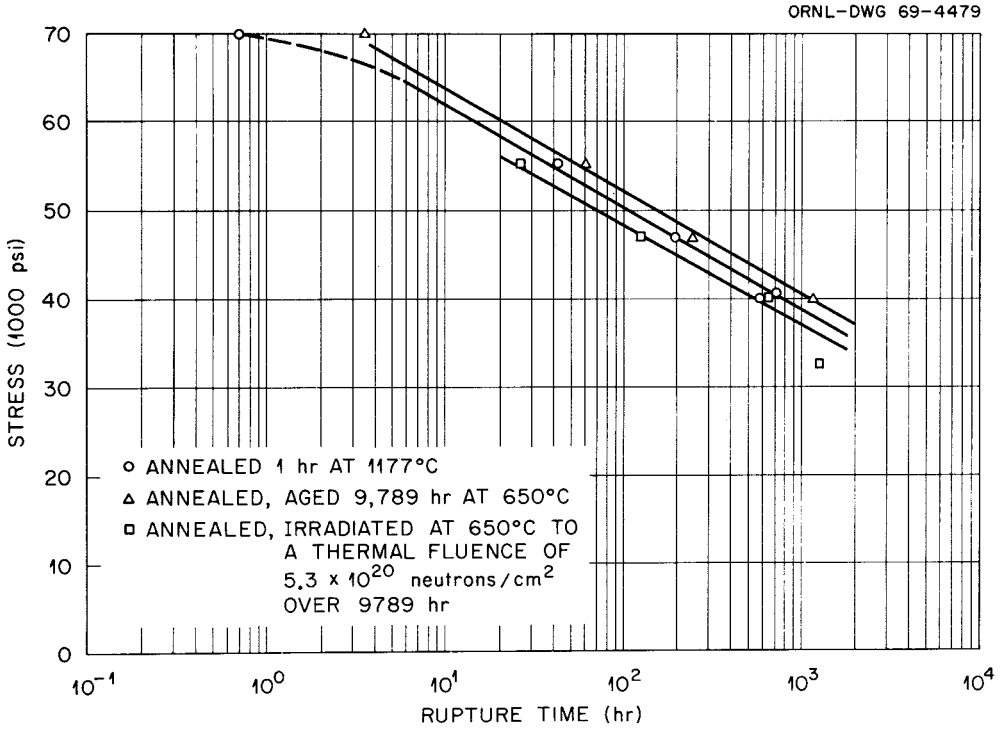

Fig. 31. Stress-Rupture Properties of Heat 67-502 at 650°C.

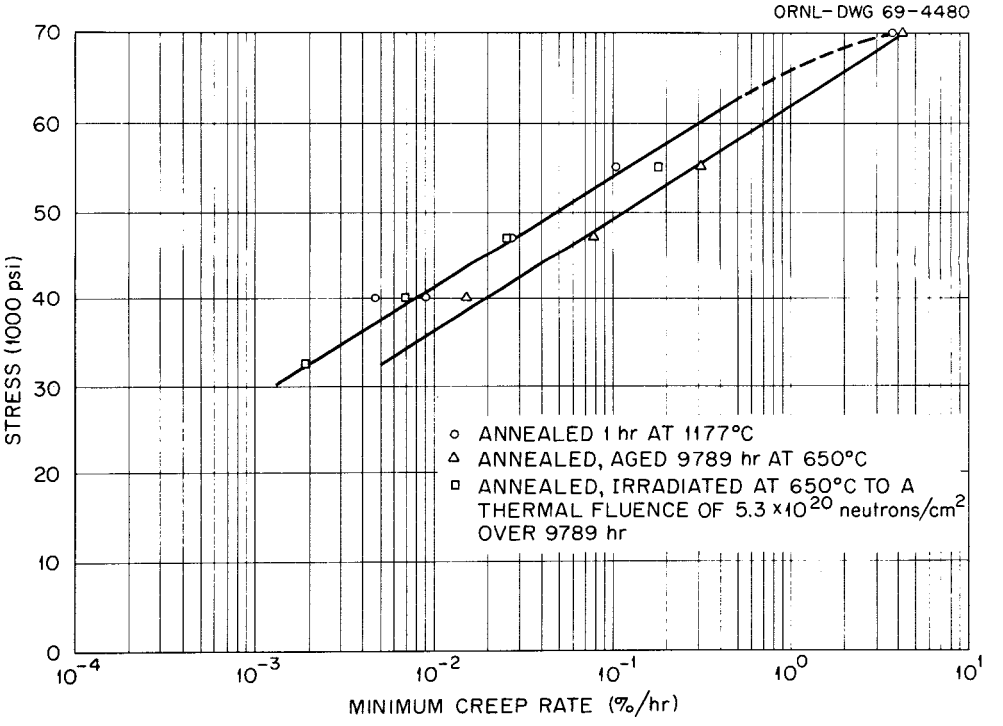

Fig. 32. Variation of Minimum Creep Rate with Stress Level for Heat 67-502 at 650°C.

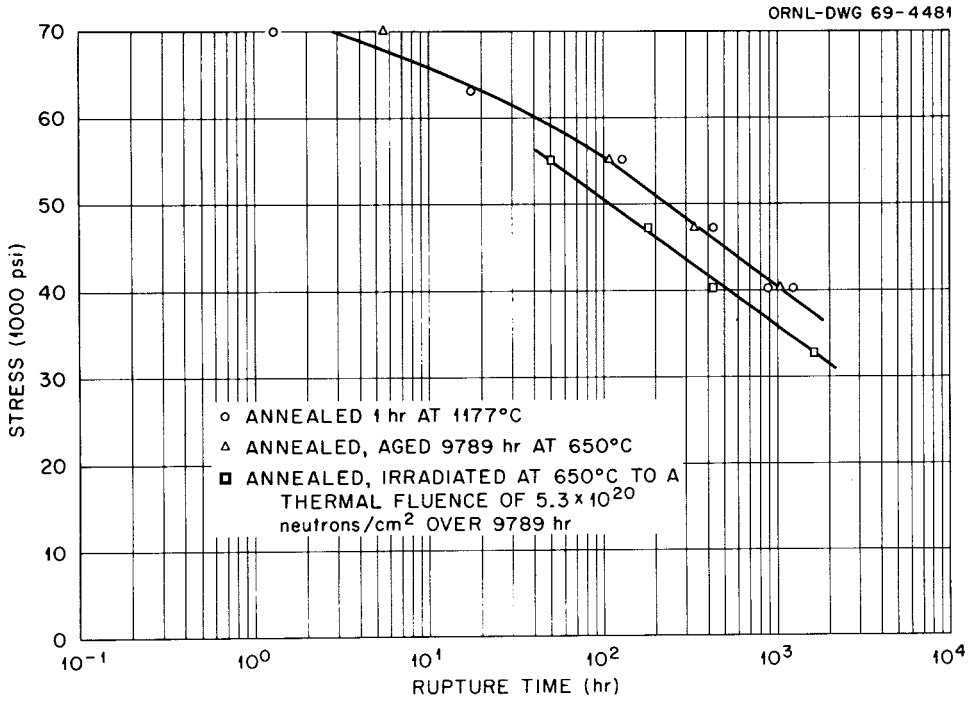

Fig. 33. Stress-Rupture Properties of Heat 67-504 at 650°C.

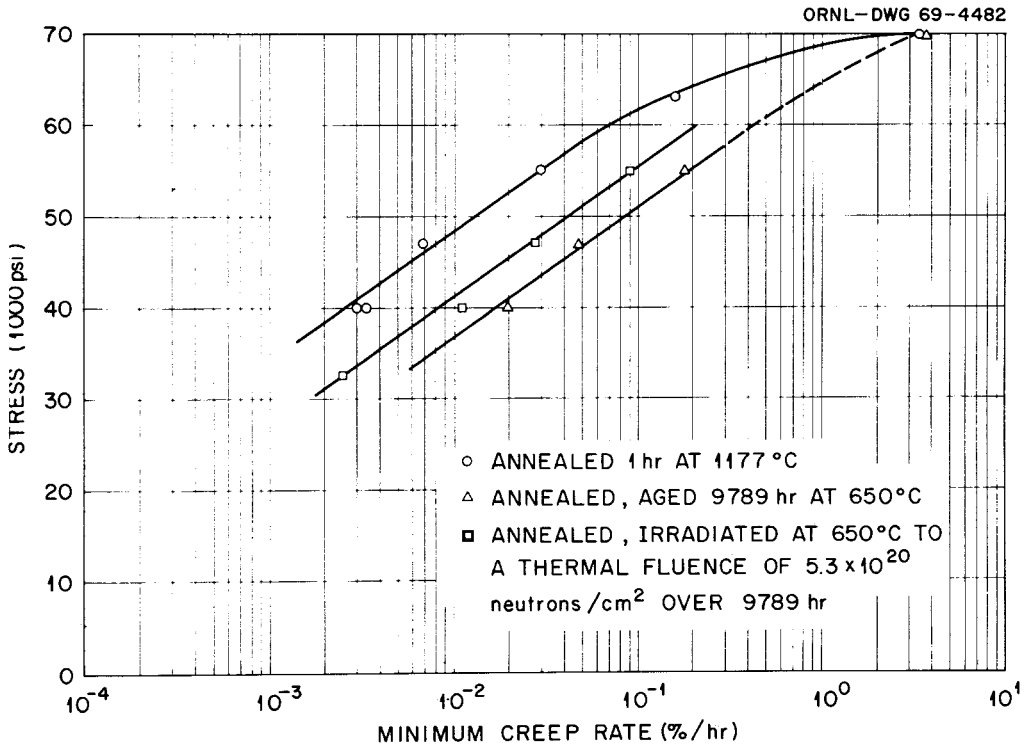

Fig. 34. Variation of Minimum Creep Rate with Stress Level for Heat 67-504 at 650°C.

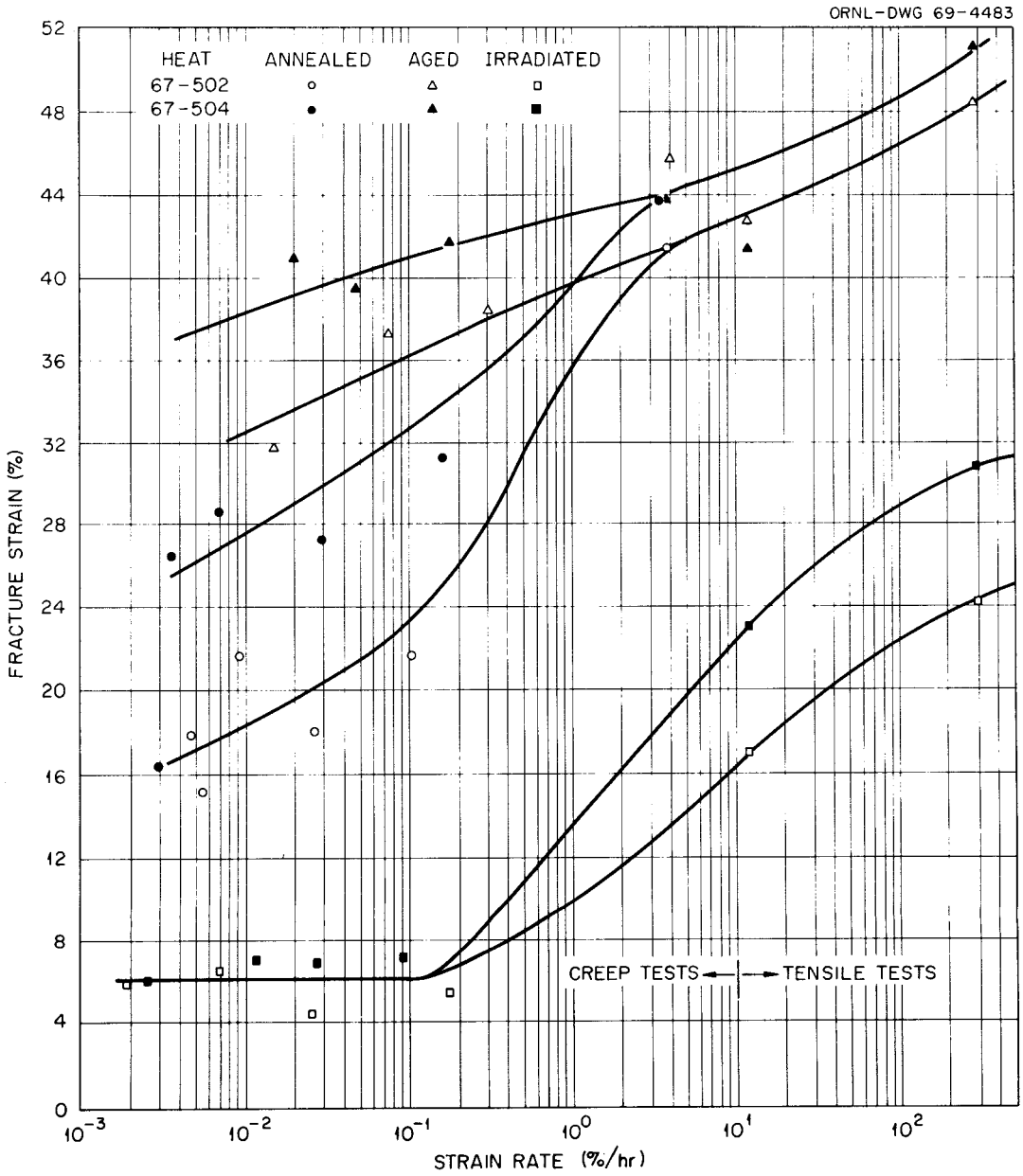

Fig. 35. Comparison of the Fracture Strains of Two Heats of Modified Hastelloy N Tested at 650°C in Various Metallurgical Conditions.

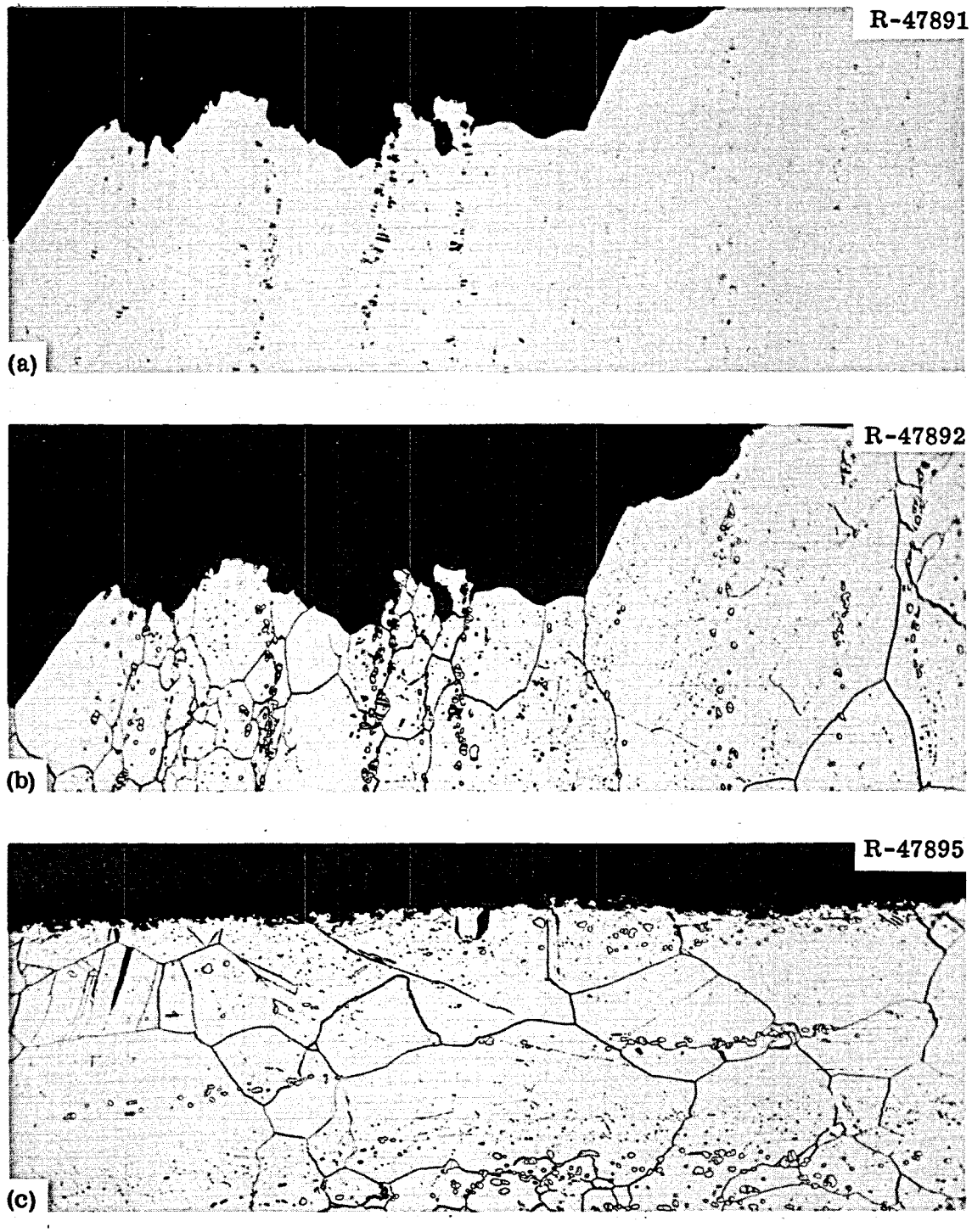

Fig. 36. Photomicrographs of a Hastelloy N (Heat 5085) Sample Tested at 25°C at a Strain Rate of 0.05 min^{-1}. Sample had been irradiated to a thermal fluence of 2.6×10^{19} neutrons/cm^2 while being exposed to the cell environment at 650°C for 20,789 hr. 100×. (a) Fracture, as polished. (b) Fracture, etched. (c) Edge of stressed portion. Etchant: aqua regia.

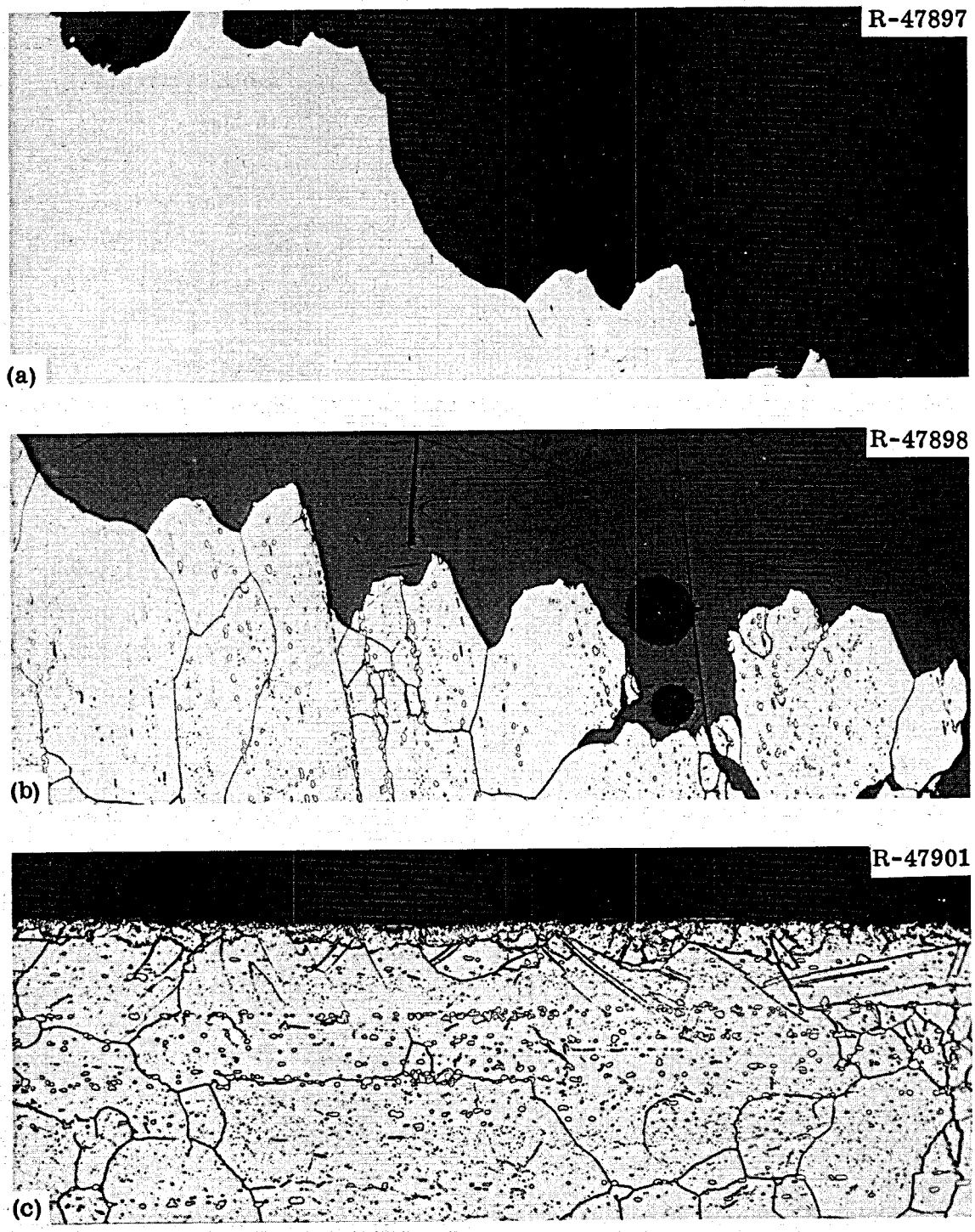

Fig. 37. Photomicrographs of a Hastelloy N (Heat 5085) Sample Tested at 650°C at a Strain Rate of 0.002 min^{-1}. Sample had been irradiated to a thermal fluence of 2.6×10^{19} neutrons/cm^2 while being exposed to the cell environment at 650°C for 20,789 hr. 100X. (a) Fracture, as polished. (b) Fracture, etched. (c) Edge of stressed portion, etched. Etchant: aqua regia.

A sample of heat 5065 that was removed from outside the vessel and tested at 25°C is shown in Fig. 38. The fracture is still partially intergranular, but the elongated grains indicate that the sample strained a large amount before failing. As shown in Fig. 12, p. 20, this sample had a fracture strain of 59.5%. A sample of heat 5065 was tested at 600°C and typical photomicrographs are shown in Fig. 39. The fracture strain of this sample was only 15% and the fracture is predominately intergranular.

The thin oxide surface layers do not seem to influence the deformation in the samples from outside the vessel. The amount of edge cracking noted in Figs. 36 through 39 is not unusual for Hastelloy N.

Typical photomicrographs of a sample of heat 5085 aged for 15,289 hr at 650°C in static barren fuel salt and tested at 200°C are shown in Fig. 40. The fracture strain of this sample was quite good (Fig. 14, p. 22) although the fracture is partially intergranular. A cross section from the stressed portion of this sample is shown in Fig. 40(b) and shows that the surface structural modification extends to a depth of about 3 mils. Figure 40(c) gives some further insight into the origin of the modified structure. The surface indentations are engraved identification numbers and would have involved heavy cold working. Note that the modified structure extends to a greater depth under these impressions. The fabrication sequence was (1) rods fabricated to approximate diameter, (2) rod segments welded together, (3) annealed for 2 hr at 900°C in argon, (4) sinterless ground to final diameter, (5) gage portions milled, (6) identification numbers engraved, and (7) samples put into surveillance facility. Thus, all surfaces were cold worked; the major diameter by grinding and the gage diameter by milling. The resulting microstructure likely results from carbide precipitation on the dislocations introduced by cold working.

Figure 41 shows several photomicrographs of a sample of heat 5085 that was irradiated in the MSRE core to a thermal fluence of 9.4×10^{20} neutrons/cm^2 and tested at 200°C. The fracture is mixed transgranular and intergranular. The grain shapes attest to the lower elongation of the irradiated sample in Fig. 41(c) compared with that of the unirradiated sample shown in Fig. 40(a). The as-polished

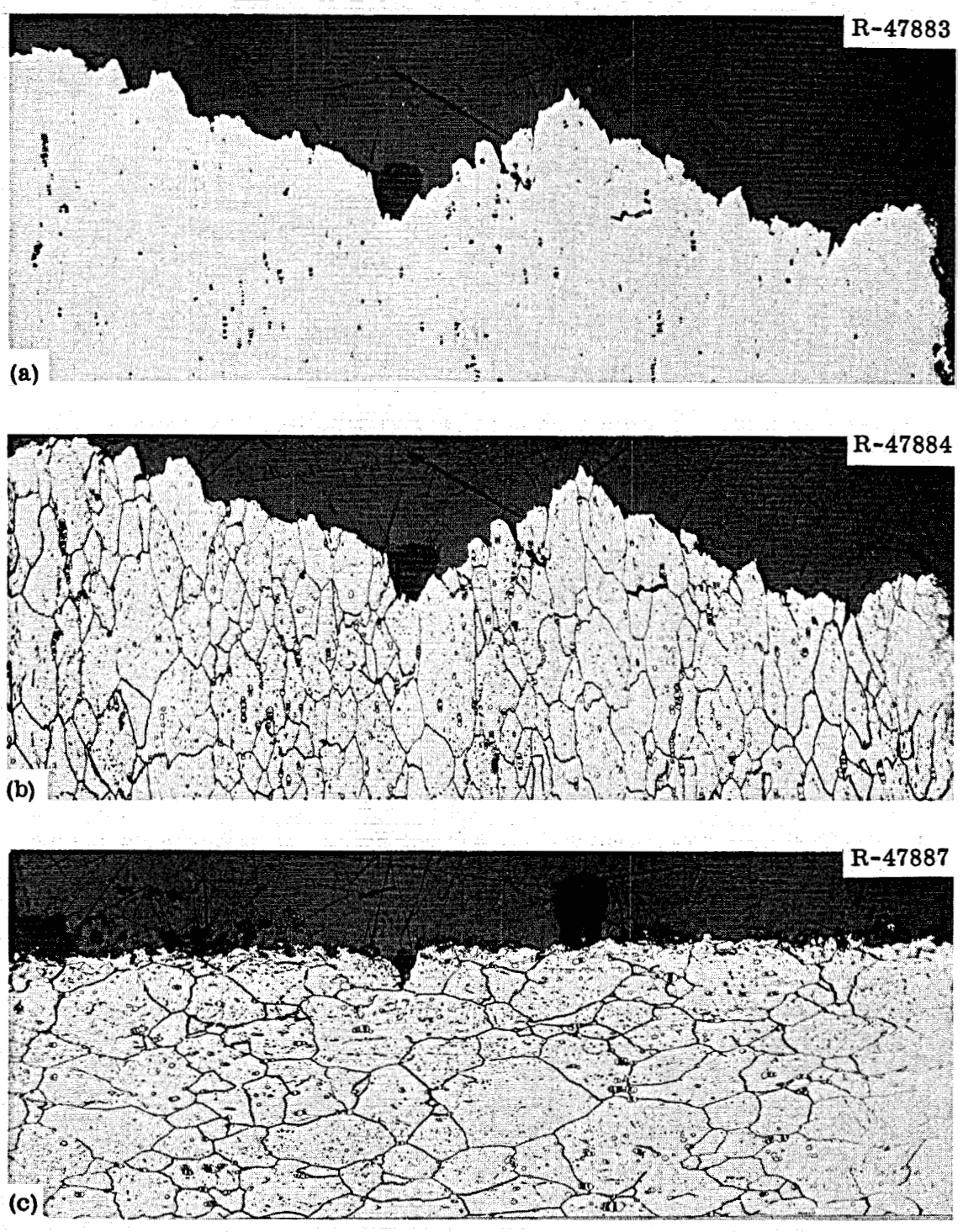

Fig. 38. Photomicrographs of a Hastelloy N (Heat 5065) Sample Tested at 25°C at a Strain Rate of 0.05 min^{-1}. Sample had been irradiated to a thermal fluence of 2.6×10^{19} neutrons/cm^2 while being exposed to the cell environment at 650°C for 20,789 hr. 100x. (a) Fracture, as polished. (b) Fracture, etched. (c) Edge of stressed portion. Etchant: aqua regia.

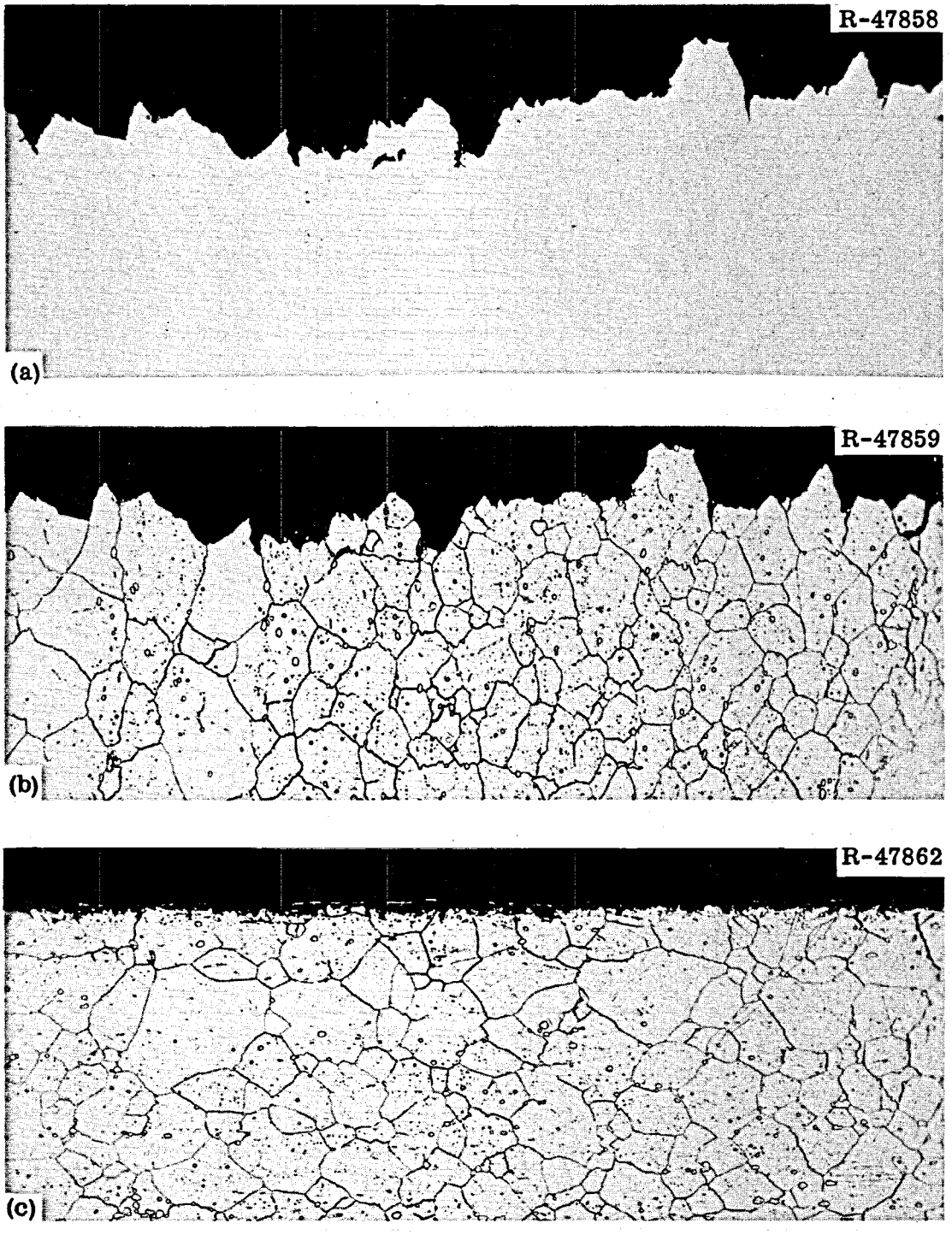

Fig. 39. Photomicrographs of a Hastelloy N (Heat 5065) Sample Tested at 600°C at a Strain Rate of 0.002 min^{-1}. Sample had been irradiated to a thermal fluence of 2.6×10^{19} neutrons/cm^2 while being exposed to the cell environment at 650°C for 20,789 hr. 100X. (a) Fracture, as polished. (b) Fracture, etched. (c) Edge of stressed portion, etched. Etchant: aqua regia.

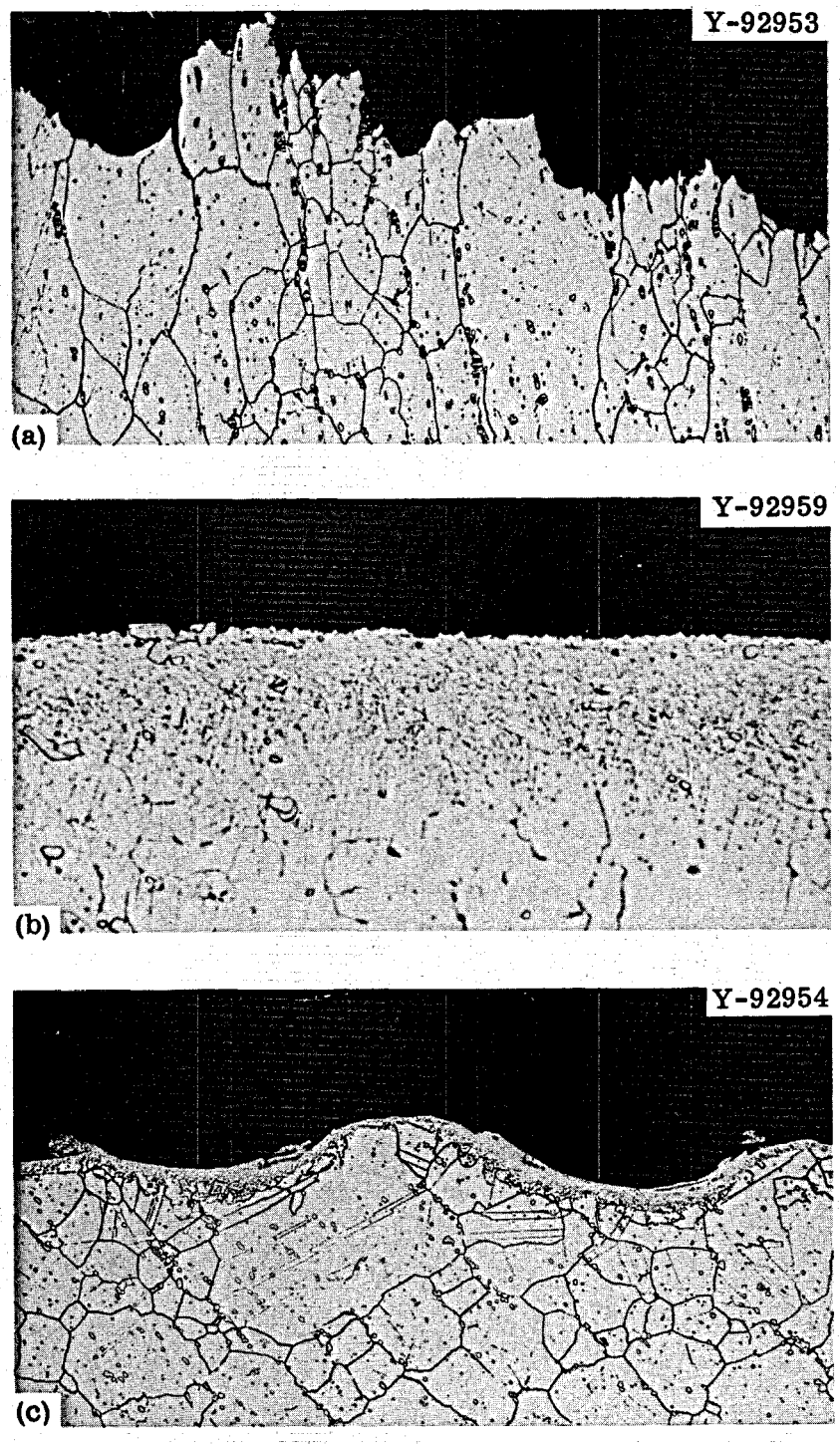

Fig. 40. Photomicrographs of a Hastelloy N (Heat 5085) Sample Exposed to Static Barren Fuel Salt for 15,289 hr at 650°C and Then Tested at 200°C. (a) Fracture. 100×. (b) Edge of cross section from stressed portion. 500×. (c) Edge of cross section from shoulder showing impressions made by engraving numbers. 100×. Etchant: glyceria regia.

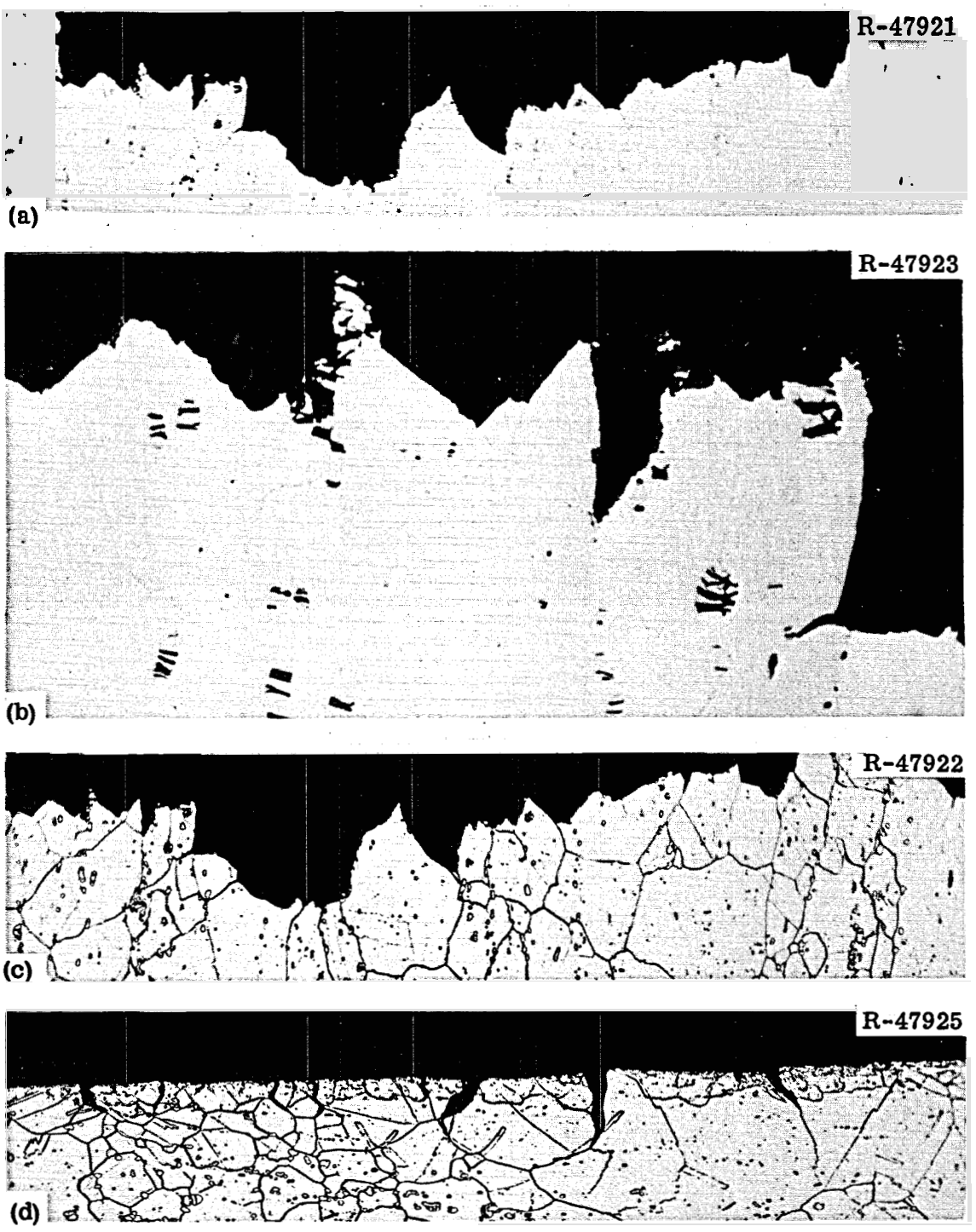

Fig. 41. Photomicrographs of a Hastelloy N (Heat 5085) Sample Exposed to Fluoride Salt in the MSRE for 15,289 hr at 650°C and Then Tested at 25°C. Thermal Fluence was 9.4×10^{20} neutrons/cm^2. (a) Fracture, as polished. 100X. (b) Fracture, as polished. 500X. (c) Fracture, etched. 100X. (d) Edge of stressed portion, etched. 100X. Etchant: aqua regia.

photomicrographs [Fig. 41(a) and (b)] show that the large carbides actually fracture during testing. Some of these cracks may propagate and contribute to fracture. (This fracturing occurs in unirradiated and irradiated samples when tested at relatively low temperatures, e.g., Figs. 36, 38, and 40.) There is a very thin layer of the modified structure near the surface of the tested sample [Fig. 41(d)], but the amount of edge cracking is not unusually high for a sample that has strained 36% (Fig. 13, p. 22).

The fracture of a sample of heat 5085 that was tested at 650°C after exposure to a static barren fuel salt for 15,289 hr at 650°C is shown in Fig. 42. The fracture is mixed transgranular and intergranular and there is considerable evidence of carbide fracturing. By contrast, the fracture shown in Fig. 43 is primarily intergranular. The sample in Fig. 43 was irradiated to a thermal fluence of 2.4×10^{20} neutrons/cm^2 and tested at 650°C. At the low fracture strain of only 5% (Fig. 13, p. 22) there is little evidence of plastic deformation with only a few fractured carbides and some separations at the carbide-metal interfaces [Fig. 43(b)].

Samples of heat 5065 that were irradiated to a thermal fluence of 2.4×10^{20} neutrons/cm^2 and the thermal controls both had fracture strains of over 40% when tested at 25°C (Figs. 15 and 16, p. 23). The fractures of these samples appear quite similar (Figs. 44 and 45). The fractures are largely intergranular although the grains have deformed extensively. Some edge cracking occurred on both samples.

When tested at 650°C an unirradiated sample of heat 5065 had a fracture with transgranular and intergranular components (Fig. 46). This sample had a fracture strain of about 17% (Fig. 16, p. 23) compared with 3.5% (Fig. 15, p. 23) for a comparable sample irradiated to a thermal fluence of 9.4×10^{20} neutrons/cm^2. The irradiated sample has an intergranular fracture with very limited intergranular and carbide cracking (Fig. 47). The modified layer near the surface has not deformed differently from the remaining sample. The fracture of a sample modified with titanium (heat 67-502) that was exposed to barren fuel salt for 9789 hr at 650°C and tested at 25°C is shown in Fig. 48. The grains have deformed extensively although the fracture is largely intergranular.

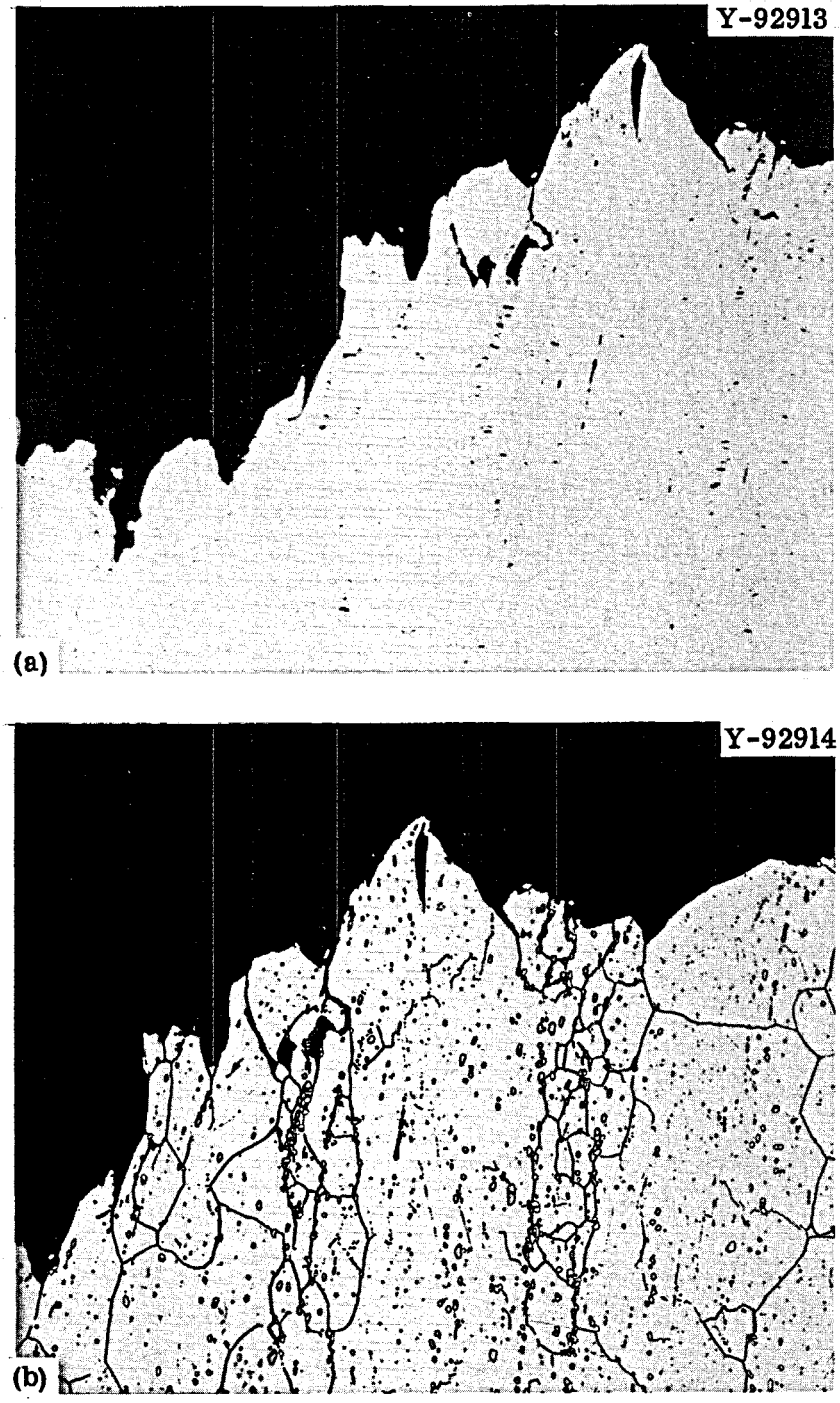

Fig. 42. Photomicrographs of a Hastelloy N (Heat 5085) Sample Exposed to Static Barren Fuel Salt for 15,289 hr at 650°C and Then Tested at 650°C and a Strain Rate of 0.002 min^{-1}. 100×. (a) Fracture, as polished. (b) Fracture, etched. Etchant: glyceria regia.

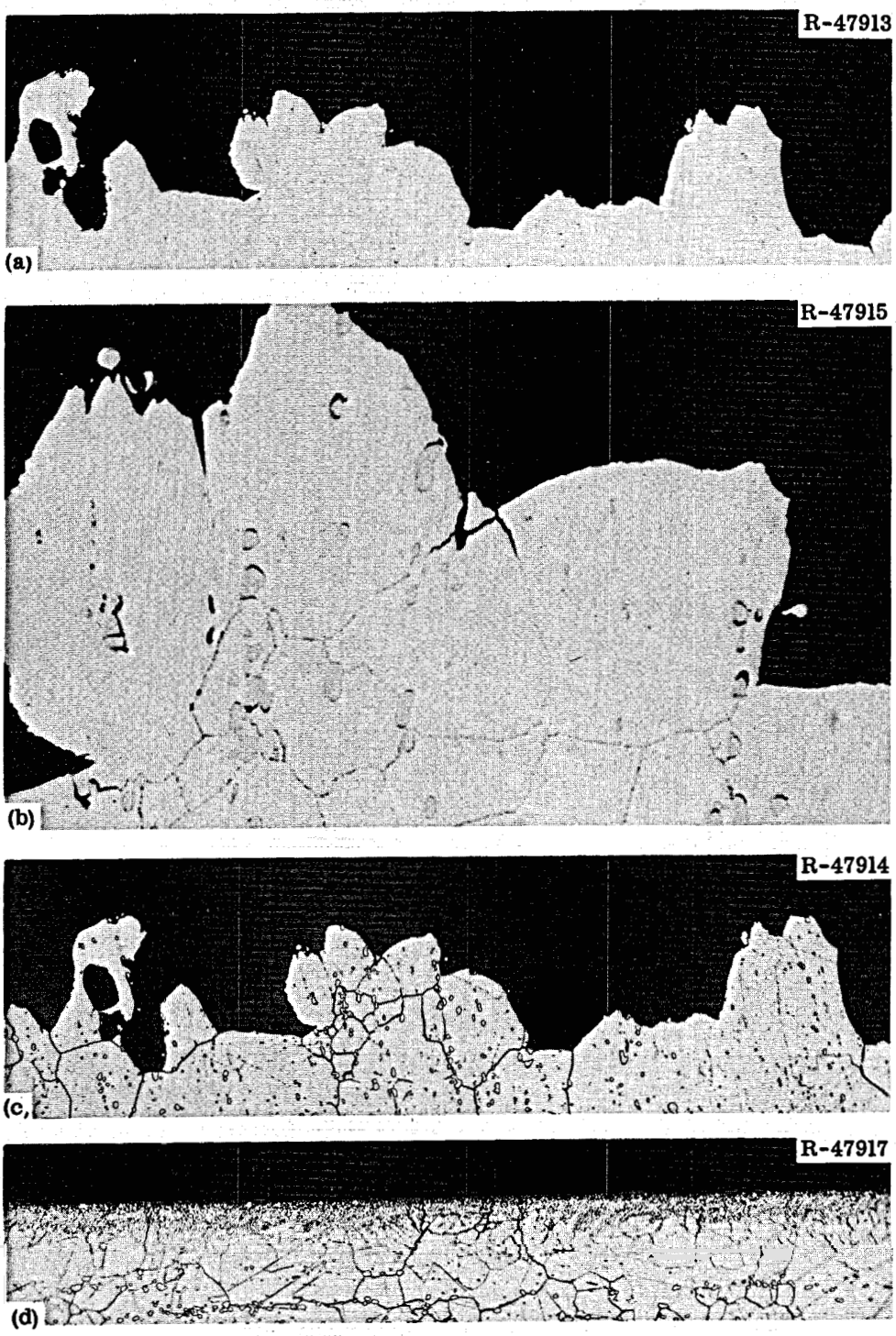

Fig. 43. Photomicrographs of a Hastelloy N (Heat 5085) Sample Exposed to Fluoride Salt in the MSRE for 15,289 hr at 650°C and Then Tested at 650°C and a Strain Rate of 0.002 min^{-1}. Thermal fluence was 9.4×10^{20} neutrons/cm^2. (a) Fracture, as polished. 100×. (b) Fracture, as polished. 500×. (c) Fracture, etched. 100×. (d) Edge of stressed portion, etched. 100×. Etchant: aqua regia. Reduced 14.5%.

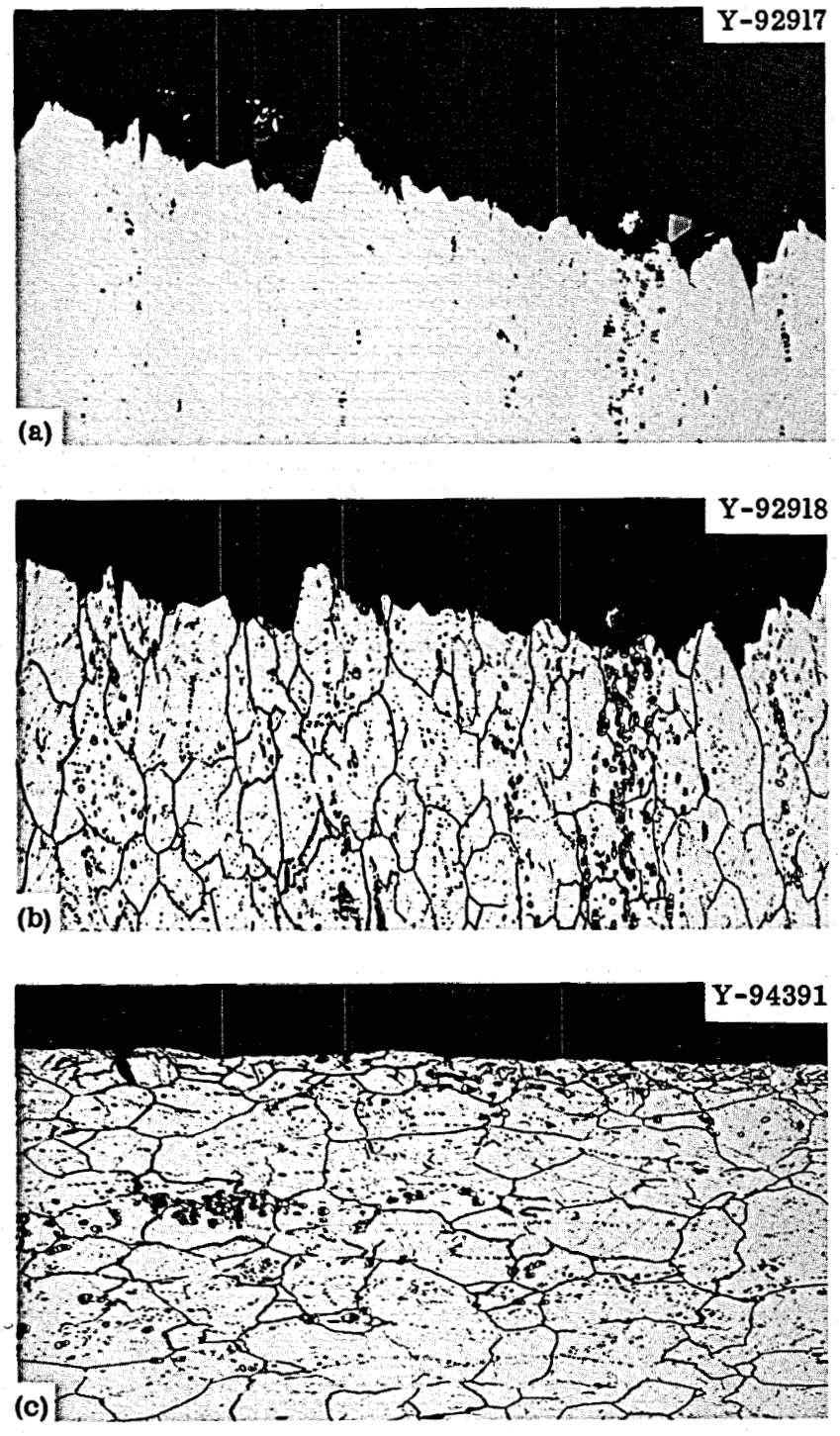

Fig. 44. Photomicrographs of a Hastelloy N (Heat 5065) Sample Exposed to Static Barren Fuel Salt for 15,289 hr at 650°C and Then Tested at 25°C and a Strain Rate of 0.05 min^{-1}. 100×. (a) Fracture, as polished. (b) Fracture, etched. (c) Edge of stressed portion, etched. Etchant: glyceria regia.

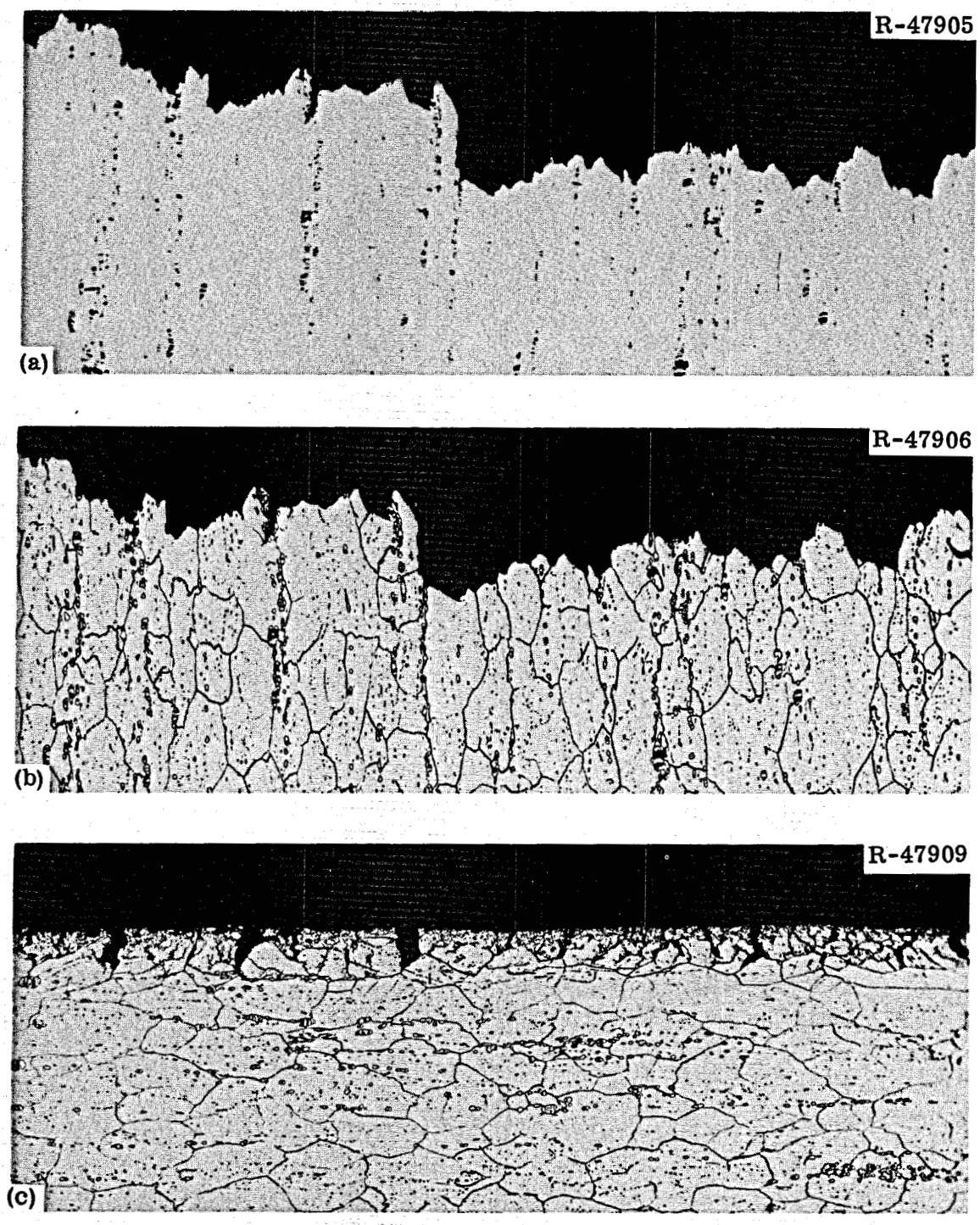

Fig. 45. Photomicrographs of a Hastelloy N (Heat 5065) Sample Exposed to Fluoride Salt in the MSRE for 15,289 hr at 650°C and Then Tested at 25°C and a Strain Rate of 0.05 min^{-1}. Thermal fluence was 9.4×10^{20} neutrons/cm^2. 100×. (a) Fracture, as polished. (b) Fracture, etched. (c) Edge of stressed portion. Etchant: aqua regia.

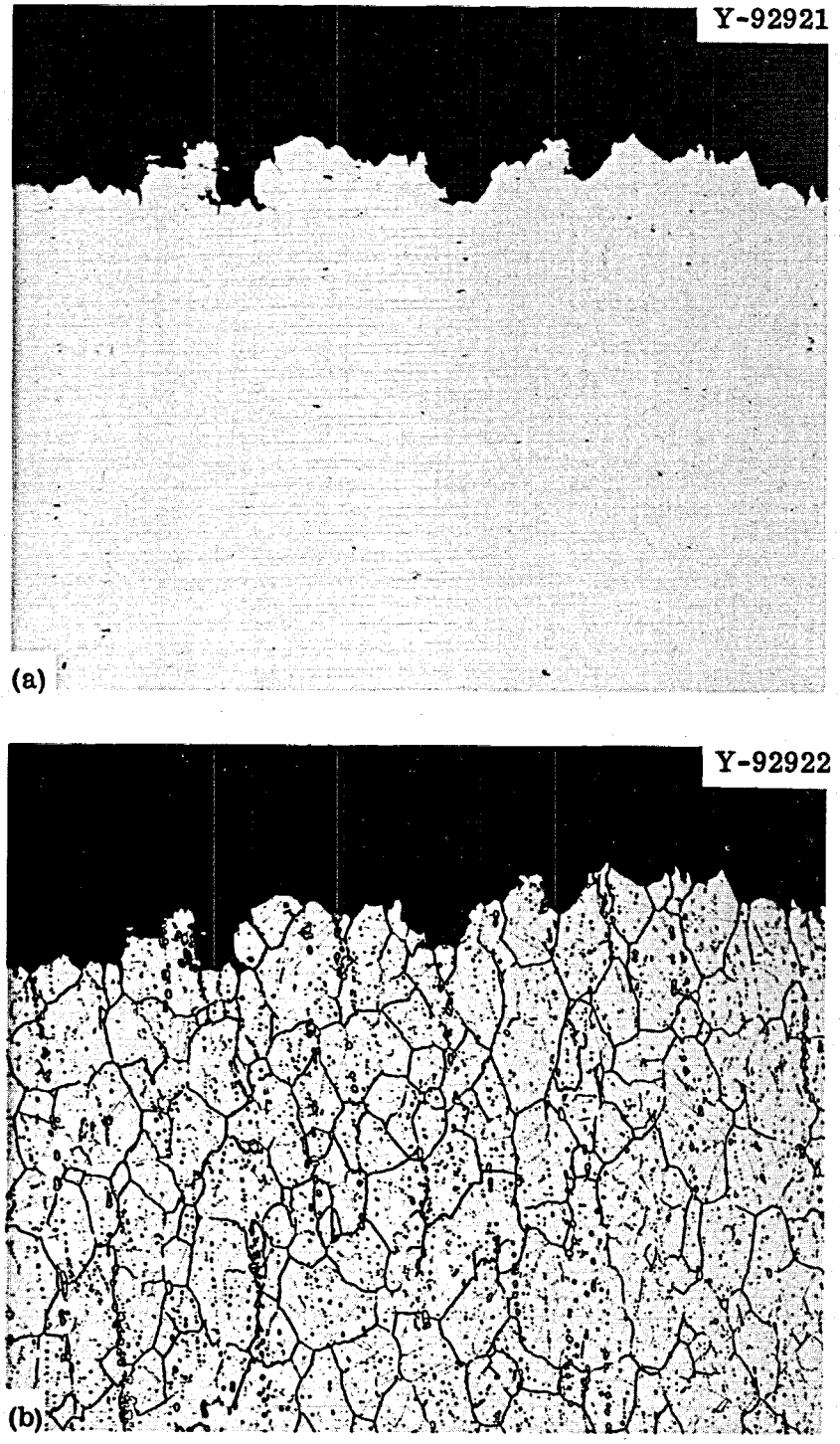

Fig. 46. Photomicrographs of a Hastelloy N (Heat 5065) Sample Exposed to Static Barren Fuel Salt for 15,289 hr at 650°C and Then Tested at 650°C and a Strain Rate of 0.002 min^{-1}. 100×. (a) Fracture, as polished. (b) Fracture, etched. Etchant: glyceria regia.

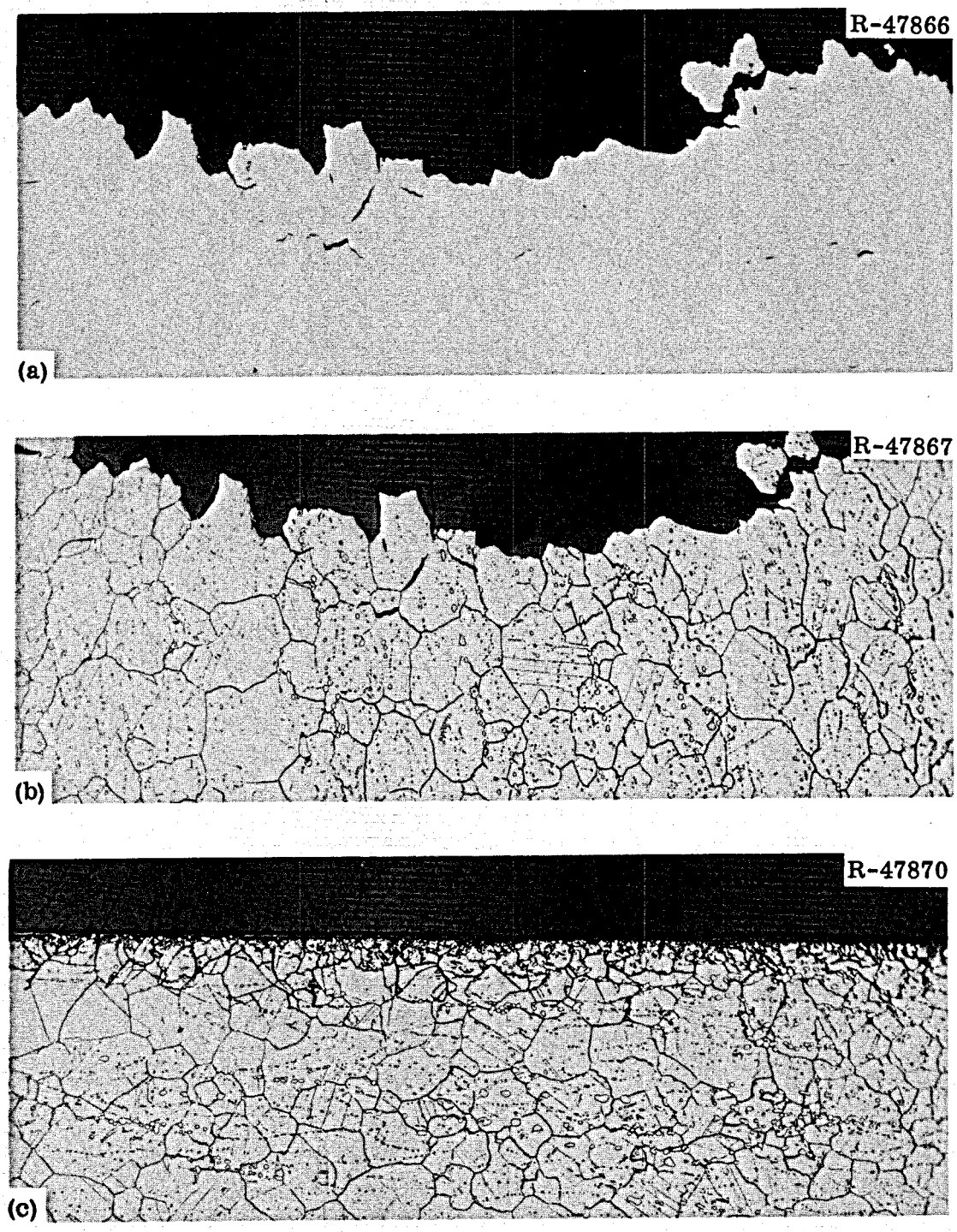

Fig. 47. Photomicrographs of a Hastelloy N (Heat 5065) Sample Exposed to Fluoride Salt in the MSRE for 15,289 hr at 650°C and Then Tested at 650°C and a Strain Rate of 0.002 min^{-1}. Thermal fluence was 9.4×10^{20} neutrons/cm^2. 100×. (a) Fracture, as polished. (b) Fracture, etched. (c) Edge of stressed portion, etched. Etchant: aqua regia.

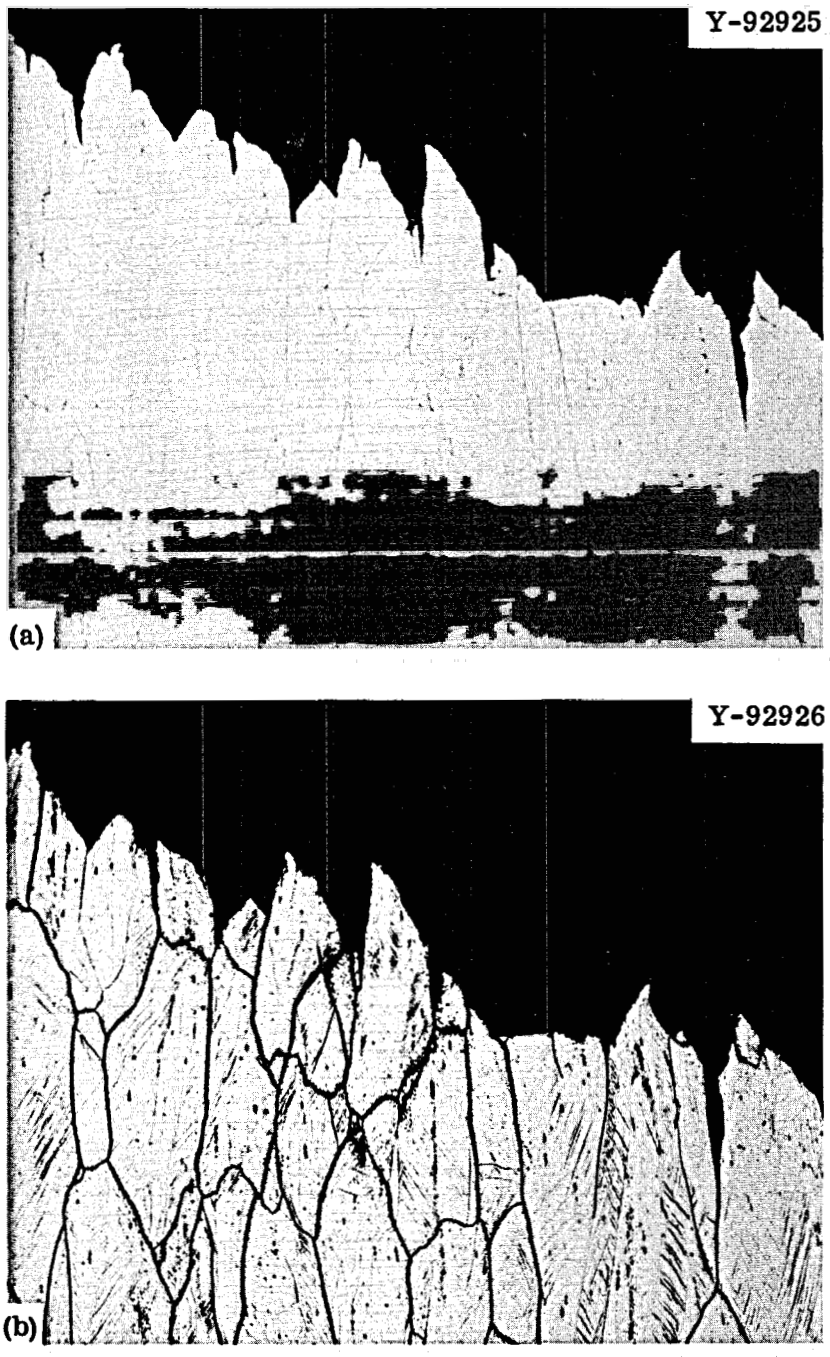

Fig. 48. Photomicrographs of a Hastelloy N (Heat 67-502) Sample Exposed to Static Barren Fuel Salt for 9789 hr at 650°C and Then Tested at 25°C. 100×. (a) Fracture, as polished. (b) Fracture, etched. Etchant: glyceria regia.

Further photomicrographs of the unstressed portion of this same sample are shown in Fig. 49. There is a very fine carbide precipitate throughout this sample and our other studies indicate that these are likely carbides of the M_2C or MC types.[10] The grain boundaries also etch quite heavily indicating the presence of heavy grain-boundary precipitation. The surface of the sample has a very thin layer that is rich in iron. This is likely a deposit since this alloy is very low in iron and the rest of the system is fabricated of material that contains 4 to 5% Fe.

A sample of heat 67-502 that was irradiated and tested at 25°C is shown in Fig. 50. The fracture strain of this sample was about as high as that for the unirradiated sample (Fig. 29, p. 35), but the grains are not nearly as elongated in the irradiated sample (Fig. 50) as in the unirradiated sample (Fig. 48). There are considerably more grain-boundary cracks in the irradiated sample than in the unirradiated sample.

The fracture of a sample of heat 67-502 that was exposed to barren fuel salt for 9789 hr and tested at 650°C is shown in Fig. 51. The fracture is transgranular, an observation consistent with the extremely high fracture strain of this sample (Fig. 29, p. 35).

The fracture at 25°C of heat 67-504 (Fig. 52) is quite similar to that noted for heat 67-502 (Fig. 48). Heat 67-504 is modified with 0.5% Hf and the photomicrographs in Fig. 53 indicate that there may be more precipitate in this alloy than in heat 67-502 that was modifed with 0.5% Ti and 2% W. However, the apparent amount of precipitation is very dependent upon the etching procedure. This heat of material is also very low in iron and iron deposition was noted [Fig. 53(a)].

The fracture of an irradiated sample of heat 67-504 tested at 25°C is shown in Fig. 54. The grains have deformed and the fracture was transgranular. As shown in Fig. 29, p. 35, the fracture strain at 25°C of heat 67-504 was lower than that of 67-502. However, the fractures (Figs. 50 and 54) give the opposite impression.

---

[10]R. E. Gelbach and S. W. Cook, MSR Program Semiann. Progr. Rept. Feb. 28, 1969, ORNL-4396, pp. 240–242.

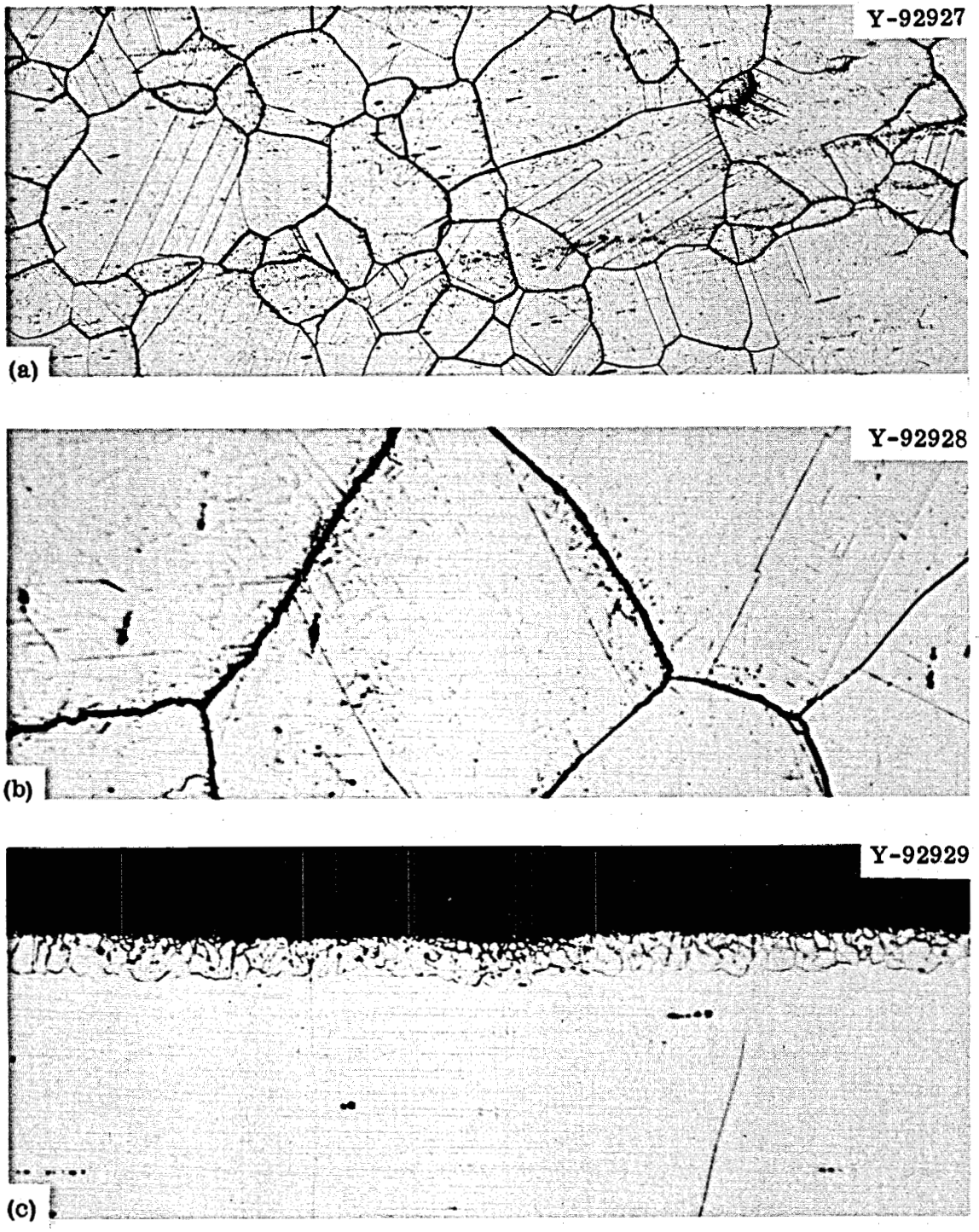

Fig. 49. Photomicrographs of the Unstressed Portion of a Hastelloy N (Heat 67-502) Sample That Was Exposed to Static Barren Fuel Salt for 9789 hr at 650°C. (a) Typical. 100×. (b) Typical. 500×. (c) Edge. 500×. Etchant: glyceria regia.

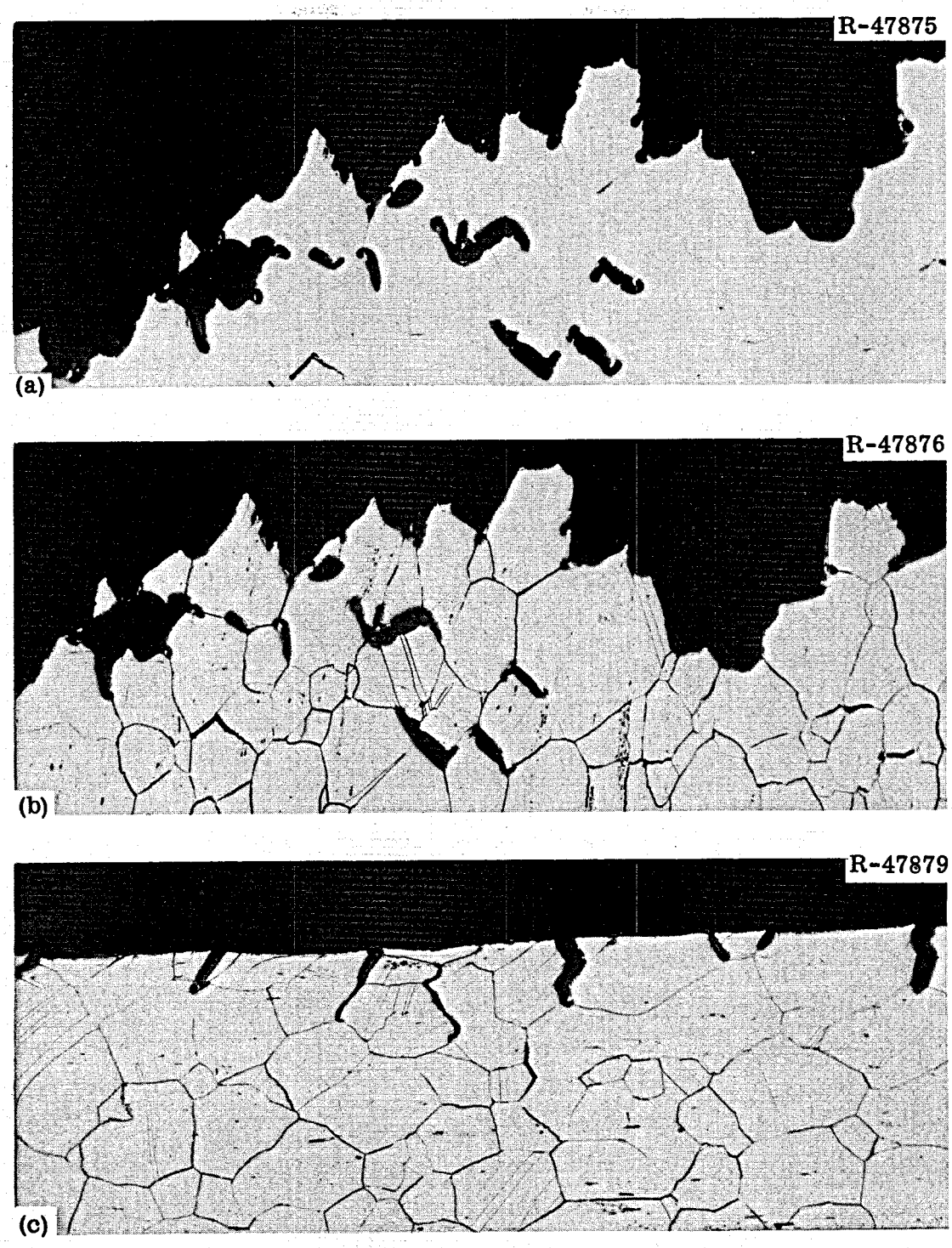

Fig. 50. Photomicrographs of a Hastelloy N (Heat 67-502) Sample Exposed to Fluoride Salt in the MSRE for 9789 hr at 650°C and Then Tested at 25°C. 100×. (a) Fracture, as polished. (b) Fracture, etched. (c) Edge of stressed portion, etched. Etchant: aqua regia.

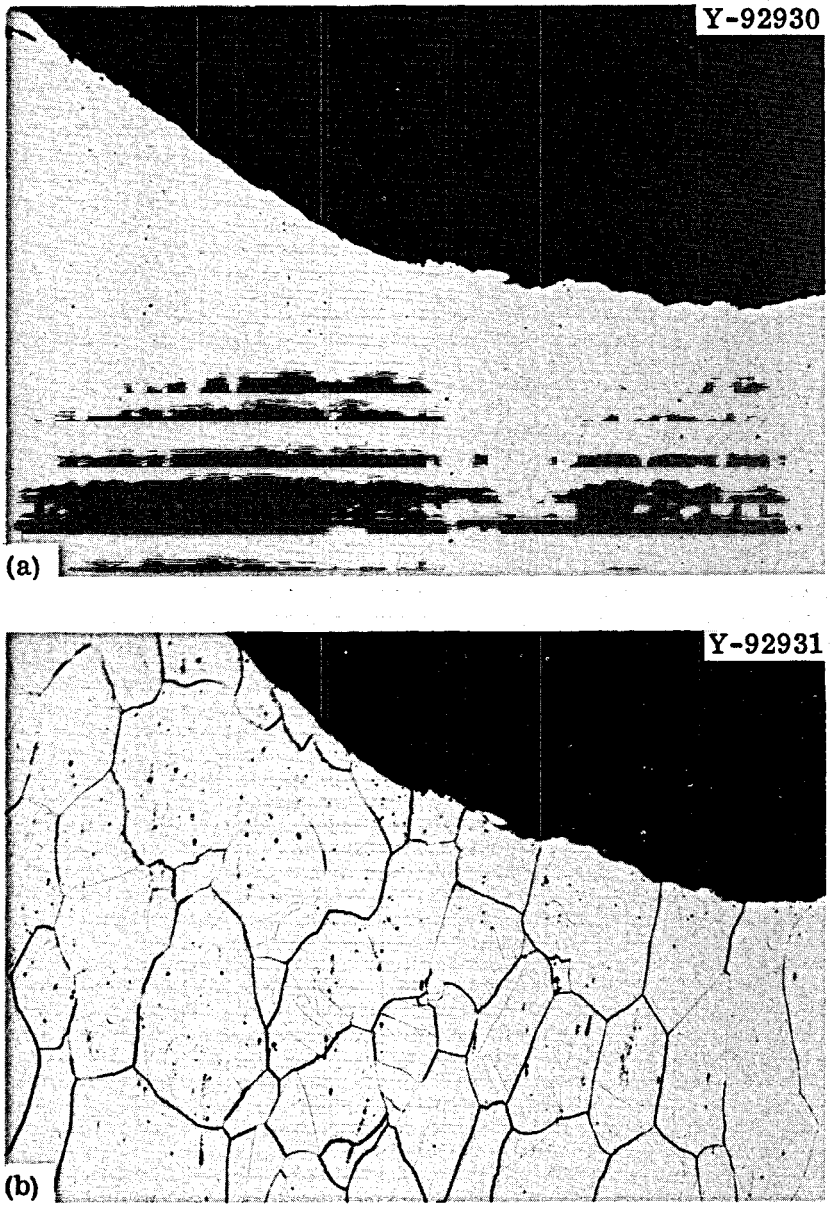

Fig. 51. Photomicrographs of the Fracture of a Hastelloy N (Heat 67-502) Sample Exposed to Static Barren Fuel Salt for 9789 hr at 650°C and Then Tested at 650°C and a Strain Rate of 0.002 min^{-1}. 100×. (a) As polished. (b) Etched. Etchant: glyceria regia.

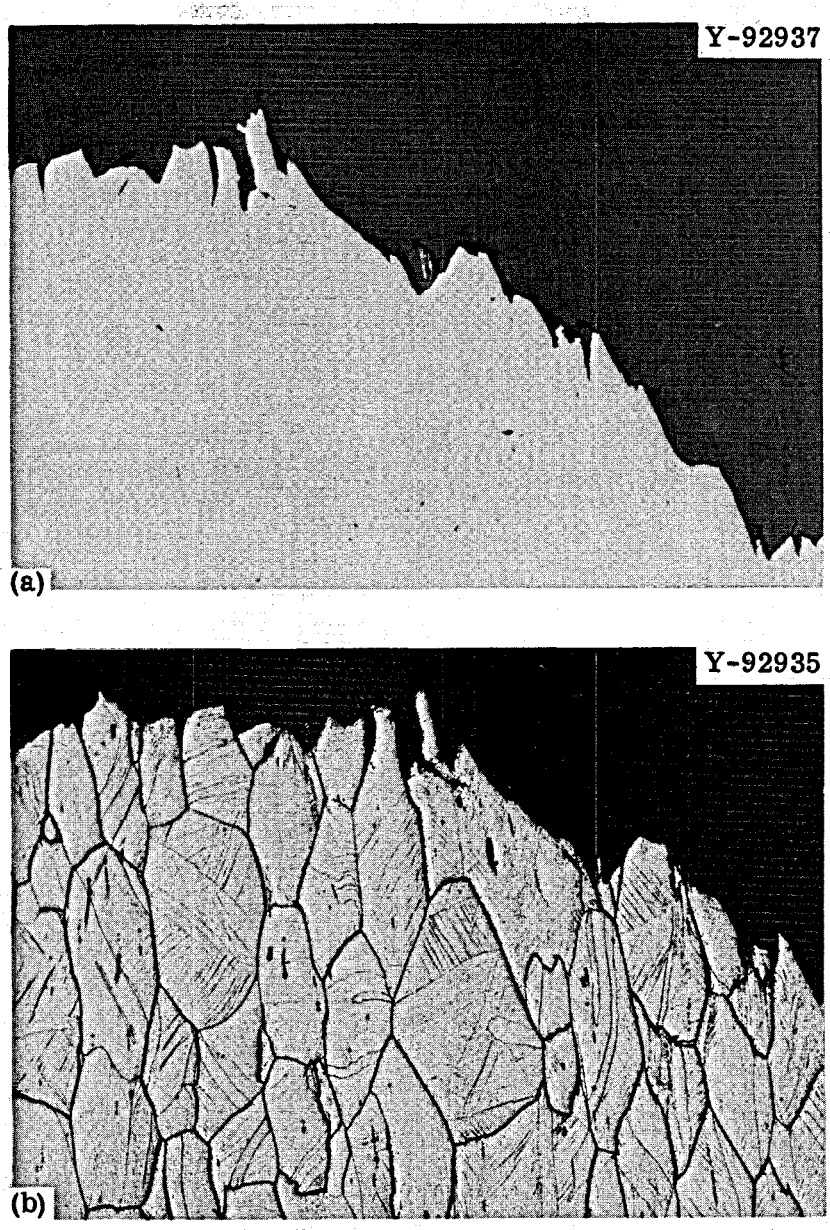

Fig. 52. Photomicrographs of the Fracture of a Hastelloy N (Heat 67-504) Sample That Was Exposed to Barren Fuel Salt for 9789 hr at 650°C and Tested at 25°C. 100×. (a) As polished. (b) Etched. Etchant: glyceria regia.

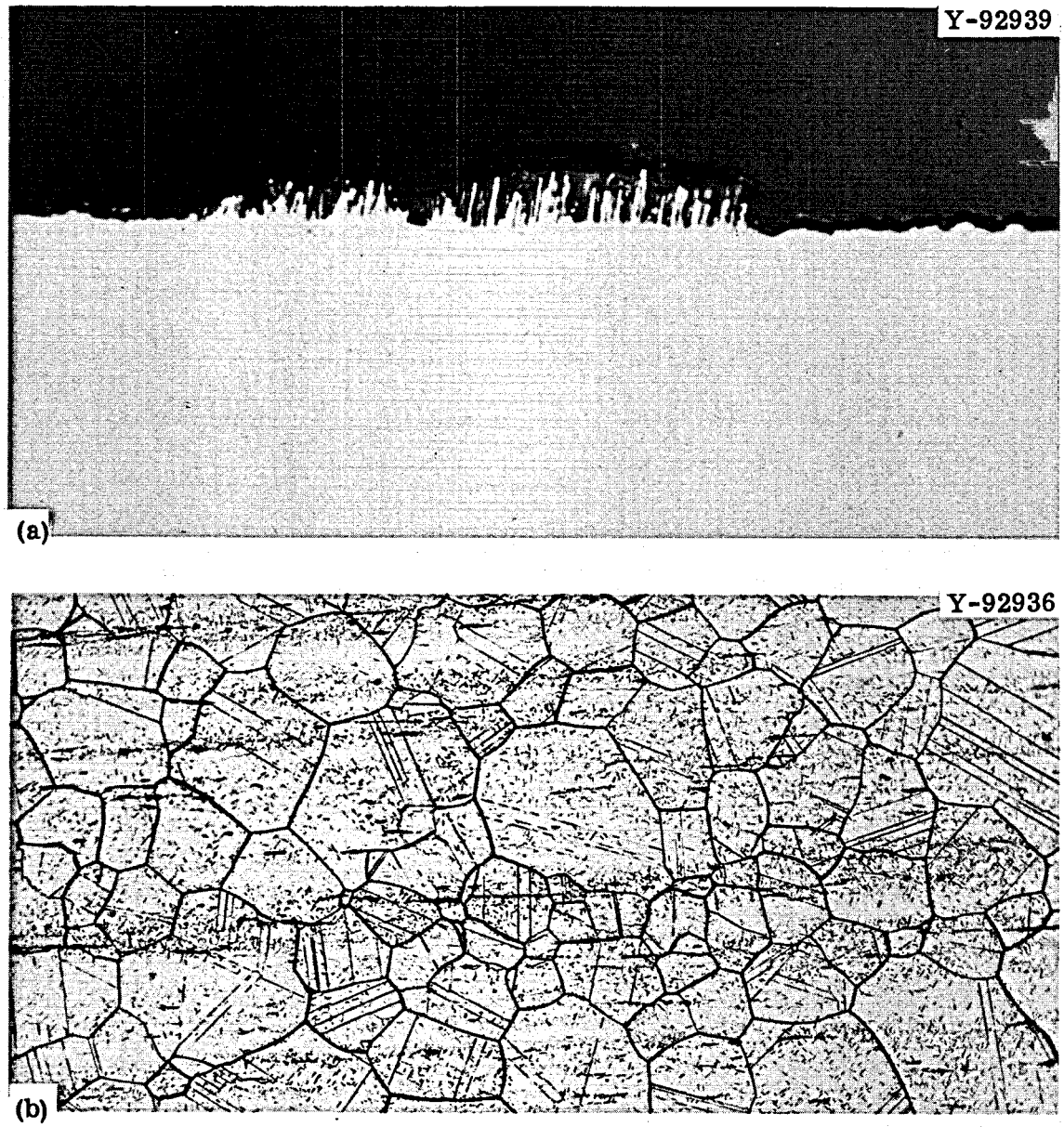

Fig. 53. Photomicrographs of the Unstressed Portions of a Hastelloy N (Heat 67-504) Sample Exposed to Barren Fuel Salt for 9789 hr at 650°C. (a) Edge, as polished. 1000X. (b) Typical microstructure, etched. 100X. Etchant: glyceria regia.

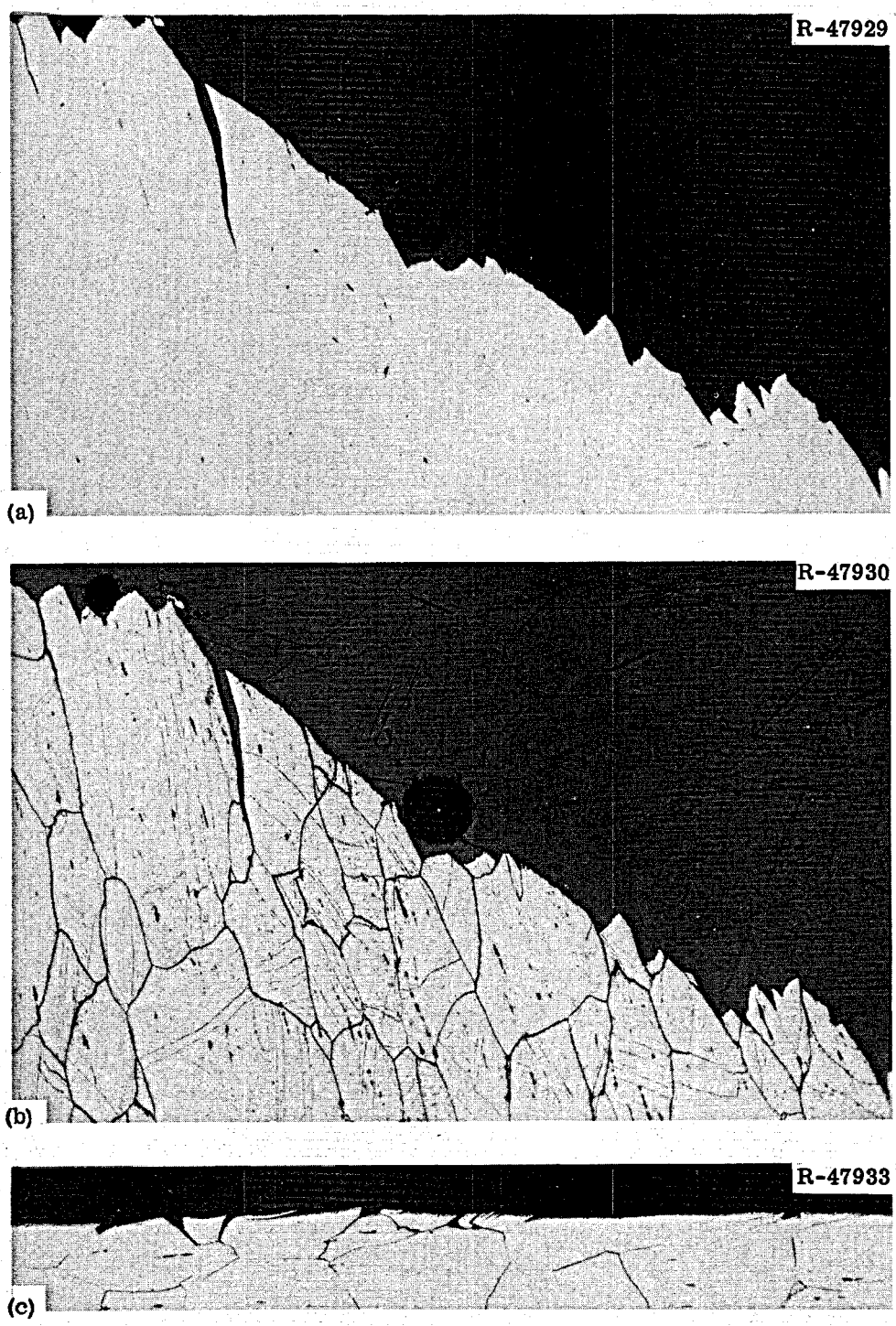

Fig. 54. Photomicrographs of a Hastelloy N (Heat 67-504) Sample Exposed to Fluoride Salt in the MSRE for 9789 hr at 650°C and Tested at 25°C. 100×. (a) Fracture, as polished. (b) Fracture, etched. (c) Edge of stressed portion, etched. Etchant: aqua regia. Reduced 10%.

Heat 67-504 also failed by a predominately transgranular mode when tested at 650°C (Fig. 55). This observation correlates quite well with the high fracture strain of this sample (Fig. 29, p. 35).

Discussion of Results

The samples of standard Hastelloy N removed from the surveillance facilities inside the MSRE core and outside the reactor vessel continue to show excellent compatibility with their respective environments of fuel salt and N_2 + 2 to 5% O_2. We could not detect the diffusion of fission products into the samples from the core. The samples exposed to the cell environment showed no evidence of nitriding and only superficial oxidation.

We have removed several groups of samples from the MSRE (Table 2, p. 6) and some valuable observations have been made regarding the changes of mechanical properties with fluence and thermal exposure. The thermal flux in the center of the core is 40 times that at the vessel wall. Only the Hastelloy N thimbles for the control rods have been exposed to the peak flux and have accumulated a thermal neutron fluence of about 1×10^{21} neutrons/cm^2. The tensile (Figs. 17 and 18, pp. 24 and 25) and the creep (Figs. 21, 23, 25, and 27, pp. 27, 29, 31, and 32) properties of Hastelloy N exposed to such a fluence are very poor; but the thimbles are stressed only slightly in compression and the observed property changes are not catastrophic.

The peak vessel thermal fluence is presently (May 1968) 2.6×10^{19} neutrons/cm^2, but the properties have already been altered markedly. The results that we obtained at higher fluences can be used to estimate the future properties of the MSRE vessel. Figure 56 has been constructed for heat 5085 and shows how the fracture strain at different strain rates varies with thermal fluence at 650°C. The fraction of the strain remaining is based on the number shown in parenthesis which is the value measured in the unirradiated starting material after a 2-hr anneal at 900°C. The corresponding curve for the burnup of ^{10}B is also

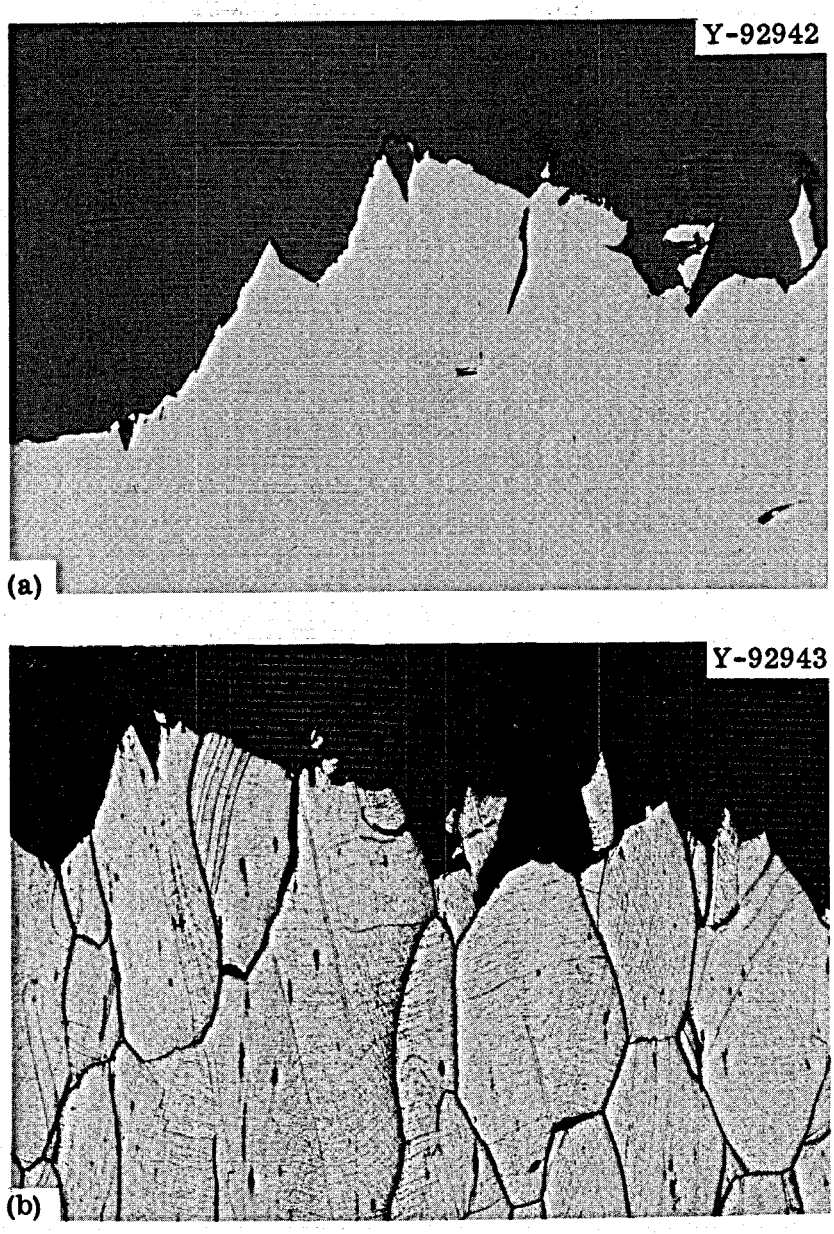

Fig. 55. Photomicrographs of the Fracture of a Hastelloy N (Heat 67-504) Sample Exposed to Static Barren Fuel Salt for 9789 hr at 650°C and Tested at 650°C and a Strain rate of 0.002 min^{-1}. 100×. (a) As polished. (b) Etched. Etchant: glyceria regia.

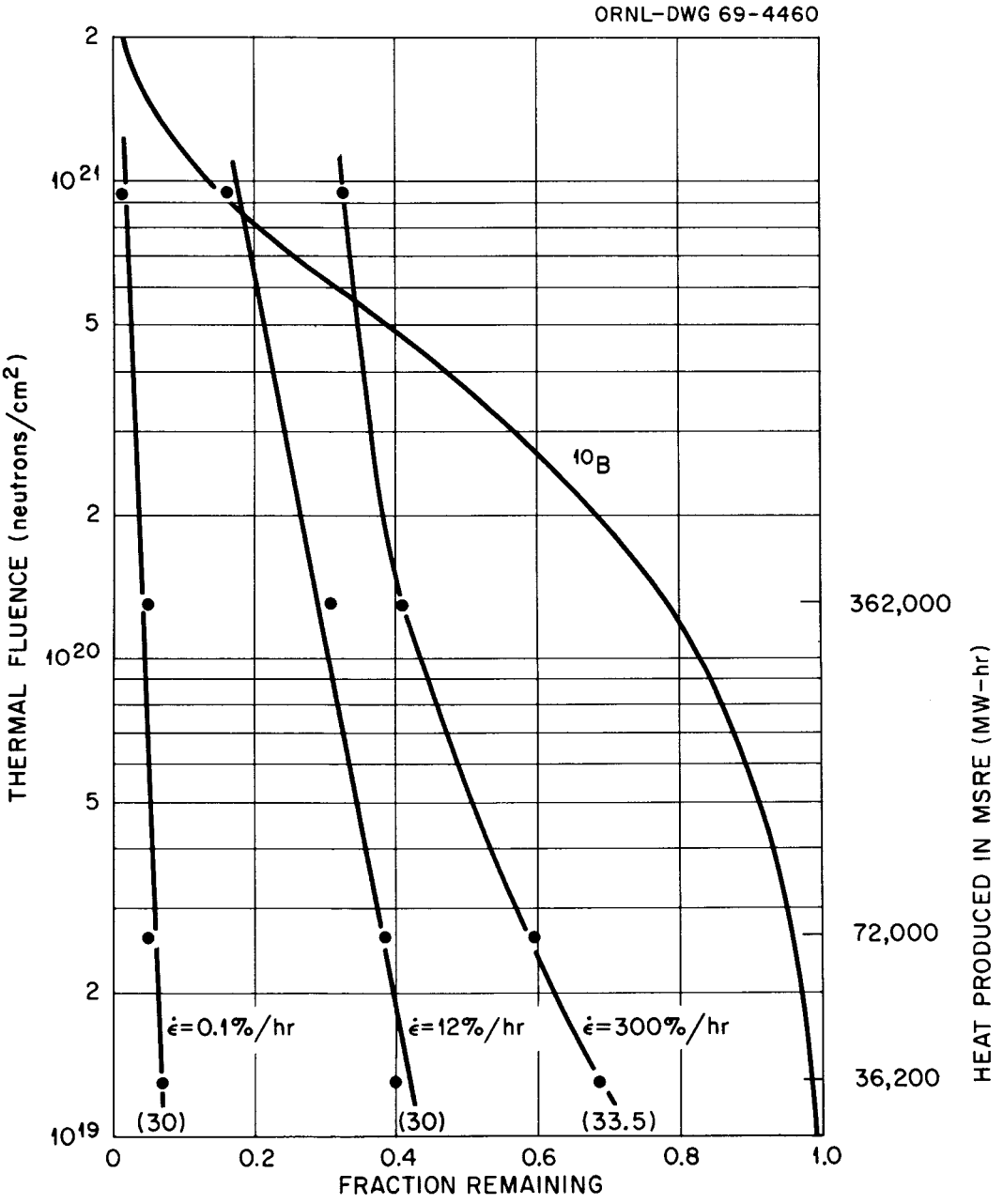

Fig. 56. Change in the Fracture Strain of Hastelloy N (Heat 5085) with Thermal Fluence for Various Strain Rates.

shown for comparison (based on a cross section of 1930 barns for MSRE spectrum[11]).

The strain rate of 300%/hr (0.05 min^{-1}) is that normally used in tensile tests and the vessel heats presently, after 72,400 Mwhr of operation, will strain about 20% at 650°C before failure. The fracture strain decreases with decreasing strain rate to a minimum value of 1.5% at a strain rate of about 0.1%/hr. These property changes are quite large when we consider that only 4% of the ^{10}B has been converted to helium (accumulated thermal fluence $\simeq 2.6 \times 10^{19}$ neutrons/cm^2). However, the results from samples exposed to higher fluences in the core indicate that the property changes are not simply proportional to the quantity of ^{10}B transmuted to helium. Although the intended operating time for the MSRE has not been established, it likely will not exceed 362,000 Mwhr (five times the energy already generated). Figure 56 indicates that the mechanical properties should not worsen drastically from those that prevail after 72,400 Mwhr of operation.

The main uncertainty associated with our estimate of the future properties of the MSRE vessel is that we have not taken into account the property changes due to thermal aging. As shown in Figs. 19 and 21, pp. 25 and 27, the tensile and creep properties of heat 5085 were changed just by annealing at 650°C. However, heat 5065 (Fig. 25, p. 31) seemed to be more resistant to aging. The noted changes in the fracture strain at lower temperatures could also conceivably become a problem. These changes also vary from heat to heat and depend on both fluence and aging time. Thus, the effects of aging cannot be taken into account adequately to improve on the property estimates made on the basis of Fig. 56.

The postirradiation properties of the two modified alloys (heats 67-502 and -504) were better than those of the standard alloys (compare Figs 28 and 35, pp. 33 and 39). We cannot explain the property changes that occurred as a result of aging these alloys in static barren salt, but our current aging studies should reveal the mechanism.

---

[11]B. E. Prince, MSR Program Semiann. Progr. Rept. Aug. 31, 1967, ORNL-4191, p. 58.

Metallographic examination showed that the standard Hastelloy N was very compatible with the fuel salt. The samples removed from outside the vessel were oxidized but there was no evidence of nitrogen absorption. The modified alloys were exposed to the fuel salt and an iron-rich layer was formed on the surface. This transfer occurred because the modified alloys contain less than 0.1% Fe and the standard Hastelloy N used in the rest of the system contains 4 to 5% Fe.

SUMMARY AND CONCLUSIONS

We have examined the third group of surveillance samples removed from the MSRE. The materials involved were (1) standard Hastelloy N exposed in the MSRE cell to an environment of N_2 + 2 to 5% O_2 for 20,789 hr at 650°C to a thermal fluence of 2.6×10^{19} neutrons/cm^2, (2) standard Hastelloy N exposed in the MSRE core to fluoride salt for 15,289 hr at 650°C to a thermal fluence of 9.4×10^{20} neutrons/cm^2, and (3) modified Hastelloy N exposed in the MSRE to fluoride salt for 9789 hr at 650°C to a thermal fluence of 5.3×10^{20} neutrons/cm^2. Postirradiation creep and tensile tests were run to evaluate the influence of the respective exposures on the mechanical properties. The property change of most concern is the reduction in the fracture strain. The fracture strain at 25°C was reduced by an amount related to both the neutron fluence and the exposure time. The fracture strain could be restored by a postirradiation anneal of 8 hr at 870°C and we propose that the reduction in fracture strain at 25°C is due to carbide precipitation. The fracture strain in tensile tests above 500°C and in creep tests at 650°C was reduced by irradiation. This embrittlement is associated with the helium that is produced by the transmutation of ^{10}B in the alloy and cannot be recovered by postirradiation annealing. We compared the results from samples irradiated to thermal fluences ranging from 1.3×10^{19} to 9.4×10^{20} neutrons/cm^2 and have an approximate picture of how the fracture strain varies with fluence. This picture is complicated by the fact that the properties of the unirradiated material change some with aging at 650°C, and we do not have sufficient data to separate the contributions of irradiation and aging to the observed embrittlement.

The modified alloys had better postirradiation properties than were measured for the standard Hastelloy N. Although the properties of these materials were affected appreciably by irradiation, the minimum fracture strain observed in postirradiation creep tests at 650°C was 6%.

ACKNOWLEDGMENTS

The author is indebted to numerous persons for assistance in this study.

W. H. Cook and A. Taboada — Design of surveillance assembly and insertion of specimens.

W. H. Cook and R. C. Steffy — Flux measurements.

J. R. Weir, Jr., R. E. Gehlbach, and C. E. Sessions — Review of manuscript.

E. J. Lawrence and J. L. Griffith — Assembled surveillance and control specimens in fixture.

P. Haubenreich and MSRE Operation Staff — Exercised extreme care in inserting and removing the surveillance specimens.

E. M. King and Hot Cell Operation Staff — Developed techniques for cutting long rods into individual specimens, determined specimen straightness, and offered assistance in running creep and tensile tests.

B. C. Williams, B. McNabb, and N. O. Pleasant — Ran tensile and creep tests on surveillance and control specimens.

E. M. Thomas and J. Feltner — Processed test data.

H. R. Tinch and E. Lee — Metallography on control and surveillance specimens.

Metals and Ceramics Reports Office — Preparation of manuscript.

Graphic Arts — Preparation of drawings.

APPENDIX

Table A-1. Postirradiation Tensile Properties of Samples of Heat 5085[a]

Specimen Number	Test Temperature (°C)	Strain Rate (min^{-1})	Stress, psi		Strain, %		Reduction in Area (%)	True Strain (%)
			Yield	Ultimate	Uniform	Total		
7976	25	0.05	46,500	99,100	32.8	32.8	24.51	28.0
7982[b]	25	0.05	46,700	111,900	48.2	48.3	34.19	42.0
7975	200	0.05	38,000	94,600	40.0	41.2	32.11	39.0
7974	400	0.05	34,700	90,800	46.8	47.2	36.46	45.0
7972	500	0.05	33,500	86,700	43.2	44.0	36.13	45.0
7970	550	0.05	32,000	76,000	29.5	30.2	30.89	37.0
7968	600	0.05	31,700	68,000	21.0	21.3	24.63	28.0
7966	650	0.05	30,400	60,900	18.8	19.7	14.82	16.0
7964	700	0.05	30,000	54,000	15.7	15.9	8.64	9.0
7962	760	0.05	30,200	43,800	8.3	8.9	12.30	13.0
7960	850	0.05	33,000	37,500	3.2	3.5	3.98	4.0
7973	400	0.002	35,000	91,500	47.3	47.8	37.20	47.0
7989	500	0.002	37,200	79,000	27.5	28.7	29.55	35.0
7969	550	0.002	33,500	67,400	19.5	20.6	18.94	21.0
7967	600	0.002	31,500	58,000	15.2	15.7	19.07	21.0
7965	650	0.002	31,300	49,900	11.1	11.6	18.61	21.0
7963	700	0.002	30,000	41,900	6.7	7.3	10.02	11.0
7961	760	0.002	28,600	37,000	4.4	5.0	8.31	9.0
7981	850	0.002	21,700	21,700	1.0	1.5	4.91	5.0
7988	500	0.0005	34,300	68,800	20.4	21.1	19.33	21.0
7987	550	0.0005	33,500	64,100	19.0	19.6	18.48	20.0
7986	600	0.0005	31,800	54,100	13.3	13.7	16.76	18.0
7985	650	0.0005	31,300	46,100	8.5	9.3	6.95	7.0
7984	700	0.0005	30,800	41,100	5.0	5.2	6.45	7.0

[a]Located outside the MSRE vessel for 20,789 hr at 650°C. Thermal fluence was 2.6×10^{19} neutrons/cm^2.

[b]Given a postirradiation anneal of 8 hr at 870°C.

Table A-2. Postirradiation Tensile Properties of Samples of Heat 5065[a]

Specimen Number	Test Temperature (°C)	Strain Rate (min^{-1})	Stress, psi		Strain, %		Reduction in Area (%)	True Strain (%)
			Yield	Ultimate	Uniform	Total		
7940	25	0.05	49,000	118,800	57.8	59.7	38.44	49.0
7939	200	0.05	40,500	105,200	55.1	57.6	40.54	52.0
7938	400	0.05	36,600	99,600	55.0	56.3	43.27	57.0
7936	500	0.05	45,400	94,800	46.6	47.2	40.83	52.0
7934	550	0.05	36,000	83,800	31.8	32.0	26.83	31.0
7946	600	0.05	33,100	79,800	33.3	33.9	31.33	38.0
7930	650	0.05	30,600	55,400	11.7	11.8	11.69	12.0
7928	700	0.05	31,100	57,200	13.5	13.6	16.83	18.0
7926	760	0.05	29,600	33,700	2.2	3.2	8.17	9.0
7924	850	0.05	32,700	36,800	3.2	3.4	3.99	4.0
7935	500	0.002	36,200	85,200	25.7	26.2	22.89	26.0
7956	500	0.002	38,100	86,900	29.5	30.2	24.14	28.0
7933	550	0.002	35,600	78,400	26.4	26.7	24.99	29.0
7931	600	0.002	34,600	63,400	14.9	15.1	8.49	9.0
7947	650	0.002	34,100	55,500	12.2	12.5	16.09	18.0
7948	700	0.002	33,500	49,900	8.6	8.7	8.31	9.0
7925	760	0.002	33,300	40,000	3.5	5.0	12.39	13.0
7945	850	0.002	22,600	23,100	1.0	2.0	2.86	3.0
7955	400	0.0005	38,200	100,700	52.8	54.2	37.37	47.0
7954	500	0.0005	36,400	80,100	28.3	28.9	25.11	29.0
7953	550	0.0005	37,500	70,200	20.3	20.9	19.59	22.0
7952	600	0.0005	27,800	61,100	16.7	17.0	18.74	21.0
7929	650	0.0005	33,700	52,700	8.8	9.1	16.02	17.0
7950	700	0.0005	32,800	46,300	4.8	6.2	5.69	6.0

[a]Located outside the MSRE vessel for 20,789 hr at 650°C. Thermal fluence was 2.6×10^{19} neutrons/cm^2.

Table A-3. Tensile Properties of Samples of Heat 5085[a]

Specimen Number	Test Temperature (°C)	Strain Rate (min^{-1})	Stress, psi		Strain, %		Reduction in Area (%)	True Strain (%)
			Yield	Ultimate	Uniform	Total		
7888	25	0.05	52,300	95,000	28.7	28.9	19.95	22.0
7889	200	0.05	43,700	92,200	36.1	36.7	30.00	36.0
7890	400	0.05	42,800	84,300	31.9	32.1	31.11	37.0
7892	500	0.05	39,600	81,200	35.0	35.2	31.33	38.0
7894	550	0.05	38,900	71,500	22.5	23.6	27.64	32.0
7881	600	0.05	38,100	58,700	11.1	11.8	18.80	21.0
7887	650	0.05	34,400	51,600	10.4	11.0	14.16	15.0
7879	700	0.05	35,900	46,200	5.8	6.3	10.70	11.0
7877	760	0.05	29,700	36,200	4.7	5.4	11.74	12.0
7875	850	0.05	30,400	31,300	1.8	2.2	6.84	7.0
7891	400	0.002	42,000	86,400	34.6	34.8	30.11	36.0
7893	500	0.002	41,100	68,000	17.0	18.1	20.08	22.0
7895	550	0.002	44,300	64,900	12.4	13.3	16.02	17.0
7880	600	0.002	34,300	46,900	6.4	7.1	16.04	17.0
7886	650	0.002	35,000	42,400	4.5	5.0	13.14	14.0
7878	700	0.002	33,700	36,100	2.1	2.2	7.63	8.0
7876	760	0.002	31,000	31,900	1.8	2.2	4.69	5.0
7874	850	0.002	22,200	22,200	1.2	1.2	1.74	2.0

[a]After exposure in the MSRE core for 15,289 hr at 650°C. Thermal fluence was 9.4×10^{20} neutrons/cm^2 and the fast fluence > 1.22 Mev was 2.3×10^{20} neutrons/cm^2.

Table A-4. Tensile Properties of Control Specimens of Heat 5085[a]

Specimen Number	Test Temperature (°C)	Strain Rate (min^{-1})	Stress, psi		Strain, %		Reduction in Area (%)	True Strain (%)
			Yield	Ultimate	Uniform	Total		
10166	25	0.05	53,900	115,900	38.4	38.6	29.66	35.0
10167	200	0.05	44,500	109,600	46.5	46.8	37.44	47.0
10165	400	0.05	39,600	102,700	49.7	50.2	39.08	50.0
10168	500	0.05	41,200	99,500	47.9	49.1	33.98	42.0
10169	550	0.05	38,600	91,400	39.3	39.5	33.20	40.0
10187	600	0.05	41,500	86,500	24.5	26.0	24.51	28.0
10170	650	0.05	38,000	70,500	18.8	19.6	20.89	23.0
10185	700	0.05	42,300	77,700	22.5	24.0	22.23	29.0
10172	760	0.05	35,800	68,600	24.8	31.3	22.23	29.0
10164	850	0.05	30,200	50,300	12.9	37.6	33.66	51.0
10183	400	0.002	41,700	107,300	48.8	49.3	36.46	45.0
10177	500	0.002	39,200	95,200	32.5	33.3	28.30	33.0
10184	550	0.002	39,600	83,500	25.6	26.6	19.20	21.0
10189	600	0.002	42,700	73,100	15.6	16.1	19.07	21.0
10190	650	0.002	37,700	64,700	17.4	18.0	19.74	22.0
10173	700	0.002	42,400	68,000	15.8	16.8	19.87	22.0
10182	760	0.002	35,500	53,100	8.6	35.5	32.55	39.0
10174	850	0.002	31,600	31,600	1.3	34.1	35.48	44.0
10175	850	0.002	29,900	29,900	1.5	31.0	32.88	40.0

[a]After exposure to static fluoride salt for 15,289 hr at 650°C.

Table A-5. Tensile Properties of Samples of Heat 5065[a]

Specimen Number	Test Temperature (°C)	Strain Rate (min^{-1})	Stress, psi		Strain, %		Reduction in Area (%)	True Strain (%)
			Yield	Ultimate	Uniform	Total		
7915	25	0.05	51,700	109,300	41.4	41.5	34.14	42.0
7916	200	0.05	62,300	102,400	38.9	39.6	35.87	44.0
7917	400	0.05	41,700	94,600	43.8	46.3	39.02	49.0
7919	500	0.05	44,100	90,600	37.0	38.0	34.63	43.0
7921	550	0.05	43,100	81,400	25.4	25.7	25.83	30.0
7908	600	0.05	38,600	62,100	11.7	11.9	13.28	14.0
7914	650	0.05	39,200	55,600	8.3	8.5	12.53	13.0
7906	700	0.05	36,200	46,800	5.4	5.5	6.75	7.0
7904	760	0.05	33,800	38,100	2.8	2.9	10.99	12.0
7900	850	0.05	34,000	34,000	1.4	1.5	5.18	5.0
7918	400	0.002	46,600	96,900	41.9	43.0	37.57	47.0
7920	500	0.002	44,300	76.800	16.3	16.6	19.46	22.0
7922	550	0.002	42,400	66.300	12.0	12.4	18.15	20.0
7907	600	0.002	37,200	49,500	5.8	5.9	12.95	14.0
7913	650	0.002	40,400	46,300	3.2	3.4	5.95	6.0
7905	700	0.002	37,400	38,200	1.7	1.8	6.10	6.0
7903	760	0.002	33,200	34,700	1.0	1.0	9.40	9.0
7901	850	0.002	20,500	20,500	1.0	1.0	4.38	4.0

[a]After exposure in MSRE core for 15,289 hr at 650°C. Thermal fluence was 9.4×10^{20} neutrons/cm^2 and fast fluence > 1.22 Mev was 2.3×10^{20} neutrons/cm^2.

Table A-6. Tensile Properties of Control Specimens of Heat 5065[a]

Specimen Number	Test Temperature (°C)	Strain Rate (min^{-1})	Stress, psi		Strain, %		Reduction in Area (%)	True Strain (%)
			Yield	Ultimate	Uniform	Total		
10215	25	0.05	60,900	126,700	46.5	47.4	39.30	50.0
10214	200	0.05	46.800	114,300	47.2	49.4	37.07	46.0
10210	400	0.05	46,700	110,300	44.4	47.4	39.30	50.0
10194	500	0.05	41,200	103,700	45.7	46.5	36.77	46.0
10213	550	0.05	42,800	98,400	41.2	41.4	35.59	44.0
10217	600	0.05	40,700	88,300	23.2	24.3	20.86	23.0
10211	650	0.05	43,400	78,200	18.4	18.8	16.56	18.0
10191	700	0.05	39,600	71.400	17.0	17.6	19.07	21.0
10195	760	0.05	36,900	69,500	20.3	29.9	21.94	25.0
10196	850	0.05	35,300	46,900	8.6	44.1	48.82	67.0
10208	400	0.002	50,700	118,500	43.4	46.5	38.34	48.0
10199	500	0.002	46,100	91,800	30.8	31.4	22.48	25.0
10200	550	0.002	46,500	84,100	18.6	19.1	17.75	20.0
10212	600	0.002	41,200	75,400	18.5	19.0	19.20	21.0
10216	650	0.002	44,200	73,300	16.0	16.5	16.83	18.0
10202	700	0.002	43,700	69,700	13.8	21.1	18.68	21.0
10198	760	0.002	41,700	50,400	7.5	34.8	36.87	46.0
10192	850	0.002	29,400	29,400	1.3	44.9	44.56	59.0

[a]After exposure to static fluoride salt for 15,289 hr at 650°C.

Table A-7. Postirradiation Creep-Rupture Properties at 650°C of Samples of Standard Hastelloy N[a]

Test Number	Specimen Number	Stress Level (psi)	Rupture Life (hr)	Rupture Strain (%)	Minimum Creep Rate (%/hr)
		Heat 5065			
R-717	7941	52,000	3.4	2.3	0.525
R-736	7942	47,000	11.6	1.0	0.0792
R-725	7943	40,000	30.8	0.97	0.0283
R-728	7944	32,400	77.7	0.72	0.0062
R-780	7949	27,000	499.2	2.0	0.0012
		Heat 5085			
R-718	7977	52,000	1.9	2.4	0.892
R-739	7978	47,000	4.1	1.9	0.400
R-724	7979	40,000	40.2	1.3	0.0209
R-729	7980	32,400	264.0	1.2	0.0029
R-781	7983	27,000	451.5	1.6	0.0021

[a]Located outside the MSRE Vessel for 20,789 hr at 650°C. Thermal fluence was 2.6×10^{19} neutrons/cm^2.

Table A-8. Creep-Rupture Properties at 650°C of Samples of Standard Hastelloy N[a]

Test Number	Specimen Number	Stress Level (psi)	Rupture Life (hr)	Rupture Strain (%)	Minimum Creep Rate (%/hr)
		Heat 5065			
R-719	7909	47,000	0.3	0.12	0.20
R-726	7912	32,400	4.7	0.18	0.0214
R-721	7911	27,000	5.1	0.09	0.0134
R-730	7910	21,500	246.3	0.28	0.0010
R-783	7923	17,000	1940.2	0.83	0.0002
		Heat 5085			
R-720	7882	47,000	0		
R-722	7884	32,400	12.6	0.52	0.0245
R-723	7885	27,000	50.6	0.81	0.0104
R-731	7883	21,500	217.8	1.1	0.0025
R-782	7873	17,000	2386.8	1.29	0.0005

[a]After exposure in the MSRE core for 15,289 hr at 650°C. Thermal fluence was 9.4×10^{20} neutrons/cm^2 and the fast fluence >1.22 Mev was 2.3×10^{20} neutrons/cm^2.

Table A-9. Creep-Rupture Properties at 650°C of Control Specimens of Standard Hastelloy N[a]

Test Number	Specimen Number	Stress Level (psi)	Rupture Life (hr)	Rupture Strain (%)	Minimum Creep Rate (%/hr)	Reduction in Area (%)
			Heat 5065			
7240	10205	55,000	14.9	15.5	0.620	16.2
7239	10206	47,000	107.5	23.3	0.145	20.5
7238	10193	40,000	416.6	28.9	0.0426	24.8
7237	10209	32,400	1234.2	27.8	0.0131	32.9
			Heat 5085			
7236	10178	55,000	10.3	18.2	0.905	18.7
7235	10188	47,000	65.2	19.6	0.156	18.8
7355	10179	40,000	526.5	20.5	0.025	24.4
7233	10186	38,200	658.3	23.2	0.0230	27.5
7416	10176	32,400	1670.6	23.7	0.0083	29.9

[a]Exposed to static fluoride salt for 15,289 hr at 650°C.

Table A-10. Tensile Properties of Heat 67-502 Surveillance Samples[a]

Specimen Number	Test Temperature (°C)	Strain Rate (min^{-1})	Stress, psi		Strain, %		Reduction in Area (%)	True Strain (%)
			Yield	Ultimate	Uniform	Total		
5329	25	0.05	65,400	119,300	50.3	51.6	34.81	43.0
5330	200	0.05	51,300	104,500	47.0	49.3	42.83	56.0
5331	400	0.05	47,500	93,800	47.9	50.2	45.68	61.0
5333	500	0.05	47,800	109,000	48.0	51.8	42.39	55.0
5335	550	0.05	40,000	104,000	43.5	44.2	39.02	49.0
5322	600	0.05	41,100	82,800	38.1	40.2	31.46	38.0
5328	650	0.05	44,100	69,600	22.5	24.1	27.13	32.0
5320	700	0.05	36,700	61,600	19.0	20.2	23.35	27.0
5318	760	0.05	33,000	58,000	14.9	16.6	8.67	9.0
5316	850	0.05	31,100	35,300	2.4	3.0	13.29	14.0
5332	400	0.002	52,300	96,800	48.4	50.0	35.22	43.0
5334	500	0.002	52,600	82,400	29.3	31.4	26.03	30.0
5336	550	0.002	51,200	66,400	10.5	13.0	22.56	26.0
5321	600	0.002	40,900	62,700	17.1	19.0	19.07	21.0
5327	650	0.002	42,200	62,900	15.6	17.1	15.36	17.0
5319	700	0.002	35,500	55,500	10.2	12.7	13.29	14.0
5317	760	0.002	35,500	42,100	4.4	8.2	9.59	10.0
5315	850	0.002	24,900	25,100	1.1	3.0	9.44	10.0

[a]Exposed to core of MSRE for 9789 hr at 650°C. Thermal fluence was 5.3×10^{20} neutrons/cm^2.

Table A-11. Tensile Properties of Heat 67-504 Surveillance Samples[a]

Specimen Number	Test Temperature (°C)	Strain Rate (min^{-1})	Stress, psi		Strain, %		Reduction in Area (%)	True Strain (%)
			Yield	Ultimate	Uniform	Total		
5086	25	0.05	102,300	119,300	26.0	27.0	33.46	41.0
5087	200	0.05	46,400	105,700	43.7	44.4	31.89	38.0
5088	400	0.05	41,000	97,700	44.0	44.5	37.20	47.0
5090	500	0.05	40,100	93,000	42.8	43.3	37.94	48.0
5092	550	0.05	39,600	112,000	46.0	46.7	36.46	45.0
5079	600	0.05	39,700	101,000	35.3	35.7	33.53	41.0
5085	650	0.05	32,900	70,000	30.0	30.7	31.45	38.0
5077	700	0.05	35,000	65,900	23.2	24.2	24.54	28.0
5075	760	0.05	34,900	57,600	12.8	13.8	18.02	20.0
5073	850	0.05	32,600	40,800	4.8	6.6	9.37	10.0
5089	400	0.002	41,700	99,000	41.8	42.9	36.36	45.0
5091	500	0.002	41,600	91,200	42.2	43.2	28.18	33.0
5093	550	0.002	38,000	78,100	28.2	29.9	21.18	24.0
5078	600	0.002	40,200	69,600	23.7	24.8	17.16	19.0
5084	650	0.002	34,700	63,900	21.9	23.1	16.96	19.0
5076	700	0.002	35,700	56,200	11.9	14.6	13.12	14.0
5074	760	0.002	37,000	42,300	4.3	6.7	11.92	13.0
5072	850	0.002	25,400	26,000	2.1	4.4	11.50	12.0

[a]Exposed to core of MSRE for 9789 hr at 650°C. Thermal fluence was 5.3×10^{20} neutrons/cm^2.

Table A-12. Tensile Properties of Control Specimens of Heat 67-502[a]

Specimen Number	Test Temperature (°C)	Strain Rate (min^{-1})	Stress, psi		Strain, %		Reduction in Area (%)	True Strain (%)
			Yield	Ultimate	Uniform	Total		
5381	25	0.05	56,600	113,400	53.7	55.4	50.04	69.0
5390	200	0.05	54,400	111,700	54.4	56.2	51.17	72.0
5393	400	0.05	48,100	106,100	58.0	60.9	52.51	74.0
5391	500	0.05	42,900	95,600	50.6	52.6	45.31	60.0
5395	550	0.05	45,600	97,600	52.9	54.9	48.16	66.0
5397	600	0.05	44,000	93,500	52.8	55.1	43.09	56.0
5394	650	0.05	51,200	98,200	46.5	48.3	35.48	44.0
5389	700	0.05	41,700	83,600	41.3	43.6	34.19	42.0
5388	760	0.05	39,200	72,800	24.5	39.7	29.44	35.0
5382	850	0.05	35,200	47,300	8.0	25.0	23.35	27.0
5386	400	0.002	49,300	105,100	54.8	56.9	48.90	67.0
5384	500	0.002	45,000	89,700	51.7	55.7	45.39	61.0
5392	550	0.002	38,800	88,100	50.4	52.9	35.48	44.0
5379	600	0.002	52,400	88,900	29.6	31.2	28.87	34.0
5387	700	0.002	41,700	75,300	18.8	34.1	31.56	38.0
5383	760	0.002	44,800	50,800	6.4	27.3	24.75	28.0
5380	850	0.002	29,000	29,400	2.9	18.1	19.07	21.0

[a]After exposure to static fluoride salt for 9789 hr at 650°C.

Table A-13. Tensile Properties of Control Specimens of Heat 67-504[a]

Specimen Number	Test Temperature (°C)	Strain Rate (min^{-1})	Stress, psi		Strain, %		Reduction in Area (%)	True Strain (%)
			Yield	Ultimate	Uniform	Total		
5058	25	0.05	67,500	132,800	50.2	52.3	43.72	57.0
5046	200	0.05	59,700	118,700	43.5	44.0	41.59	54.0
5057	400	0.05	45,500	105,100	46.2	47.2	36.41	45.0
5061	500	0.05	43,100	99,900	50.6	52.1	41.30	53.0
5045	550	0.05	45,300	101,500	47.9	49.4	36.87	46.0
5055	600	0.05	45,400	97,700	49.1	50.9	36.67	46.0
5065	650	0.05	43,300	94,300	48.8	50.9	37.37	47.0
5067	700	0.05	53,300	94,600	30.8	39.5	36.00	45.0
5066	760	0.05	44,200	75,400	20.3	43.5	38.44	49.0
5060	850	0.05	34,900	47,800	7.7	38.7	35.48	44.0
5064	400	0.002	53,400	122,800	46.2	47.9	34.19	42.0
5041	500	0.002	61,300	115,500	44.5	46.1	33.52	41.0
5053	550	0.002	49,200	99,700	47.2	48.5	39.59	50.0
5044	600	0.002	45,800	91,300	41.9	43.7	37.27	47.0
5042	650	0.002	44,900	80,200	30.0	41.2	38.14	48.0
5048	700	0.002	42,100	68,100	16.2	45.8	40.64	52.0
5047	760	0.002	42,700	50,800	6.0	38.9	41.78	54.0
5056	850	0.002	31,500	32,400	2.9	34.8	34.29	42.0

[a]After exposure to static fluoride salt for 9789 hr at 650°C.

Table A-14. Creep-Rupture Properties at 650°C of Surveillance Specimens of Modified Hastelloy N[a]

Test Number	Specimen Number	Stress Level (psi)	Rupture Life (hr)	Rupture Strain (%)	Minimum Creep Rate (%/hr)
		Heat 67-502			
R-735	729	55,000	26.0	5.8	0.178
R-716	711	47,000	126.4	4.3	0.0248
R-709	704	40,000	655.2	6.4	0.0068
R-735	730	32,400	1274.7	5.8	0.0019
		Heat 67-504			
R-733	728	55,000	59.6	7.0	0.0905
R-715	710	47,000	181.7	6.8	0.0272
R-708	703	40,000	467.2	6.9	0.0113
R-732	727	32,400	1643.8	5.9	0.0025

[a]Exposed to the core of the MSRE for 9789 hr at 650°C. Thermal fluence was 5.3×10^{20} neutrons/cm^2.

Table A-15. Creep-Rupture Properties at 650°C of Control Specimens of Modified Hastelloy N[a]

Test Number	Specimen Number	Stress Level (psi)	Rupture Life (hr)	Rupture Strain (%)	Minimum Creep Rate (%/hr)	Reduction in Area (%)
		Heat 67-502				
7232	5401	70,000	3.6	45.6	4.15	39.5
7231	5402	55,000	60.1	38.3	0.308	38.3
7230	5403	47,000	242.2	37.2	0.0775	34.7
7229	5404	40,000	1148.6	31.7	0.0148	29.2
		Heat 67-504				
7228	5050	70,000	5.5	43.7	3.80	43.9
7227	5043	55,000	108.3	41.7	0.180	39.6
7226	5049	47,000	329.2	39.4	0.0485	43.3
7225	5062	40,000	1014.6	40.8	0.0200	48.0

[a]Exposed to static fluoride salt for 9789 hr at 650°C.

INTERNAL DISTRIBUTION

1–3. Central Research Library
4–5. ORNL Y-12 Technical Library Document Reference Section
6–25. Laboratory Records
26. Laboratory Records, ORNL RC
27. ORNL Patent Office
28. R. K. Adams
29. G. M. Adamson, Jr.
30. R. G. Affel
31. J. L. Anderson
32. R. F. Apple
33. W. E. Atkinson
34. C. F. Baes
35. J. M. Baker
36. S. J. Ball
37. C. E. Bamberger
38. C. J. Barton
39. H. F. Bauman
40. M. S. Bautista
41. S. E. Beall
42. R. L. Beatty
43. M. J. Bell
44. M. Bender
45. C. E. Bettis
46. E. S. Bettis
47. D. S. Billington
48. R. E. Blanco
49. F. F. Blankenship
50. J. O. Blomeke
51. E. E. Bloom
52. R. Blumberg
53. E. G. Bohlmann
54. B. S. Borie
55. C. J. Borkowski
56. H. I. Bowers
57. C. M. Boyd
58. G. E. Boyd
59. J. Braunstein
60. M. A. Bredig
61. R. B. Briggs
62. H. R. Bronstein
63. G. D. Brunton
64. O. W. Burke
65. S. Cantor
66. D. W. Cardwell
67. J. H. Carswell, Jr.
68. W. L. Carter
69. G. I. Cathers
70. J. E. Caton
71. O. B. Cavin
72. A. G. Cepolina
73. J. M. Chandler
74. C. J. Claffey
75. F. H. Clark
76. H. D. Cochran
77. Nancy Cole
78. C. W. Collins
79. E. L. Compere
80. K. V. Cook
81. W. H. Cook
82. J. W. Cooke
83. L. T. Corbin
84. B. Cox
85. J. L. Crowley
86. F. L. Culler
87. D. R. Cuneo
88. J. E. Cunningham
89. J. M. Dale
90. D. G. Davis
91. R. J. DeBakker
92. J. H. DeVan
93. J. R. DiStefano
94. S. J. Ditto
95. F. A. Doss
96. A. S. Dworkin
97. W. P. Eatherly
98. J. R. Engel
99. E. P. Epler
100. J. I. Federer
101. D. E. Ferguson
102. L. M. Ferris
103. A. P. Fraas
104. J. K. Franzreb
105. H. A. Friedman
106. D. N. Fry
107. J. H Frye, Jr.
108. L. C. Fuller
109. W. K. Furlong
110. C. H. Gabbard
111. R. B. Gallaher
112. R. E. Gehlbach
113. J. H. Gibbons

114. L. O. Gilpatrick
115. G. Goldberg
116. W. R. Grimes
117. A. G. Grindell
118. R. W. Gunkel
119. R. H. Guymon
120. J. P. Hammond
121. R. L. Hamner
122. T. H. Handley
123. B. A. Hannaford
124. P. H. Harley
125. D. G. Harman
126. W. O. Harms
127. C. S. Harrill
128. P. N. Haubenreich
129. F. K. Heacker
130. R. E. Helms
131. P. G. Herndon
132. D. N. Hess
133. J. R. Hightower
134–136. M. R. Hill
137. E. C. Hise
138. B. F. Hitch
139. H. W. Hoffman
140. D. K. Holmes
141. P. P. Holz
142. R. W. Horton
143. A. Houtzeel
144. T. L. Hudson
145. W. R. Huntley
146. H. Inouye
147. W. H. Jordan
148. P. R. Kasten
149. R. J. Kedl
150. C. W. Kee
151. M. T. Kelley
152. M. J. Kelly
153. C. R. Kennedy
154. T. W. Kerlin
155. H. T. Kerr
156. J. J. Keyes
157. R. T. King
158. S. S. Kirslis
159. L. R. Koffman
160. J. W. Koger
161. H. W. Kohn
162. R. B. Korsmeyer
163. A. I. Krakoviak
164. T. S. Kress
165. J. W. Krewson
166. C. E. Lamb
167. J. A. Lane
168. M. S. Lin
169. R. B. Lindauer
170. A. P. Litman
171. E. L. Long
172. A. L. Lotts
173. M. I. Lundin
174. R. N. Lyon
175. R. L. Macklin
176. H. G. MacPherson
177. R. E. MacPherson
178. J. C. Mailen
179. D. L. Manning
180. C. D. Martin
181. W. R. Martin
182. R. W. McClung
183–187. H. E. McCoy
188. D. L. McElroy
189. C. K. McGlothlan
190. C. J. McHargue
191. H. A. McLain
192. B. McNabb
193. L. E. McNeese
194. J. R. McWherter
195. H. J. Metz
196. A. S. Meyer
197. R. L. Moore
198. C. A. Mossman
199. D. M. Moulton
200. T. R. Mueller
201. M. L. Myers
202. H. H. Nichol
203. J. P. Nichols
204. E. L. Nicholson
205. T. S. Noggle
206. L. C. Oakes
207. S. M. Ohr
208. P. Patriarca
209. A. M. Perry
210. T. W. Pickel
211. H. B. Piper
212. C. B. Pollock
213. B. E. Prince
214. G. L. Ragan
215. J. L. Redford
216. J. D. Redman
217. D. M. Richardson
218. M. Richardson
219. G. D. Robbins
220. R. C. Robertson
221. K. A. Romberger

222. M. W. Rosenthal
223. R. G. Ross
224. J. Roth
225. J. P. Sanders
226. H. C. Savage
227. W. F. Schaffer
228. C. E. Schilling
229. Dunlap Scott
230. J. L. Scott
231. H. E. Seagren
232. C. E. Sessions
233. J. H. Shaffer
234. W. H. Sides
235. M. J. Skinner
236. G. M. Slaughter
237. A. N. Smith
238. F. J. Smith
239. G. P. Smith
240. O. L. Smith 1
241. P. G. Smith
242. I. Spiewak
243. R. C. Steffy
244. H. H. Stone
245. R. A. Strehlow
246. R. D. Stulting
247. R. W. Swindeman
248. J. R. Tallackson
249. E. H. Taylor
250. W. Terry
251. R. E. Thoma
252. P. F. Thomason
253. L. M. Toth
254. A. L. Travaglini
255. D. B. Trauger
256. Chia-Pao Tung
257. W. E. Unger
258. G. M. Watson
259. J. S. Watson
260. H. L. Watts
261. C. F. Weaver
262. B. H. Webster
263. A. M. Weinberg
264. J. R. Weir
265. K. W. West
266. H. L. Whaley
267. M. E. Whatley
268. J. C. White
269. R. P. Wichner
270. L. V. Wilson
271. Gale Young
272. H. C. Young
273. J. P. Young
274. E. L. Youngblood
275. F. C. Zapp

EXTERNAL DISTRIBUTION

276. G. G. Allaria, Atomics International
277. J. G. Asquith, Atomics International
278. D. F. Cope, RDT, SSR, AEC, Oak Ridge National Laboratory
279. C. B. Deering, AEC, OSR, Oak Ridge National Laboratory
280. A. R. DeGrazia, AEC, Washington
281. H. M. Dieckamp, Atomics International
282. David Elias, AEC, Washington
283. A. Giambusso, AEC, Washington
284. J. E. Fox, AEC, Washington
285. F. D. Haines, AEC, Washington
286. C. E. Johnson, AEC, Washington
287. W. L. Kitterman, AEC, Washington
288. W. J. Larkin, AEC, Oak Ridge Operations
289. Kermit Laughon, AEC, OSR, Oak Ridge National Laboratory
290. C. L. Matthews. AEC, OSR, Oak Ridge National Laboratory
291–292. T. W. McIntosh, AEC, Washington
293. A. B. Martin, Atomics International
294. D. G. Mason, Atomics International
295. G. W. Meyers, Atomics International
296. D. E. Reardon, AEC, Canoga Park Area Office

297. D. R. Riley, AEC, Washington
298. H. M. Roth, AEC, Oak Ridge Operations
299. M. Shaw, AEC, Washington
300. J. M. Simmons, AEC, Washington
301. T. G. Schleiter, AEC, Washington
302. W. L. Smalley, AEC, Washington
303. S. R. Stamp, AEC, Canoga Park Area Office
304. E. E. Stansbury, the University of Tennessee
305. D. K. Stevens, AEC, Washington
306. R. F. Sweek, AEC, Washington
307. A. Taboada, AEC, Washington
308. M. J. Whitman, AEC, Washington
309. R. F. Wilson, Atomics International
310. Laboratory and University Division, AEC, Oak Ridge Operations
311–325. Division of Technical Information Extension